No. 71 – March 1993

ESO, CNRS and MPI Sign Agreement on Enhancement of the VLT Interferometer

On December 18, 1992, a ceremony took place at the ESO Headquarters during which an important tripartite agreement was signed that will significantly enhance the scientific possibilities of the Very Large Telescope.

After a period of intense negotiations, Dr. A. Berroir (Director of CNRS-INSU), Dr. W. Hasenclever (General Secretary of the MPI) and Prof. H. van der Laan (ESO Director General) on behalf of their respective organizations put their signatures on a contract which will permit the construction of a third 1.8-metre movable telescope for the VLT Interferometer (VLTI). This took place in the presence of several important guests, including Prof. P. Léna, French delegate to the ESO Council and actively involved in the ESO interferometric programme, and Dr. G. Preiß and Mr. D. von Staden from the Max-Planck Society. Several ESO staff members were also present.

In his introduction, Prof. van der Laan mentioned the history of interferometry, from the early work in the radio domain

Figure 1: *Signing ceremony at the ESO Headquarters (from left to right): Prof. P. Léna, member of the ESO Council; Dr. A. Berroir, Director of CNRS-INSU; Prof. H. van der Laan, Director General of ESO; Dr. W. Hasenclever, MPG General Secretary; Dr. G. Preiß, MPG; Mr. D. von Staden, MPG.*

to the great opportunities with modern optical arrays. He specifically stated the unanimous support of the VLTI project by the ESO Scientific and Technical Committee (STC) and was followed by the manager of the VLT project, Prof. M. Tarenghi, who likened the VLTI with an astronomer's dream coming true. Nobody knows for sure which new discoveries will be made with this absolutely unique instrument in the future.

The representatives of ESO's German and French partners spoke about the not so easy task of finding money for such a project in these days of limited ressources, but also how happy they were to bless a truly European undertaking of this dimension. Both Dr. Hasenclever and Dr. Berroir were sure that the new instrument would be of enormous interest to the scientific communities in their respective countries and they were looking forward to the implementation of the new facility at Paranal.

Figure 2: *Discussing the project (from left to right): Prof. H. van der Laan, Director General of ESO; Dr. A. Berroir, Director of CNRS-INSU; Dr. W. Hasenclever, MPG General Secretary, and Prof. M. Tarenghi, VLT Programme Manager.*

Prof. Léna reminded those present of the fact that although the medical science has proven that it is possible to dream a complete dream in just a few seconds, in this case, it has taken European astronomers almost 20 years to realize this particular dream. He congratulated all involved, scientists and engineers, with the excellent preparations, which have finally born fruit. He briefly compared the VLT with other large telescope projects and concluded that it is exactly the great and unique interferometric possibilities which lets ESO's project stand out among the others. As an astronomer, he was looking forward to participate in some of the most important scientific tasks to be undertaken with the VLTI, including the study of proto-planetary systems and the centre of the Milky Way.

The photos from the ceremony were taken by ESO photographer H.-H. Heyer.

The Editor

The VLT Main Structure

M. QUATTRI, ESO

The VLT Programme

During the development of the project the VLT programme was broken down into several subsystems, each of them with clearly identifiable functional requirements and interfaces with the other parts of the project. These subsystems would have lately been contracted to ESO member countries' industrial firms for design and construction. The unit 8-m telescope main structure is one of these subsystems.

The Main Structure

The main structure is a telescope without mirrors and field derotator.

In Figure 1 the items which compose the main structure are indicated. The major components are:

- the telescope steel structure (tube and fork),
- the motors which make it move around the altitude and azimuth axes (drives),
- the angular measurement system which gives the position of the two axes (encoders),
- the supporting system of the telescope (hydrostatic bearings),
- the cooling system used to cool the different power sources placed on the telescope,
- all the equipment which provide safety functions (brakes, locking device to lock the telescope in defined positions for maintenance, emergency stop buttons system),
- the auxiliary systems to monitor the temperature of the steel structure to model the thermal displacements of the attached mirror units,
- the equipment to access the different parts of the structure for maintenance or operations,
- the dummies simulating the inertia characteristics of the mirror units.

The Functional Requirements

Like any instrument of measure, a telescope, once its modes of use are defined according to the scientific needs, must reduce to the minimum acceptable the induced disturbance to the measurements it has to perform.

When the modes of use are different, and imply contradictory requirements, and all of them must be implemented in the same telescope, an accurate evaluation at system level has to be done in order to define the best combination of parameters which characterize the design and which can be clearly specified to a subcontractor, who has to design a part of the complete system without knowing the top level requirements. At the same time, in order to proceed in parallel with the design of the other subsystems, all the interface requirements and boundary conditions have to be defined. This was the job performed at ESO. To derive the functional requirements which would have been specified for the main structure we have started from the following basic requirements:

1. pointing better than 1″
2. tracking better than 0.05″ (both under a wind speed of 18 m/s max. with wind gusts up to 27 m/s)
3. stability of the secondary mirror after chopping of 0.2″ peak to valley with a chopping amplitude of 1′ at 5 Hz and 80 % duty cycle (infrared mode)
4. stability of the Optical Path Distance within 14 nm for an integration time of 10 ms, 50 nm for an integration time of 48 ms and 225 nm for an integration time of 290 ms under a wind speed of 10 m/s (interferometric mode)
5. stability of the position of the altitude and the azimuth axes during the rotation of the telescope
6. stability of the attachment points of the instrumentation during the rotation of the telescope
7. stability of the alignment of the mirror units (primary, secondary and tertiary) within a relative displacement between the mirrors which will not cause a displacement of the image in the Nasmyth focal plane higher than the blind pointing requirement. Because the differential displacement of the mirrors due to the main structure is only one of the contributions to the displacement of the image in the focal plane (others are the deformation inside the mirror units themselves), we required that the contribution of the main structure should not be higher than 0.″3

8. the surfaces of the telescope in contact with the air within ±1 degree C in order to avoid perturbation of the atmosphere surrounding the telescope and consequent seeing deterioration.

Main Structure Specifications

As already described above, the main structure is an electro-mechanical system, and in this sense only electric and mechanical functional requirements, like deflections, eigenfrequencies, weights, wind resistance, motor torque, encoder accuracy, and so on, can be specified and tested on the final product.

The job to derive these parameters kept us busy for quite a long period, during which a large amount of parametric analyses, trade-off among different possible solutions and a lot of conceptual design were carried out.

During this period all the electro-mechanical parameters to specify the main structure were defined, and at the same time a large number of requirements were imposed to all the other subsystems of the VLT.

Since the beginning, and also based on the direct experience we made with the NTT, a few things appeared to be very important to achieve the performance requirements of the VLT:

1. the mechanical structure must be very light, stiff and compact
2. elimination or reduction to the very minimum of all the effects which could have caused disturbance to a smooth motion of the telescope around the axes (for example step-wise motion due to sticking effects coming from the use of ball bearings, or contact between gear-teeth)
3. very good accuracy encoders had to be directly mounted on the axes of the telescope avoiding any gear or friction wheel coupling
4. accurate aerodynamic design of the parts of the main structure exposed to the wind in order to reduce disturbance caused by wind turbulence.

The Preliminary Design

Based on the technical specifications derived as described above, a call for tender was issued to a selected group of companies in the ESO member countries.

After a hard job of selection and analysis of the offers, a consortium of Italian companies was selected. The AES consortium is composed of Ansaldo Componenti (ACO), situated in Genova, European Industrial Engineering (EIE), situated in Venice, and SOIMI, situated in Milan.

On 23 September 1991 the contract was signed. After about 1 year the preliminary design (Figs. 2 and 3) was completed, and the Preliminary Design Review (PDR) was carried out in Venice by an ESO team which included about 15 people to cover all the technical aspects of the project, and two well-known external telescope experts, Pierre Bely of the Space Telescope Institute and Torben Andersen of the Nordic Telescope Group.

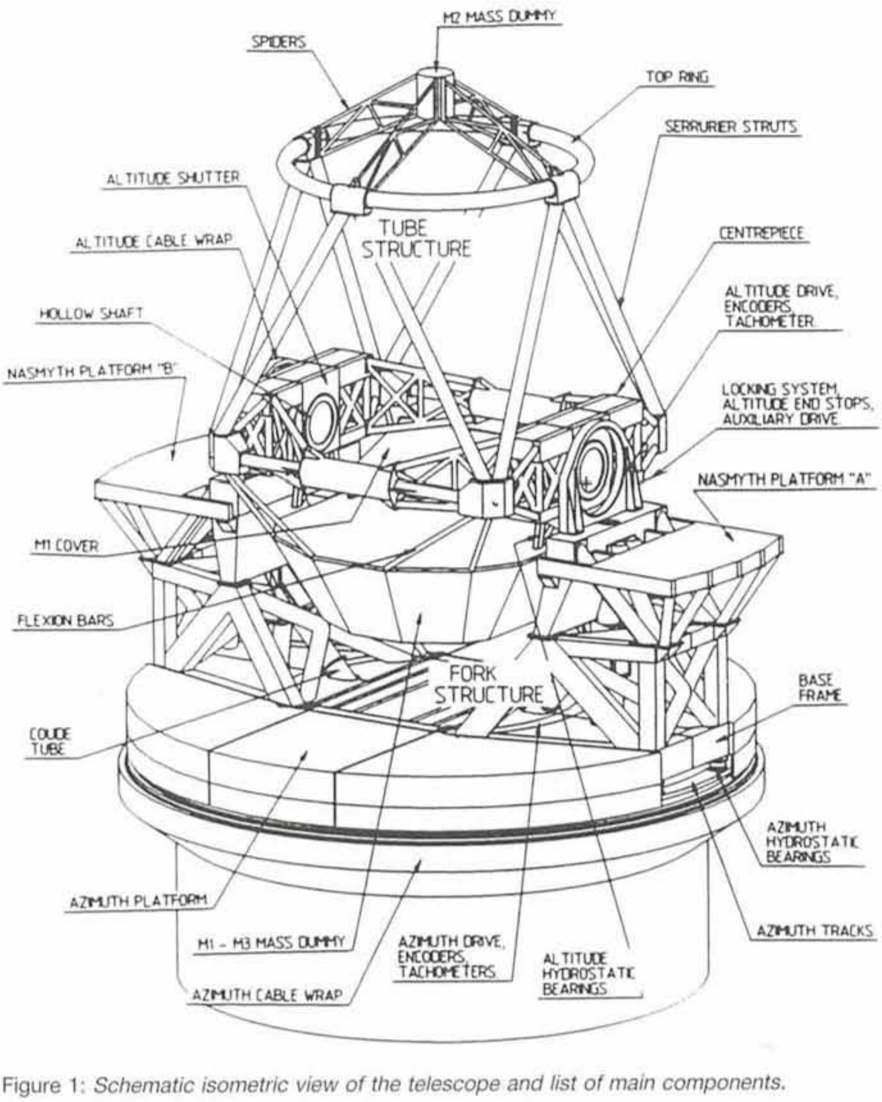

Figure 1: *Schematic isometric view of the telescope and list of main components.*

Riccardo Giacconi Receives High NASA Honour

Professor Riccardo Giacconi, Director General of ESO since the beginning of this year and before then Director of the Space Telescope Science Institute in Baltimore, U.S.A., has just been awarded the "NASA Distinguished Public Service Medal".

The Director of NASA, Mr. John M. Klineberg, has conveyed his personal congratulations to Prof. Giacconi, informing at the same time that this medal is given only to individuals whose distinguished accomplishments contributed substantially to the NASA mission. Moreover, the contribution must be so extraordinary that other forms of recognition by NASA would be inadequate. It is the highest honour that NASA confers to a non-government individual.

All of us at ESO heartily congratulate Prof. Giacconi to this unique distinction, so rightly deserved through many years of hard work to the benefit of astronomers on all continents.

The Editor

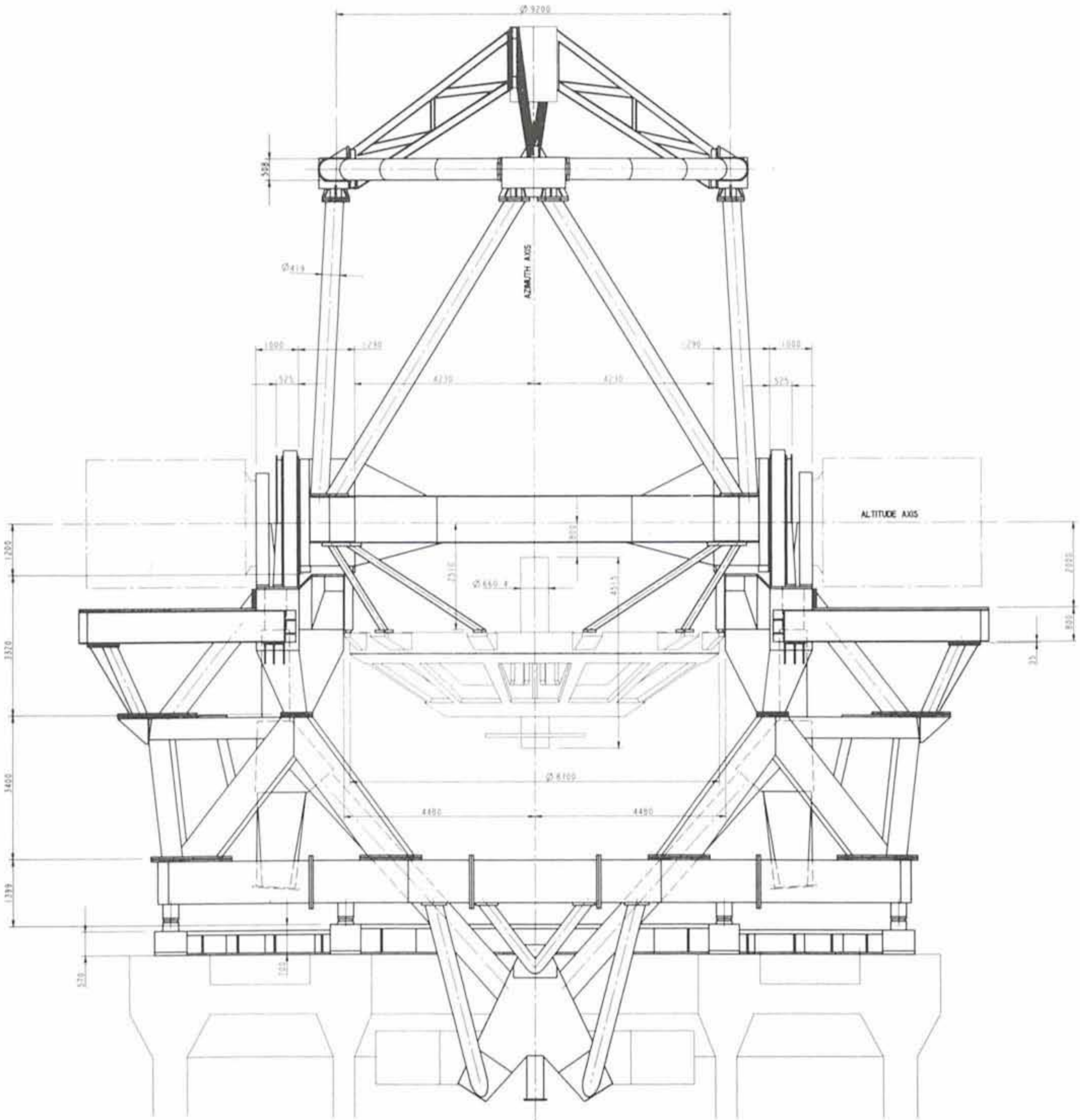

Figure 2: *Front and side view of the preliminary design of the main structure.*

The main features of AES' design are:

1. segmented direct drives on both altitude (about 3 m diameter) and azimuth axes (about 10 m diameter)
2. thrust and centring hydrostatic bearings on both axes
3. double azimuth bearing tracks
4. direct mounted optical encoders on both altitude (about 2.6 m diameter) and azimuth (about 10 m diameter). At the moment both classical graduated steel tape with optical reader heads and laser encoders, based on light phase shift measurement, are being investigated. The aim is to determine which solution fulfills at the best the stringent accuracy requirement of 0.1″ RMS
5. the steel structure makes use of aerodynamically optimized structural profiles, even though some more optimization is needed, and is a trusses structure that realizes the best ratio stiffness/weight for these dimensions of the order of 20 m.
6. the cable wraps are motorized in order not to introduce friction in the telescope,
7. no rotating machinery, like pumps or fans, are installed on the structure, in order to avoid the introduction of vibrations.

The weight of the rotating mass is about 400 t (including the weigths of the mirror units), the lowest eigenfrequency, indicative of the stiffness of the structure, is about 8 Hz. For the sake of comparison, the ESO 3.6-m telescope has a lowest eigenfrequency of 1.4 Hz and weighs about 300 t, the NTT has the lowest eigenfrequency of about 9 Hz and weighs 120 t.

The Next Steps

Since the completion of the PDR the final design phase has been started during which the final optimizations of the design and all the tests needed to validate the adopted solutions will be performed.

At the end a Final Design Review, at the moment foreseen at the end of September 1993, will assess the results of this phase and will give the start to the phase of fabrication.

The first main structure will then be assembled in Milan starting from the end of 1994, and tested for six months by ESO, starting beginning July 1995 till the end of December 1995, with the option to continue till the end of March 1996.

At the same time, after the preliminary acceptance of the first main structure, the second main structure will be erected in Chile, and in April 1996 the provisional acceptance will take place.

Then at the rhythm of one about every 6 months, the other three main structures will be ready for provisional acceptance and for starting the integration of the other VLT subsystems. The last structure will be ready in April 1998.

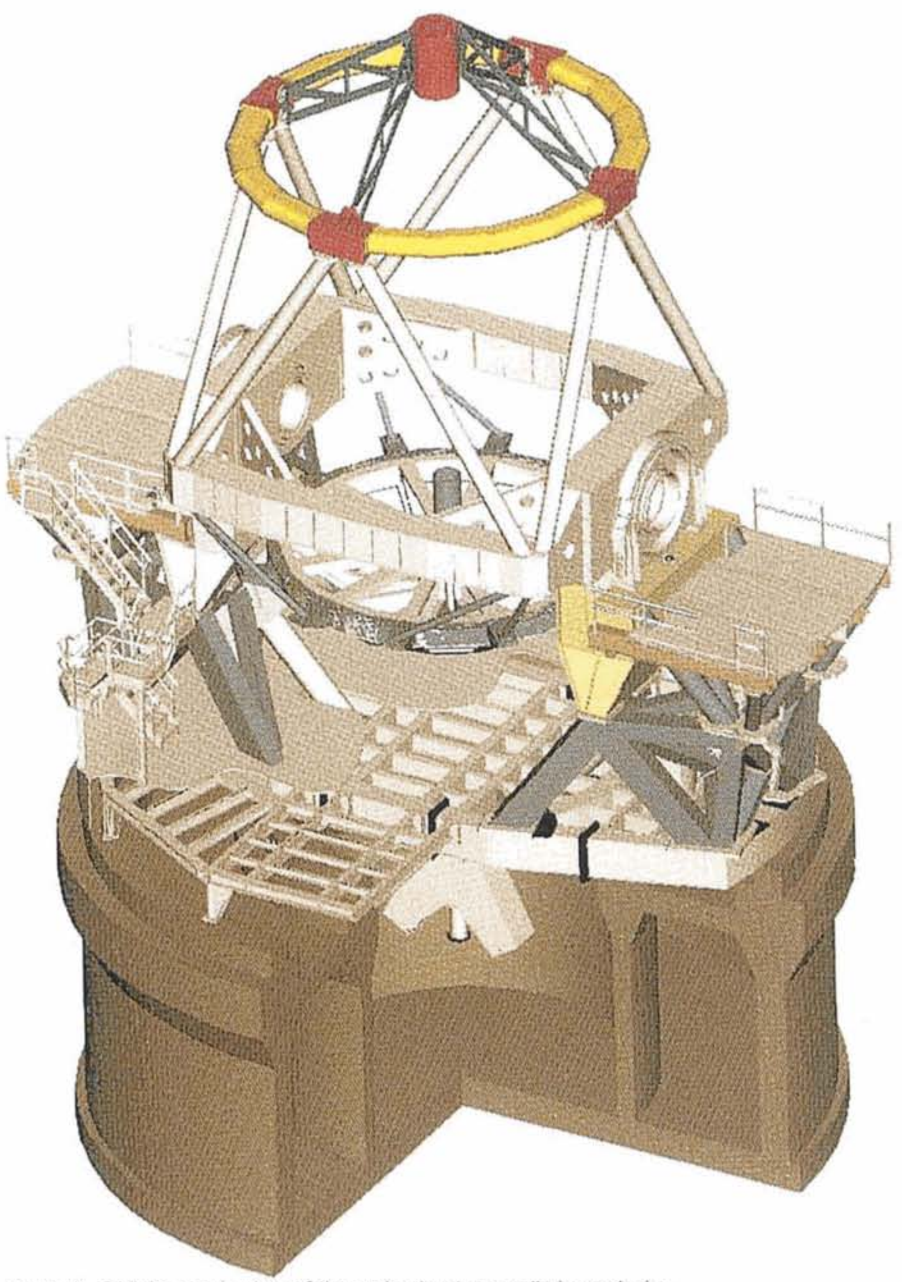

Figure 3: *CAD isometric view of the main structure preliminary design.*

All Those Who Contributed

A job like the one described above requires the close collaboration of many people with very different competences, and, most of the time, supporting requirements in contrast to each other. Moreover, in the case of the companies involved, most of the time the economical constraints require a large amount of continuous exchange of information without which it would not be possible to achieve any of the results foreseen.

For this reason I would like to mention here all those who have contributed to the definition and design of the main structure: E. Brunetto and M. Kraus, who found solutions to many difficult problems, F. Koch, who supported the definition of many requirements with large and complex F.E.M. calculations, L. Zago, who supported the aerodynamic design, M. Schneermann, who was responsible for the first definition of the basic requirements, M. Ravensbergen, responsible for the electric and control design and tracking performance of the main structure, F. Ploetz, who performed the first assessment of the tracking performance, D. Enard, who has been, since ever, the engineering team leader of the VLT. A special mention deserve the engineering teams of Ansaldo, EIE and SOIMI, who have to struggle daily to design, according to the requirements and within budget, the VLT main structure.

Manufacturing of the 8.2-m Zerodur Blanks for the VLT Primary Mirrors – a Progress Report

P. DIERICKX, ESO

The manufacturing of the Zerodur glass-ceramics blanks for the VLT primary mirrors was contracted by ESO to SCHOTT Glaswerke Mainz in 1988. Since then, spectacular progress has been achieved, and the first blank is due to delivery and transport to the plant of the optical manufacturer [REOSC] by August 1993.

The erection of the VLT blanks production facility in Mainz started on July 6, 1989. Seventeen months later, 45 tons of liquid glass were cast in an 8.6-m mold for the first time. Given the difficulty and size of the problem, this

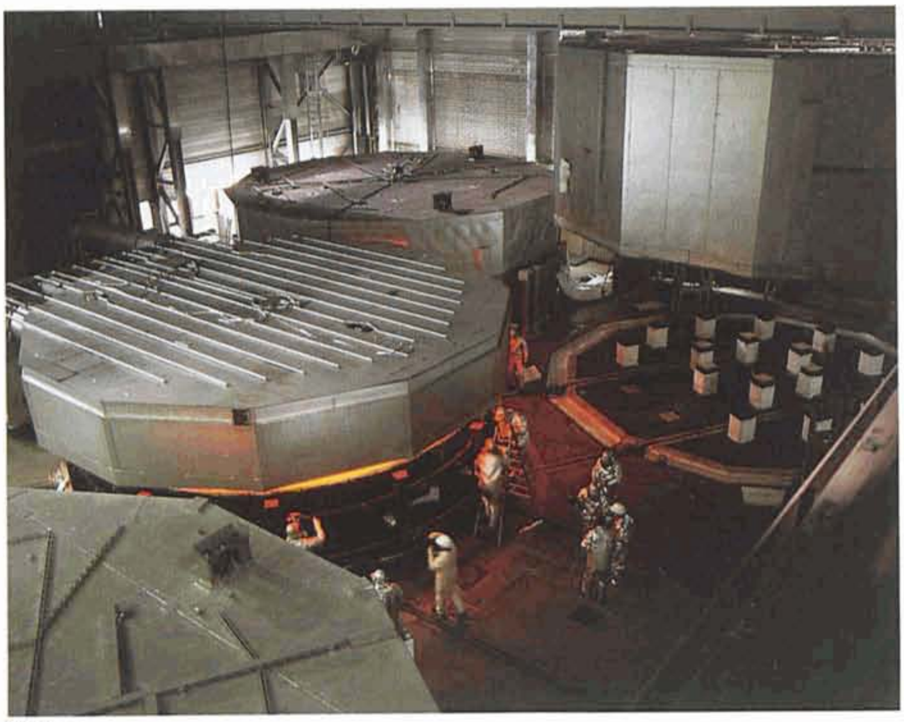

Figure 1.

has undoubtedly been a fantastic achievement.

However, manufacturing an 8-m-class Zerodur blank is a fairly delicate task, which eventually requires full-scale tests, even after validating the spin-cast technology up to the 4-m range. The key issue is that a crystalline layer inevitably builds up at the bottom and outer edges of the blank, where the liquid glass comes into contact with the insulating material of the mold. This crystalline layer has a different coefficient of thermal expansion than the glassy Zerodur, stresses build up during the cooling phase and may eventually lead to an overall breakage. By a proper selection of the insulating material and, to a lesser extent by an accurate thermal control of the casting process, the thickness of the crystalline layer may be reduced. With the first castings, the layer was a few millimetres thick, a figure that has now been brought down to about 0.2 mm. According to an analysis made on the first castings, the homogeneity of the material is exceptionally high.

The manufacturing process includes the following major steps:

1. casting, which lasts several hours;
2. annealing: the blank is cooled down and annealed in a dedicated furnace (about 4 months);
3. machining of both concave and convex sides;
4. ceramization (about 8 months);
5. drilling of the central hole;
6. fine annealing;
7. fine machining.

Probably the most critical operation, apart from the annealing, is the handling of a mirror blank when it comes out of its first annealing cycle. At this stage the crystalline layer is still partially adhering to the blank, which is therefore extremely fragile. While the blank is being transported and turned upside down onto the grinding machine, chips of glass are falling from the convex side. The noise is almost imperceptible...and definitely frightening. In order to provide the smoothest possible handling conditions, SCHOTT designed and built an 18-cup vacuum lifter, which performed remarkably well.

With the last upgrade of the insulating material, the convex surface is very smooth and there are no longer chips of glass to gather for decoration of one's desk.

The zero-expansion property of Zerodur is achieved after the ceramization cycle. Following very successful results obtained with 4-m-class prototypes, it has been tried to skip the annealing cycle, i.e. directly ceramize the blank after casting. The trial was unfortunately not successful.

During ceramization the active mold follows the shrinkage of the material, in order to ensure a proper distribution of the weight of the blank onto its support. By the time this article is published, the first ceramized Zerodur blank should come out of the furnace. After final machining it will have a mass of about 23 metric tons.

For the time being there are 5 blanks in the production line. The pictures shown here were taken upon the last casting early February 1993. After casting, the mold is transported from below the melting tank onto a rotating platform where it is spun for about one hour, after that the cover of the mold was lifted a few centimetres. The temperature of the liquid glass is about 1300 C. It solidifies fairly rapidly. After spinning, the cover is removed and a cooling cover is brought over the mold (Fig. 1). The few minutes where the glass is uncovered are just enough to understand what is thermal

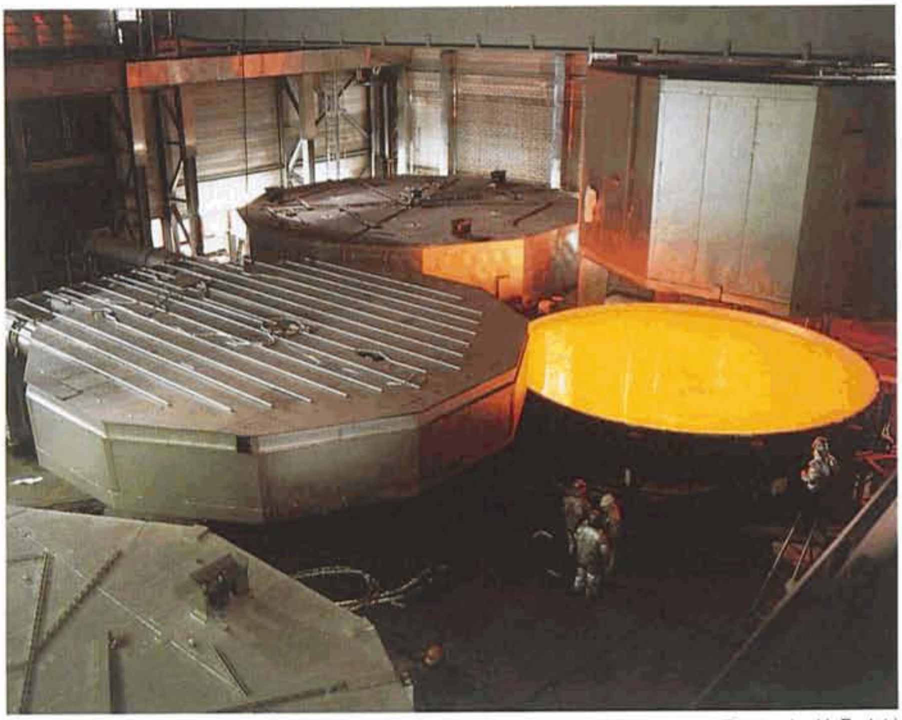

Figure 2.

(Photos by H. Zodet.)

radiation. Once the glass has cooled down to about 800 – 900 C, the mold is brought into the annealing furnace (Fig. 2) where it will stay for several months.

There will be one more casting, the goal for SCHOTT being to manufacture a total of 6 blanks, four of which will be delivered to ESO and the two others will wait for potential customers. At the latest in July the melting tank which has been in continuous operation since 1990 will be shut down.

Glass making is a very specialized field, which combines tradition, dedicated experience and modern technologies. Making 8-m-class blanks is a fascinating achievement. Moreover, other fascinating achievements are still to come, with the work of the polishing tools.

Seeing at Paranal: Mapping the VLT Observatory

M. SARAZIN, ESO-Garching, and J. NAVARRETE, ESO-Paranal

Modifying the shape of a summit after it was chosen for its outstanding qualities in optical turbulence raised justified concerns in the community about possible perturbations of the local flow pattern and their possible negative effect on the astronomical seeing. Numerical simulations had been performed at RISOE, Denmark, for various input wind conditions predicting neglectable effects at the northern and southern edge of the new 25,000 square metre telescope area. It was nevertheless not without some apprehension that we pushed the "start" key of the seeing monitor, now located on the newly formed VLT platform, on November 29, 1992.

The VLT observatory was greeting its first pieces of optics with the impressive sight of perfect flatness only broken by four huge holes giving the scale of the future observatory (Fig. 1). The Differential Image Motion seeing monitor which was used that night (DIMM1) was incidentally the same as the one started in April 1987, on the same summit, then 28 m higher when the seeing survey was initiated. During this survey, the 35-cm diameter Cassegrain telescopes were operated on concrete platforms at 5 m above ground. This was considered a lower height limit for the position of the primary mirror of modern telescopes.

Because of manpower shortage, it was unfortunately impossible for the VLT civil engineering department to design, for the new measurements, a tower which could be easily removed during the VLT erection phase. The DIMM1 telescope was thus installed on a 1 m high platform convenient to protect the optics from local dust. This was however not high enough to escape thermal turbulence in the surface layer,

Figure 1: *Location of the seeing monitoring stations in the new VLT telescope area.*

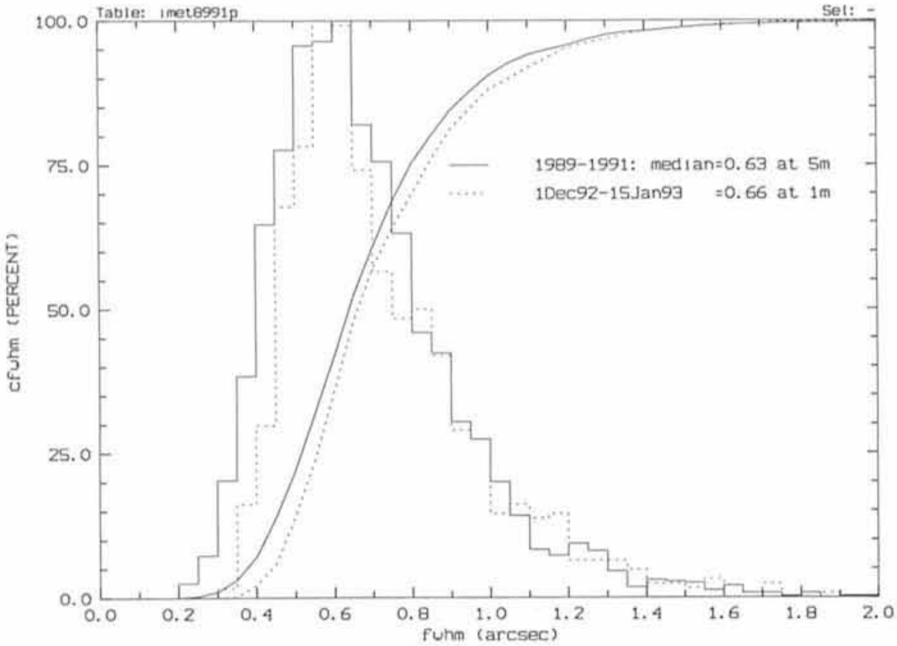

Figure 2: *Statistics of seeing measurements before and after summit levelling. Seeing is computed for equivalent 20-min exposures obtained at 0.5 μm at zenith with a perfect large telescope.*

inducing an artificial increase of local seeing particularly sensitive in extremely good overall conditions.

Such local effects are illustrated in Figure 2, comparing one and a half month of measurements at the northern edge of the telescope area with the statistics available for the Paranal peak until the disruption of measurements in July 1991. While the upper tail of the probability distribution (seeing is computed for equivalent 20-min exposures at 0.5 μm at zenith) is virtually unchanged, the five percentile increases from 0.37 arcsec at 5 m above ground to 0.44 arcsec at 1 m above ground.

Another identical system (DIMM3) was used in the same conditions as DIMM1 to monitor the southern edge of the telescope area. One month of common data summarized in Figure 3 did not permit to detect any permanent differential effect related to the position with respect to the incident wind flow. The spread of the regression is however linked to a sporadic increase of local turbulence at either location, the strongest events taking place at low (< 2 m/s) wind speed.

With a median seeing of 0.66 arcsec at 1 m above ground, Paranal has clearly survived the blasting. More seeing observations will be made at 5 m height on a tower currently under design at the Observatory of Capodimonte, Italy. Strange as it appears, the next threat for site quality will be the VLT itself. This is why great care is taken in the design of the observatory to avoid heat and cold sources both inside and outside the enclosures.

We thank the VLT Site and Buildings Group for providing the infrastructure at Paranal. The monitors are operated by the Paranal Meteorology team composed of F. Gomez, D. Mazat and A. Vargas.

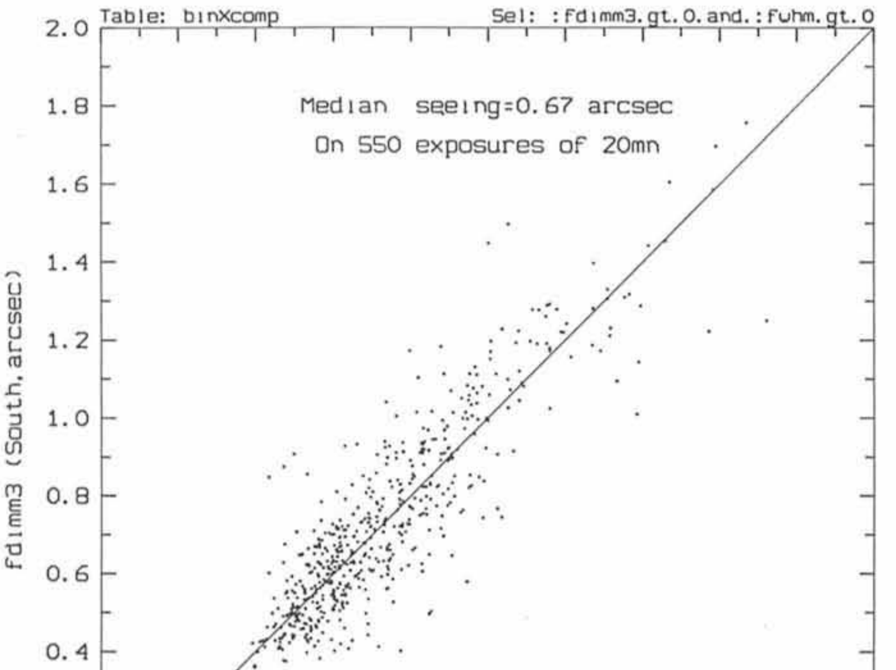

Figure 3: *Comparison of seeing measurements made at the southern and northern edges of the telescope area.*

Tentative Time-table of Council Sessions and Committee Meetings in 1993

March 30	Finance Committee
April 1	Council
May 3–4	Users Committee
May 6–7	Scientific Technical Committee
May 10–11	Finance Committee
May 27–28	Observing Programmes Committee, Copenhagen
June 1–2	Council
November 4–5	Scientific Technical Committee
November 8–9	Finance Committee
November 25–26	Observing Programmes Committee
December 1–2	Council

All meetings will take place in Garching, unless stated otherwise.

The ESO Historical Archives (EHA)

INVENTORY PER DECEMBER 1992

A. BLAAUW

Historical archives provide us with the beacons along which historians steer their stories about the past. When I wrote my articles on the history of ESO for *The Messenger* and the book "ESO's Early History", I was guided by a small, but very valuable collection of documents pertaining to the years of ESO's beginning. They originated from people who had been intimately involved in the creation of ESO (J.H. Oort, O. Heckmann, J.H. Bannier and myself) and had been transferred to ESO as a nucleus for its Historical Archives; a nucleus to be cherished and, hopefully, to be extended in the years to come. Most of the documents dated from before 1975. Subsequently some more recent items were incorporated, however only on the basis of provisional classification; their incorporation should be subject to future scrutiny.

Naturally, these archives are useful only if there is a guide to tell the student what is available and where it may be found. Such a guide is now provided in my booklet "ESO's Historical Archives (EHA); Inventory per December 1992" that appeared in December 1992. In it, the documents (letters, circular letters, maps, etc.) have been ordered in a system that takes into account the origin of the document and subsequently classifies it into categories and subcategories. For instance, item I.C.2.3.a refers to a report on a meeting of the Working Group for site tests in South Africa of January 1958, and in this case the first, roman classification number, I, tells that this document belongs to one of the collections originating from outside ESO; the letter C means that it belonged to the collection contributed by myself; the next number, 2, refers to the subdivision dealing with the early site testing; and the subsequent number, 3, to the folder containing some test reports. The system was used in my historical accounts mentioned before.

For the moment, the booklet is primarily meant as an internal ESO publication and therefore has been distributed outside ESO on a limited scale only, among some historians of astronomy or astronomers known to have a strong historical interest. A wider distribution may be considered at a later stage.

The Collection is in the care of ESO's Librarian at the Garching Headquarters. The documents are stored in cardboard boxes in a special room where it is supervised by the Librarian, and access may be requested through her. As some of the correspondence in the archives still is of a confidential nature, not everything is accessible yet.

Access to the ESO Historical Archives

The ESO Historical Archives described here, are accessible to outside professional researchers by special permission only. Note, however, that the Archive is still in the process of being supplemented with new materials from different sources and that certain, more recent parts are not yet released for general use.

For more information, please contact:

Uta Michold
ESO Library
Karl-Schwarzschild-Straße 2
D-W-8046 Garching
Germany

The ESO C&EE Programme Begins

The ESO programme to support astronomers in Central and Eastern European countries, also known as the ESO C&EE Programme, was adopted by the ESO Council in its meeting in December 1992, cf. *The Messenger* **70**, p. 8 (December 1992).

By this important action, the ESO Council recognizes the great potential of astronomy and astrophysics in the C&EE countries and the need to ensure its continuation during the present transitional period. The Programme will begin in early 1993 and have an initial duration of 3 years. It will be carried out within the financial frame stipulated by the ESO Council, and will be administered with a minimum of bureaucracy.

The details of the Programme were worked out during the month of January and a document, from now on referred to as the "Application Document", was produced. It contains all details about how to apply, the general conditions of the Programme, and the standardized application forms and was sent to about 1000 addresses at the end of January 1993. This included more than 700 astronomers, most of which are IAU members, in the C&EE countries and all major astronomical institutes in the ESO member states. Additional copies of the Application Document may be obtained by request at the address listed below. Judging from the number of inquieries received since then, the interest is intensive and by early March quite a few applications had already been received at ESO.

A guiding principle of the ESO C&EE Programme is that *support will be provided on the basis of scientific and technical merit.* It is the aim to *help C&EE astronomers to continue to do good research at their home institutes,* thus contributing to the maintenance of the scientific level and, thereby, to the survival of C&EE astronomy, and also *to provide potential benefits to astronomy in ESO member states.*

The Programme initially encompasses a number of well-defined subprogrammes, with the following titles and definitions (all further details are available in the Applications Document):

A. ESO C&EE Scientific and Technical Programmes: support of a well-specified and/or technical Programme within astronomy and astrophysics, to be carried out at one or more C&EE institutes/observatories;

B. ESO C&EE Fellows: support of individual C&EE astronomers to perform specific research programmes in astronomy or astrophysics;

C. ESO Visiting Astronomers: support of individual astronomers from ESO members states to visit C&EE institutes;

D. Participation in ESO Conferences: support of participation of C&EE astronomers in conferences organized or sponsored by ESO;

E. Exchange of Software: support of travels by C&EE astronomers to institutes/observatories in ESO member states in order to exchange software, install software systems, etc.; and

F. ESO Publications: free copies of ESO publications to C&EE institutes.

These subprogrammes are not necessarily exhaustive; they may be adjusted and others may be added, if and when other suitable modes are identified.

The first deadline for receipt of applications at the ESO Headquarters in Garching has been fixed as *15 April 1993* and the next ones will follow at three-month intervals. All applications which are received in time will be scrutinized by a special ESO C&EE Committee, composed of a small number of astronomers from in- and outside the Organization. The outcome will be announced to the applicants immediately thereafter, in most cases within one month after the deadline.

All correspondence related to this Programme shall be directed to: ESO C&EE Programme, Karl-Schwarzschild-Str. 2, D-8046 Garching bei München, Germany (Tel.: +49-89-320060; Fax: +49-89-3202362; Tlx.: 528 282 0 eo d).

It is expected that the next issue of *The Messenger* will contain an overview of the initial experience and include a list of the first support allocations.

R.M. WEST, ESO

Availability of Schmidt Plate Emulsions

On January 18, 1993, a malfunction in a compressor combined with problems in the safety system caused overheating in the cold storage plate vault outside the Schmidt building and the unexposed plates kept there were destroyed. Already exposed plates are kept in the Schmidt building itself and were not affected. Most of the plates lost were old and were used only for focus determinations and other tests. Unfortunately, our latest shipment of plates from Kodak had recently arrived and been stored, and they were lost, thus jeopardizing the scientific work at the Schmidt telescope.

To everybody's relief, Kodak was able to deliver IIIa-J, IIIa-F and IV-N plates with only four weeks' delivery time. For IIa-O, 098-04 and 103a-D emulsions, Kodak presently has problems with manufacture, and they will not be available until the end of the year. Instead of the IIa-O plates, which are the most commonly used at the Schmidt, we are looking into purchasing plates with the very similar ZU-21 emulsion from the German company ORWO. With the stock of plates that were kept in the freezers in the Schmidt building we are able to carry on with the Schmidt operations until the new plates arrive, and there will therfore be only a minor impact on the majority of programmes carried out at the Schmidt telescope.

Work is planned to begin later this year on a new plateholder that will accept emulsions on film rather than on glass. Apart from very substantial savings in operational costs, this means that programmes which are not aimed at astrometric work can benefit from new highly sensitive and fine-grained emulsions like the Kodak 4415 emulsion. Programmes that require glass plates will of course be carried out as always. After we have gained experience with this new facility, an announcement of availability will be made here in *The Messenger*.

BO REIPURTH, ESO-La Silla

Physical Study of Trojan Asteroids: a Photometric Survey

M. DI MARTINO[1], M. GONANO-BEURER[2], S. MOTTOLA[2], G. NEUKUM[2]

[1]Osservatorio Astronomico di Torino, Pino Torinese, Italy

[2]DLR German Aerospace Research Establishment, Oberpfaffenhofen, Germany

Introduction

Since their formation in the solar nebula, asteroids belonging to the main belt have been altered mainly by mutual collisions, which take place at typical impact velocities of about 5 kilometres per second. The projectile-to-target mass ratios quite frequently reach values of the order of 10^{-3}, which can produce that catastrophic fragmentation of the target asteroid. According to many investigators, this ongoing collisional process has had a number of important consequences, ranging from the formation of dynamical families and dust bands to the insertion of meteroids and Aten-Apollo-Amor objects into planet-crossing orbits and to the generation of a variety of peculiar collisional outcomes (for example, "rubble pile", asteroids, binaries, "naked" metallic cores).

One of the main motivations for studying asteroids is that they are believed to be more "primitive" than planets, i.e. closer in size, composition, and other physical properties to the population of planetesimals from which the planets accreted. It is then natural to wonder which properties are just products of collisions and which ones in some way "remember" the primordial state, when disruptive impacts did not occur and planetesimals, in the asteroid belt as well as in other zones of the solar nebula, were gradually accumulating into planetary embryos.

Were it possible to quantitatively model the subsequent collisional evolution of

Figure 1: *The DLR CCD camera installed at the ESO 1-m telescope.*

asteroids, one could in principle reconstruct from the current asteroid properties (e.g. size distribution, relative velocities, rotations, shapes) those of planetesimals, and thus constrain the theories of planetary formation. This task is very complex and uncertain. We still know too little about the properties of asteroidal material and about the way solid bodies respond to catastrophic impacts at sizes 10^6 times larger than those observable in the laboratory. An alternative approach is that of looking in the asteroid population for subsets of objects for which we have reason to believe that the collisional process has been less intense and less effective than the average. This is just the case for Trojan, Hilda and Cybele asteroid groups (objects whose orbits have a semimajor axis larger than 3.3 AU), which hold considerable interest as they are likely to represent a set of relatively primitive bodies which may have experienced little thermal and collisional evolution since the time of their formation.

The dynamical scenario of the outer belt is strongly influenced by the gravitational interaction with Jupiter. With a few exceptions, the outer belt asteroids (OBA) have orbits which are either in resonance with the giant planet or are confined between two different resonances. The Cybeles are located between the 2:1 and 5:3 resonances with Jupiter (mean semi-major axis a = 3.4 AU), the Hildas are found at the 3:2 resonance (a = 4.0 AU) and the Trojans are trapped in the L4 and L5 Lagrangian points of Jupiter's orbit at a = 5.2 AU. 279 Thule is the sole object known to occupy the 4:3 resonance. There, both the number density of asteroids and their relative velocities are significantly lower than in the main belt. Therefore, these bodies should show a lesser degree of collisional alteration, and could allow us to look farther and more clearly into the primordial properties of planetesimals. At the same time, any differences in physical properties with respect to the main belt might provide evidence on the way collisions are currently causing the asteroids to evolve away from their primordial state.

Most of the OBA bear evidences of redder and darker surfaces when compared with the main belt asteroids and their spectra show a reddening in the spectral slope with increasing heliocentric distance, which implies a change in composition. The major taxonomic types among the distant asteroids are quite rare in the main belt and are currently unrepresented in terrestrial meteorite collections. The investigations of the physical properties of the OBA, and the subsequent understanding of their nature and origin, will have a direct implication for any theoretical study on the evolution of the solar system.

Rotational Properties of Outer Belt Asteroids

Some important physical properties of the asteroids can be inferred from lightcurve observations. These include the rotational period and, through some modelling effort and/or by using simplifying assumptions, the overall shape of the body and the direction of its polar axis. Statistical analyses of these rotational properties have been carried out and have revealed a complex scenario, where collisions do indeed appear to have played a dominant role (see Binzel et al. 1989).

The lack of photometric information about OBA is due to their great heliocentric distance and their corresponding faintness, nevertheless the advances in astronomical detector technology have brought the most of the OBA at reach of the small- and medium-sized telescopes, allowing American and European groups to carry out observations to study these faint objects (French, 1987; Hartmann et al., 1988; Zappalá et al., 1989; Binzel and Sauter, 1992). The first results of these studies

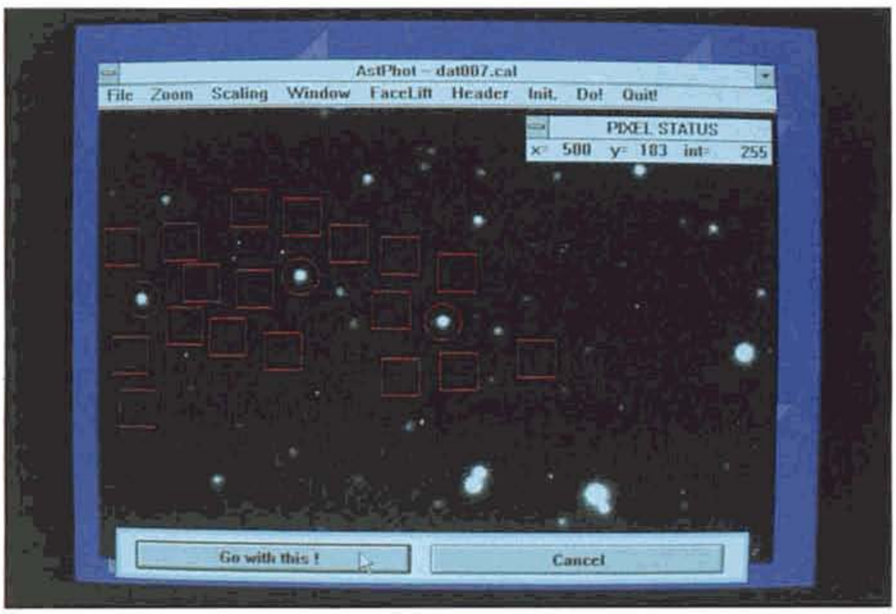

Figure 2: *This picture shows a session of the photometric reduction package in use at DLR. The circles define the integration area for the asteroid and the comparison stars. The sky background is sampled in the areas delimited by the square boxes.*

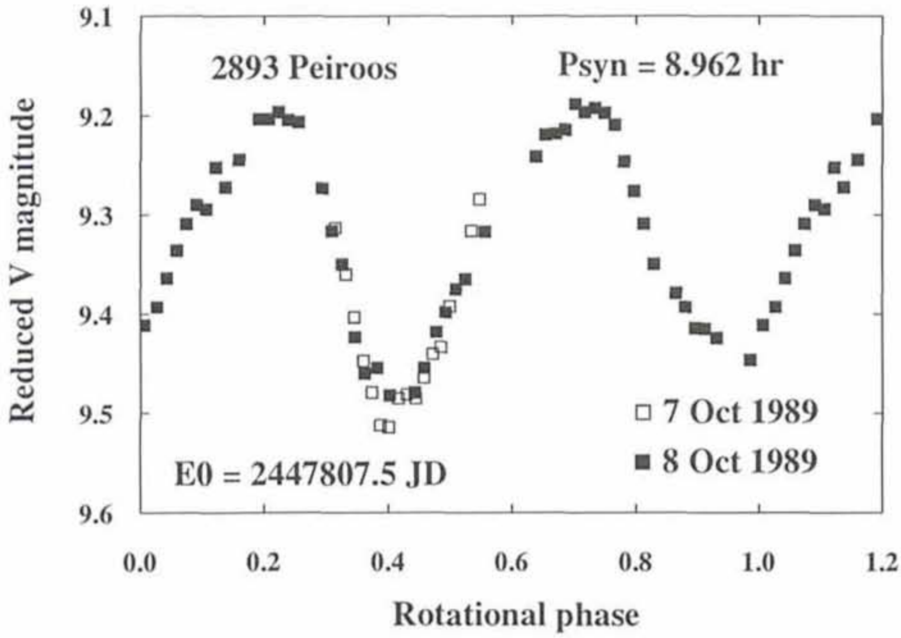

Figure 3: *Photometric measurements, extracted from repetitive imaging as shown in Figure 2, are used to determine the rotational lightcurve of the asteroid. From measurements of October 1989, we obtained this composite V-lightcurve for 2893 Peiroos. The data points beyond the rotational phase 1.0 are repeated.*

have outlined an interesting trend: the Trojan asteroids, and possibly the asteroids belonging to the Hilda group, would display larger average lightcurve amplitudes compared to those of the main belt asteroids (MBA), implying a more elongated shape. At this stage, however, it is not clear whether the high lightcurve amplitude is a common feature among the Trojans, or whether it is due to the presence in the amplitude distribution of a tail of very few, very high amplitude asteroids (Hartmann and Tholen, 1990).

Should the collisional evolution of the MBA be significantly different from that of the OBA, we would also expect to observe differences in their rotational rate distribution. In the main belt for example, Binzel et al. (1989) found that the rotational period distribution of the asteroids in the size range 50–125 km can be fitted with a linear combination of two different Maxwellians, this fact being interpreted as the evidence of the coexistence of two families of rotators at a different stage of collisional evolution. At present, however, it is impossible to perform such an analysis on the rotational rates of the Trojans with sufficient level of reliability, owing to the poor data set available.

The Survey

To contribute to establish a statistically representative sample of the rotational properties of the OBA, we started in 1988 a systematic survey to collect photometric lightcurves of the asteroids belonging to the Trojan, Hilda and Cybele groups, which is still on-going (Mottola et al., 1990; Gonano et al., 1991; Di Martino et al., 1992).

Most of our observations were carried out at the ESO 1-m telescope using the DLR CCD Camera, an easily transportable system, that we have optimized both in the hardware and in the software for the application in this field of research. In Figure 1 the DLR CCD Camera installed at the ESO 1-m telescope is shown. The DLR CCD Camera was manufactured by Photometrics Ltd. (USA), it utilizes a Thomson TH-7882 charge-coupled device and is controlled by a 486 PC.

A CCD sensor presents several advantages in dealing with some of the peculiar experimental difficulties in asteroid observations. The determination of the rotational properties implies to observe the asteroid continuously and for long runs. For this reason it is often necessary to observe at high values of airmass or during dawn or dusk. The imaging capabilities of the detector allow to perform differential photometry with comparison stars present in the field, making it possible to have an accurate extinction correction and sky background subtraction even under these critical conditions. The two-dimensional information provided by the array is also essential to overcome the problems of performing an accurate photometry when the asteroid crosses crowded stellar fields and relaxes the constraints on tracking. Furthermore the high quantum efficiency, the linearity of the solid state detector and its low read-out noise are necessary conditions to obtain the required photometric accuracy to detect features in the lightcurves, which have sometimes an amplitude of only a few hundredths of a magnitude.

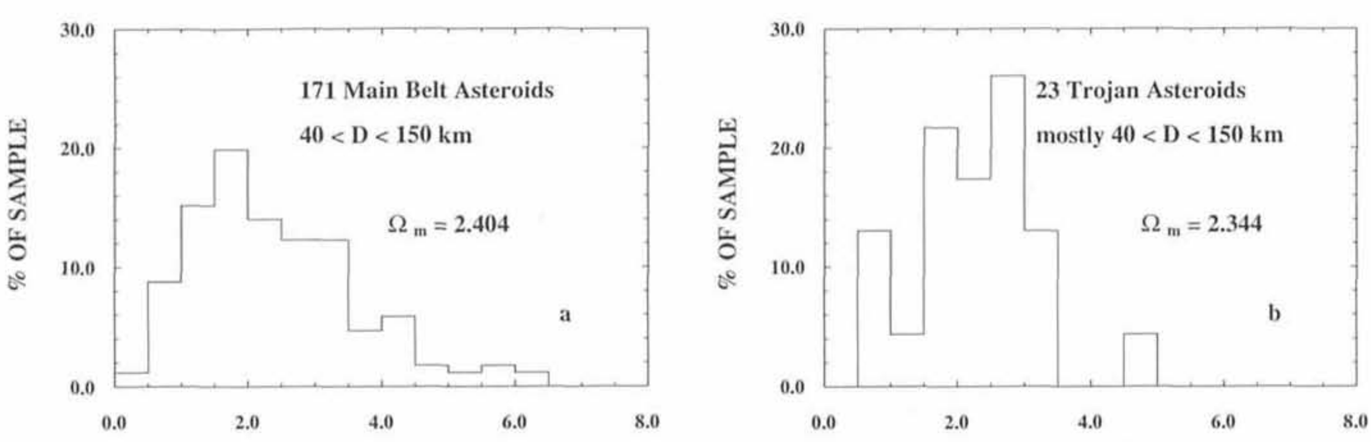

Figure 4: *(a) Histogram of the rotation rates for a sample of main belt asteroids, where the range of 0 to 8 revolutions/day has been divided into 16 equal bins. (b) The same as (a) but for the Trojan asteroids with known rotational period.*

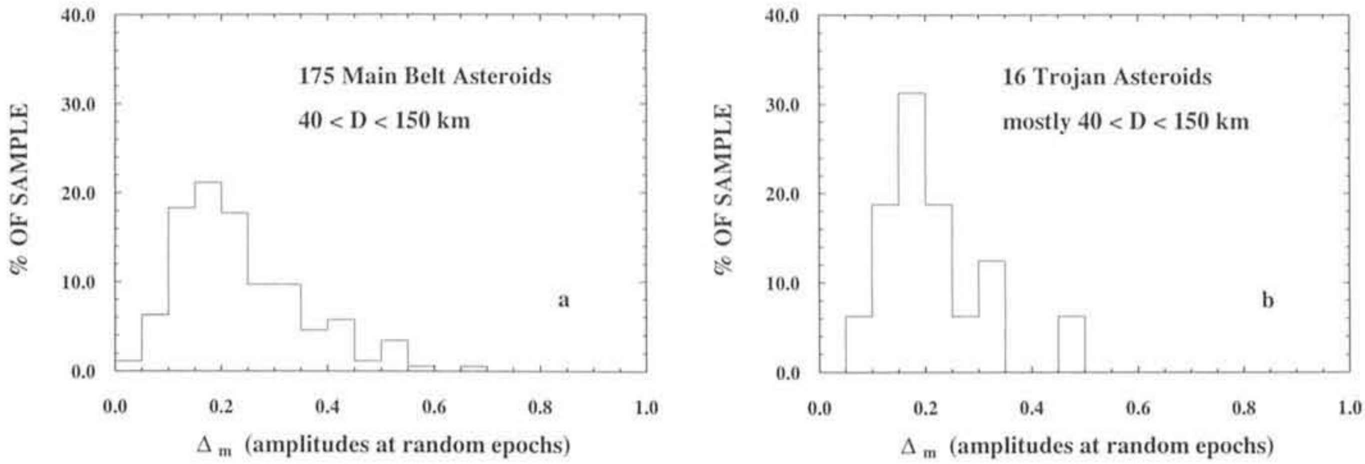

Figure 5: *(a) Histogram of the lightcurve amplitudes for a sample of main belt asteroids. (b) The same as (a) for the Trojan asteroids observed during the survey.*

Since the good time-sampling is essential to compute reliable amplitudes and rotational periods from the lightcurves, the manual intervention (and hence the occurrence of mistakes) during the operation of the camera at the telescope has been reduced. The entire acquisition sequence is preprogrammed and played back by the camera computer. This automatic sequence includes the filter positioning, the exposure timing, the display and storage of the scientific frames, and the flagging of the saturated pixels. Some of the operations are performed concurrently (e.g. image exposure and storage of the previous frame). The dead times between two exposures are then significantly reduced, limited in some cases only by the readout time of the CCD.

The data reduction is performed in the camera computer using the software package for CCD image processing developed at DLR. This allows us to perform the complete reduction of the data during daytime after each observing night, to optimize the sharing of the telescope time between the different targets, preserving the good sampling and the completeness of the lightcurve coverage. The instrumental fluxes of the asteroid and of the comparison stars present in the frame are evaluated applying a synthetic aperture photometry procedure (see Fig. 2). The "light growth curve" method (Howell, 1989) is used to determine the best aperture size and the background level.

Composites are derived combining the single lightcurves by using a Fourier fitting procedure (Harris et al., 1989). The order of the Fourier polynomials is chosen according to the temporal sampling of the lightcurves. The best-fit polynomial is then evaluated for the different trial periods and the solution is determined by comparing the residuals of the different fits. As an example of the final output, in Figure 3 we show the composite obtained from our lightcurves for the Trojan asteroid 2893 Peiroos.

Preliminary Results of the Survey

We have compared the distributions of the rotational periods and the lightcurve amplitudes of Trojan asteroids with the distributions of a selected sample of main belt asteroids. As a reference group we chose a sample of main belt asteroids in the diameter range 40–150 km from the Asteroid Photometric Catalogue (Lagerkvist et al., 1989). Particular care has been devoted to the selection of the reference sample, in order to limit the incidence of the observational bias present in the catalogue (see discussion in Binzel et al. 1989).

The sample of Trojan asteroids we used for the analysis of the rotational period distribution is based on the present results of our observational survey and also includes several objects observed by French (1987), Hartmann et al. (1988), Zappalà et al. (1989), Hartmann and Tholen (1990), Binzel and Sauter (1992) and by others. Figures 4 a and b show the histogram of the rotational frequencies of a reference group of 171 main belt asteroids and that of 23 Trojans, respectively. By applying the Kolmogorov-Smirnov test, we have checked the null hypothesis that the two observed distributions derive from the same population. The result of the test is that the two distributions cannot be distinguished at the 90 % confidence level.

We have similarly compared the distribution of the lightcurve amplitudes of 16 Trojans observed during this survey and of a reference group of 175 main belt asteroids (see Fig. 5 a, b). To account for the fact that the main belt asteroids are normally observed at larger solar phase angles than the distant Trojans, we have reduced the observed amplitudes of the MBA group to zero phase angle by using the Amplitude-Phase relationship (APR) described by Zappalà et al. (1990). Also in this case the Kolmogorov-Smirnov test gives $Q \ll 90$ %, indicating that no systematic difference between the two distributions is detected with this data sample. It is interesting to note that the distribution of the amplitudes we measured for the Trojans in this survey has a mean value (A = 0.21 mag), which is very close to that of the main belt asteroids (A = 0.22 mag) in this diameter range. In this sense our sample taken by itself does not provide the evidence for the presence of anomalously elongated shapes among the Trojans. These results on the comparison between the rotational period and lightcurve amplitude distributions of main belt and Trojan asteroids are not conclusive yet. More observations to increase the sample sizes are needed to improve the power of the statistical results. The completion of this survey will provide the required observational data set to take the first steps on the origin and the evolution of the distant asteroids.

References

Binzel, R.P. and Sauter L.M., 1992, *Icarus* **95**, 222–238.

Binzel R.P., Farinella P., Zappalà V., and Cellino A., 1989, in *Asteroids II* (R.P. Binzel, T. Gehrels, M.S. Matthews, eds.), pp. 416–441. University of Arizona Press, Tucson.

Di Martino M., Gonano-Beurer M., Mottola S., Neukum G., 1992, in *Asteroids, Comets, Meteors 1991* (E. Bowell and A.W. Harris eds.).

French L.M., 1987, *Icarus* **72**, 325–342.

Gonano M., Di Martino M., Mottola S., and Neukum G. 1991, *Adv. Space Res.*, Vol. 11, No. 12, 197–200.

Hartmann W.K., and Tholen D.J., 1990, *Icarus* **86**, 448–454.
Hartmann W.K., Tholen D.J., Goguen J., Cruikshank D.P., and Binzel R.P., 1988, *Icarus* **73**, 487–498.
Howell S.M., 1989, Pub. *A.S.P.*, **101**, 616.
Lagerkvist C.-I., Harris A., and Zappalà V., 1989, In *Asteroids II* (R.P. Binzel, T. Gehrels, M.S. Matthews, eds.), pp. 1162–1179. University of Arizona Press, Tucson.
Mottola S., Gonano M., Rebhan H., and Neukum G., 1990, in *Asteroids, Comets, Meteors III* (C.-I. Lagerkvist, H. Rickman, B.A. Lindblad, M. Lindgren, eds.), pp. 151–154. Uppsala Universitet, Uppsala.
Zappalà V., Di Martino M., Cellino A., Farinella P., De Sanctis G., and Ferreri W., 1989, *Icarus* **82**, 354–368.
Zappalà V., Cellino A., Barucci M.A., Fulchignoni M., Lupishko D.F., 1990, *Astron. Astrophys.* **231**, 548–560.

Dust in the Earth's Atmosphere Before and After the Passage of Halley's Comet (1984–1987)

G. MATESHVILI and Y. MATESHVILI, Abastumani Astrophysical Observatory, Georgia

Everybody knows that with the exception of those who study the Sun, members of the astronomical profession must work at night to be able to record the faint light from the objects of their interest. It is true that CCD flat fields are often made at twilight, but otherwise it is necessary to wait until the Sun is far below the horizon and there is no more straylight in the atmosphere, before the "real" astronomical observations can start.

It is therefore always a surprise, especially to visiting colleagues, to meet astronomers/physicists, who are busy observing during twilight and dawn, when the sky is still very bright. And it seems even more strange that when it finally gets dark, then these observers close their telescopes and return to their offices and homes!

At the Abastumani Astrophysical Observatory in the Republic of Georgia, located near the border with Turkey in the southern part of the Caucasus mountains, you will meet observers of all three types. While some of them study the Sun with imaging and spectroscopic telescopes, others like ourselves observe the emissions from the Earth's atmosphere in the daytime, during twilight and dawn, and also during the night, when still other colleagues are busy unlocking the secrets of distant stars and galaxies.

We know that most astronomers have little experience with our kind of research and would therefore like to illustrate it by some examples. It is of course normally considered to be more of "geophysical" than of "astronomical" nature, but, as we shall see below, it may however also have some implications which are of interest to solar system astronomers.

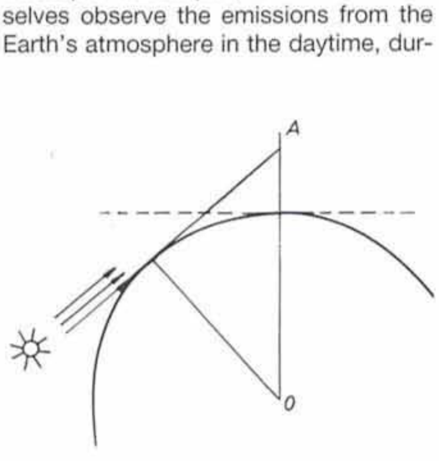

Figure 1: *The twilight phenomenon. An observer on the Earth's surface who looks up towards the zenith, only receives scattered light from those layers which are illuminated by the Sun's rays.*

The Twilight Sounding Method

Among the many interesting questions which concern the meteor showers associated with comet P/Halley, i.e. the *Orionids* with a maximum around October 21 and the *Eta Aquarids* (around May 4), is whether or not a particular activity was connected with the latest approach of this famous comet to the terrestrial orbit in 1985–1987.

Meteoric aerosol which enters into the Earth's atmosphere can be detected by the method of *twilight sounding*; this has been done many times in the past, see e.g. Fehrenbach et al. (1972); Divari and Mateshvili (1973), Mateshvili (1974), Link (1975) and Mateshvili and Mateshvili (1989).

The twilight phenomenon is explained by the fact that when the Sun sets below the horizon, its rays continue to illuminate the higher layers of the atmosphere. To begin with, these rays reach all layers, but as the Sun sinks, progressively higher layers come into the Earth's shadow and cease to be in the sunlight. The scattered light from the sky comes increasingly from the highest layers, but since the scattering efficiency falls off with the altitude (i.e. with the density) rather rapidly, we receive at any time mostly the scattered light from a rather narrow, sunlit atmospheric layer. A simplified scheme of the twilight phenomenon is shown in Figure 1.

The intensity of scattered light from point A is given by the relation:

$$I(\lambda) = I_0(\lambda)\,\omega_0\,P^m(\lambda)\,m\tau(\bar{H})$$

where $I_o(\lambda)$ is the extra-atmospheric solar brightness, ω_o is the size of the solar disk, m is the air mass, P is the vertical transmittance of the atmosphere, $\bar{H}(\lambda)$ is the instantaneous altitude of the Earth's shadow, τ is the optical thickness which is given by the expression:

$$r(\bar{H}) = \int_{\bar{H}}^{\infty} \sigma(\bar{H})\, d\bar{H}$$

where $\sigma(\bar{H})$ is the volumetric scattering coefficient (Rosenberg 1963). So, $I(\lambda)$ is therefore proportional to scattering coefficient $\sigma(\bar{H})$ and N_{aer}, the aerosol or particle content per unit of volume.

In Abastumani, we use for our twilight observations a photoelectric photometer with an interference filter that is centred at λ610 nm. During the evening twilight phase we then register the decreasing total intensity from a sky area

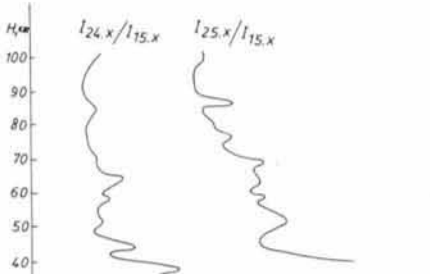

Figure 2: *Intensity ratios as a function of altitude, as observed on October 24 and 25, 1986, relative to October 15, 1986, i.e. before the Orionid period. The ratios are much larger than unity, and the scattering is therefore much larger at and after the maximum of the stream, than before. This shows the injection into the atmosphere of dust particles.*

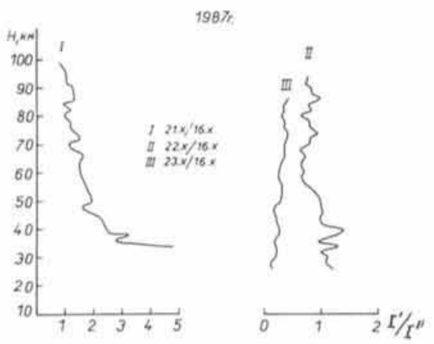

Figure 3: *As Figure 2, but for three dates in 1987. Now the intensity ratios are closer to unity than in 1986.*

defined by the optics of our instrument and in the morning twilight, we obtain a similar intensity curve in the reverse sense.

If there exists at a certain time in the atmosphere a layer with a higher scattering power and if it has a great horizontal extent, it will become apparent in our curve as an intensity excess at the same value of $\bar{H}$ in different sighting directions and therefore, at different values of ζ (the solar depression angle) and at different moments.

Our observations are usually carried out in two points of the sky on the solar vertical (the great circle through the Sun and the zenith); the zenith angles of these points are $\pm 60°$, that is, one point is in the general direction of the Sun and the other is in the opposite direction. The intensity is continuously recorded in each direction during one minute, then the system is switched to the other direction. A calibration standard is always recorded before and after the observations. This relative observing method to a large extent eliminates instrumental sensitivity drifts, etc.

Observations at the Time of Orionid Meteor Shower Activity

The observation dates in the Orionid periods of 1984, 1986 and 1987 are given in Table 1.

In Figure 2, we show the ratio of the sky intensity, as observed on October 24 and 25, 1986, respectively, to that on October 15, 1986, i.e. at a time when there should be no effect of the Orionid meteor shower. In comparison, the 1987 intensity ratios before and after the maximum of the stream (Fig. 3) are much closer to unity and reveal no significant increase. Thus, in 1986, after the maximum of the stream had been passed, the intensity of scattered light increased throughout the Earth's atmosphere. This implies that some matter was deposited into it, consisting of different fractions that moved downwards (precipitated) at different rates. When calculating the ratio of the intensities obtained in 1986 to those of 1984, i.e. before and after the passage of Comet Halley (Fig. 4), we find that the intensity of scattered light, depending on the altitude, increased from 4 to 14 times.

Observations at the Time of the Eta Aquarid Meteor Shower Activity

During the Eta Aquarid period in April/May 1987, we were only able to to compare the intensity $I(\lambda)$ with that obtained on the day preceding the onset of the activity of this meteor shower. The observations were carried out in the morning (9 times) and evening twilight (10 times), beginning on April 27 and ending on May 17, 1987.

The evening twilight observation on April 27 was chosen as the reference. When we plot the intensity ratios for the various series of observations, it is obvious that also during this period, the dust content in the upper atmospheric layers increased.

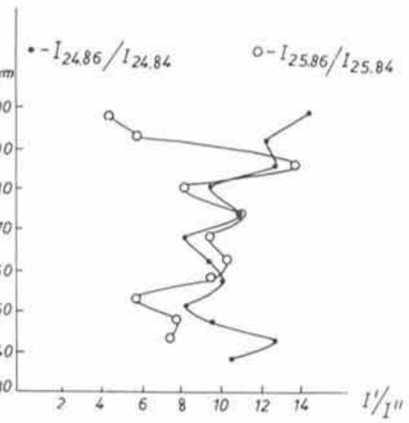

Figure 4: *A comparison of the dust content in the atmosphere on dates soon after the Orionid maxima in 1986 and 1987. The intensity ratios for the same dates in the two years are much larger than unity, i.e. there was much more dust in the atmosphere in 1986 than in 1987.*

How Big Are These Particles?

It would of course be very interesting to know the sizes of the particles which cause the increased scattering. We normally calculate this by three different methods:

1. The mean sizes are determined from the sedimentation velocities of the observed aerosol layers. The particle sedimentation velocity was determined using the Stokes-Cunningham law with the Cunningham correction

$$v_t = \frac{2r^2}{9\eta} g(\varrho - \varrho_a)(1 + \frac{Bl}{r})$$

where η is the air viscosity, ϱ_a is the density of particles, ϱ is the air density for the appropriate altitude, l is the mean free path of a molecule, and B is a factor which for $l/\varrho \geq 10$ equals 1.65.

2. The size of the particles can also be calculated from the relation

$$r = \left(\frac{9LkTV}{8\pi\varrho_a g} \right)^{1/5}$$

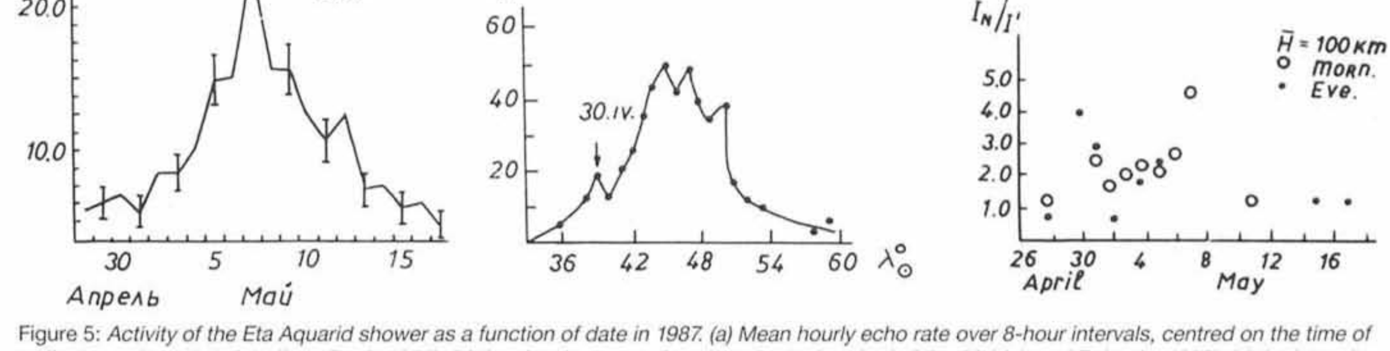

Figure 5: *Activity of the Eta Aquarid shower as a function of date in 1987. (a) Mean hourly echo rate over 8-hour intervals, centred on the time of radiant transit on that date (from Poole 1988); (b) the visual rate as a function of solar longitude (after Hajduk and Buhagiar 1982); (c) the intensity of twilight scattering at altitude 100 km in 1987 as measured in the morning and evening twilight from Abastumani (normalized to the level outside the shower period).*

Table 1. *Observation dates at the time of the Orionid shower (M: Morning (dawn) observations; E: Evening (twilight) observations)*

October	15	16	17	18	19	20	21	22	23	24	25	26	27
1984	–	–	–	–	–	–	–	E	E	E	E	E	M
1986	M	–	–	–	–	–	–	–	–	E	E	–	E
1987	–	E	–	–	–	E	E	M	–	–	–	–	–

where L is the thickness of the aerosol layer, k is the Boltzmann constant, T is the absolute temperature, g is acceleration due to gravity and $v=2.2\cdot10^{-10}\sigma(\bar{H})km^{-1}$, an empirical relation, where $\sigma(\bar{H})$ is the volumetric scattering coefficient.

3. Finally, the size of the particles may also be obtained by comparison of experimental sedimentation velocities with theoretical ones, calculated for different particle size and density (Ivlev 1982).

For the Orionids in 1984, the mean particle sedimentation velocity on October 22–27 and at altitudes 70–80 km, was 5.747 cm sec^{-1}. The estimated particle radii were ~0.08 μm. In 1986, the mean particle radius was about the same, ~ 0.065 μm. A great amount of cosmic matter consisting of particles with a wide range of sizes was injected into the atmosphere during the 1987 Eta Aquarid activity period. Very small particles with radii of the order of 0.0005 to 0.005 μm accumulated at an altitude of 100 to 120 km and those with r = 0.5 mm at $\bar{H}$=60 to $\bar{H}$=80 km. Moreover, the background aerosol content increased at all altitudes.

Time variations of the intensities at different altitudes reflect the intrusion of the particles ($\bar{H}$>70 km) and their subsequent rearrangement in the atmosphere ($\bar{H}$<70 km). The time variation of I_N/I' coincide with those of meteor hourly rates from the radar (Poole 1988) and visual (Hajduk and Buhagiar 1982) observations (Fig. 5).

Conclusions

Thus, it is clear that twilight observations of the type described here may be used to reveal structures of meteor showers. We plan to continue this work and hope eventually to accumulate enough material to be able to make more explicit statements about this.

The apparent increase in the aerosol content of the upper atmosphere when the Earth passed through the two meteor streams associated with P/Halley for the first time after the recent passage of this comet, is indeed very intriguing. We can offer no easy explanation to this at this moment.

References

Divari, N., Mateshvili, Y.: 1973, Sov. Astron. Circ 744, 3.

Fehrenbach, M., Frimout, D., Link, F., Lippens, C.: 1971, C.R. Acad. Sci. Paris **15**, 70.

Hajduk, A., Buhagiar, M.: 1982, Bull. Astron. Inst. Czech. **33**, 262.

Ivlev, L.: 1982, *Chemical composition and structure of atmospheric aerosols*, Leningrad.

Link, F.: 1975, *Planet. Space Sci.* **6**, 1011.

Mateshvili, G.: 1974, Sov. Astron. Circ. 849, 5.

Mateshvili, G., Mateshvili, Y.: 1989, in *Interstellar Dust*, IAU Symposium 135, eds. A.G.G.M. Tielens and L.J. Allamandola, NASA CP 3036, 463.

Poole, L.M.G.: 1988, *J. atmos. terr. Phys.* **50**, 585.

Rosenberg, G.: 1963, *Twilight*, Moscow.

Visiting Astronomers

(April 1 – October 1, 1993)

Observing time has now been allocated for Period 51 (April 1 – October 1, 1993). The demand for telescope time was again much greater than the time actually available.

The following list gives the names of the visiting astronomers, by telescope and in chronological order. The complete list, with dates, equipment and programme titles, is available from ESO-Garching.

3.6-m Telescope

April 1993: De Graauw et al. (9-003-49K), Danziger/Bouchet/Gouiffes/Lucy/Fransson/Mazzali/Della Valle, Böhringer et al. (1-023-49K), Shaver/Wall/Kellermann, Jablonka/Bica/Alloin, Turatto et al. (4-004-45K), Danziger/Bouchet/Gouiffes/Lucy/Fransson/Mazzali/Della Valle, De Graauw et al. (9-003-49K),

May 1993: De Graauw et al. (9-003-49K), van der Hucht/Williams/Yudiawati Anggraeni/Bouchet, Habing et al. (7-008-51K), Danziger/Bouchet/Gouiffes/Lucy/Fransson/Mazzali/Della Valle, Kudritzki/Pakull/Méndez/Conti/Gabler/Motch, Danziger/Bouchet/Gouiffes/Lucy/Fransson/Mazzali/Della Valle, Magazzù/Martín/Rebolo, Macchetto/Sparks, Danziger/Bouchet/Gouiffes/Lucy/Fransson/Mazzali/Della Valle, Amram/Balkowski/Boulesteix/Le Coarer/Marcelin/Cayatte/Sullivan, Lagage/Cabrit/André/Pantin/Olofsson/Nordh.

June 1993: Lagage/Cabrit/André/Pantin/Olofsson/Nord, Lagage/Pantin, Nissen/Lambert/Smith, Lemoine/Ferlet/Vidal-Madjar/Emerich, Baade/Kjeldsen, Leone/Pasquini, Mermilliod/Raboud/Levato, Barbuy/Renzini/Ortolani/Bica, Lagrange-Henri/Corporon/Bouvier.

July 1993: Rouan/Hofmann/Normand/Alloin/Cuby/Tacconi-Garman/Gallais, Beuzit/Lagrange-Henri/Tessier/Vidal-Madjar/Ferlet/Beust/Hubin, Dougados/Rouan/Lopez/Coudé du Foresto/Forveille, Ménard/Léna/Malbet/Dougados/Monin/Schuster, Rigaut/Léna/Gehring/Hofmann/Cuby, Della Valle/Bianchini/Duerbeck/Ögelman/Orio, Borkowski/Tsvetanov/Harrington, Danziger/Gilmozzi/Zimmermann/Hasinger/Macgillivray, Tadhunter/Morganti/Fosbury/Danziger/Shaw, Tinney/Mould/Reid, Molaro/Pasquini/Castelli/Bonifacio.

August 1993: Molaro/Pasquini/Castelli/Bonifacio, Zaggia/Capaccioli/Piotto/Stiavelli, Bedding/Beckers/von der Lühe/Weigelt/Urban/Beckman/Grieger/Kohl/van Elst, Danziger/Bouchet/Gouiffes/Lucy/Fransson/Mazzali/Della Valle, Barbon/Notni/Radovich/Rafanelli/Schulz, Véron, P./Hawkins, Seitter/Spiekermann/Schücker/Böhringer/Hartner/Crudacce, Fosbury/Villar/Binette, Danziger/Bouchet/Gouiffes/Lucy/Fransson/Mazzali/Della Valle, Schulz/Mücke, Molaro/Primas/Castelli/Bonifacio.

September 1993: Saint-Pé/Combes, M./Rigaut/Tiphène/Demailly/Tacconi-Garman, Combes, M./Saint-Pé/Tomasko/Demailly/Fauchèrre, Vettolani et al. (1-019-47K), Mazure/Rhee et al. (1-014/005-43K), Hainaut/West R.M., Møller/Warren, Kneer/Bender/Krautter, Danziger/Bouchet/Gouiffes/Lucy/Fransson/Mazzali/Della Valle, Habing et al. (7-008-51K).

3.5-m NTT

April 1993: Moorwood/Oliva/Origlia/Kotilainen, Oliva/Marconi/Salvati/Moorwood, Miley/van Ojik/Röttgering/Moorwood, Oliva/Marconi/Salvati/Moorwood, Miley et al. (2-001-43K), Turatto et al. (4-004-45K), Tammann et al. (1-022-47K), Thomsen/Sodemann, Held/Renzini/Cappi.

May 1993: Gredel/Zinnecker, Gry/Baluteau/Cox/Armand/Emery, Lutz/Genzel/Drapatz/Cameron/Harris/Najarro/Hillier/Kudritzki, Bertola/Amico/Zeilinger, Motch/Pakull/Pietsch, Danziger/Méndez/Kudritzki/Mazzali/Lucy/Ciardullo/Jacoby/Roth, Tammann et al. (1-022-47K), West/Hainaut/Mars-

More 1910 Halley Memorabilia

In addition to observing the meteoritic dust from comet P/Halley, Giuli and Yura Mateshvili recently found among their family belongings some memorabilia from the 1910 passage of this comet.

On these pictures are shown a cigarette box with the name "Halley" in cyrillic letters and two postcards, which were sent from Geneva to Lausanne in Switzerland at the time when P/Halley approached the Earth in April 1910. Of particular interest is the French text, which clearly shows the concerns of the sender about what would happen when the Earth passed through the tail of the comet – . . . humanity, which maybe perishes this night . . . (above), and, . . . it approaches, ouf! (below).

There is nothing new under the sky, or is there?

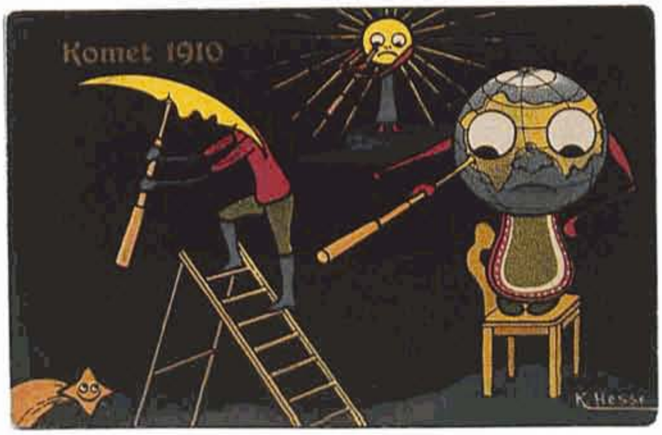

den/Smette, Della Valle/Danziger/Lucy/Mazzali, Brandner/Zinnecker.

June 1993: Origlia/Oliva/Moorwood, Käufl/Aringer/Dorfi/Hron/Stift/Wiedemann, Ortolani/Renzini/Rich, Ortolani/Barbuy/Bica, Cimatti/di Serego Alighieri/Fosbury, Habing et al. (5-007-45K), Caraveo/Bignami/Mereghetti/Grosso.

July 1993: Wampler, Webb/Barcons/Carswell/Lanzetta/Tytler, Piotto/Cacciari/Ferraro/Fusi Pecci/Djorgovski, Fort et al. (1-015-45K), Soucail/Fort/Mellier/Rieutord, Alcaino/Liller/Alvarado/Wenderoth, Moehler/Heber/de Boer/Rupprecht, Eckart/Genzel/Hofmann/Drapatz/Sams/Tacconi-Garman, Sams/Eckart/Hofmann/Tacconi-Garman.

August 1993: Ageorges/Monin/Ménard/Eckart/Drapatz, Leinert/Weitzel/Eckart, von der Lühe/Bedding/Eckart/Gehring, Ellis/Fosbury/Couch/Bower/Smail/Sharples, Surdej et al., Meylan/Djorgovski/Thompson, Bender et al. (1-004-43K), Macchetto/Giavalisco/Sparks, Kotilainen/Moorwood.

September 1993: D'Odorico et al. (2-013-49K), De Lapparent et al. (1-003-43K), Kudritzki/Roth/Méndez/Ciardullo/Jacoby, Bergeron/Guillemin,Heydari-Malayeri, Danziger/Bouchet/Gouiffes/Lucy/Fransson/Mazzali/Della Valle.

2.2-m Telescope

April 1993: MPI Time, Habing et al. (7-008-51K).

May 1993: Habing et al. (7-008-51K), van der Hucht/Williams/Yudiawati Anggraeni, Prusti/Whittet/Chiar/Smith, Prusti/Whittet/Chiar/Smith, Hutsemékers/van Drom, Grosbøl/Patsis, Tinney, Labhardt/Tammann, Grebel/Roberts, Weigelt/Appenzeller/Wagner/Zinnecker/Seggewiss/Beckmann/Kohl/van Elst/Grieger/Urban, Carollo/Danziger.

June 1993: Carollo/Danziger, Mirabel/Duc, Oliva/Reconditi/Origlia/Moorwood, Aspin/Reipurth, Pagel/Thejll/Jørgensen/Jimenez, Blietz/Cameron/Drapatz/Eckart/Genzel/Krabbe/v. d. Werf, Krenz/Genzel/Harris/Krabbe/Lutz/Geballe, Miley et al. (2-001-43K), Megeath/Wilson, Guarnieri/Moneti/Ferraro/Fusi Pecci/Testa/Ortolani.

July 1993: Guarnieri/Moneti/Ferraro/Fusi Pecci/Testa/Ortolani, van der Klis/Augusteijn/Kuulkers/van Paradijs, Simien/Mamon/Héraudeau, Grebel/Richtler, Fasano/Falomo, Lagerkvist/Dahlgren/Williams I./Fitzsimmons, Tinney, MPI Time.

August 1993: MPI Time, Bergvall/Östlin/Rönnback, Caulet/McCaughrean/Käufl.

September 1993: Tsvetanov/Ward/Ford/Fosbury/Kotilainen, Kotilainen/Ward/Hughes, Tinney, Beuermann/Grupe/Thomas/Reinsch/Fink, Held/Piotto, Barbieri et al. (2-007-43K), Habing et al. (7-008-51K).

1.5-m Spectrographic Telescope

April 1993: Gerbaldi et al. (5-004-43K), Prieto/Zeilinger, Barucci/Dotto, Jørgensen/Kjærgaard/Franx, Liu/Danziger, Guglielmo/Epchtein, Hensberge et al. (5-005-47K).

May 1993: Hensberge et al. (5-005-47K), Stefl/Baade/Cuypers, Courvoisier/Bouchet/Blecha, Ramella/daCosta/Focardi/Geller/Nonino/Smith/Raychaudury, Kudritzki/Pakull/Méndez/Conti/Gabler/Motch, Calvani/Sulentic/Marziani, Pottasch S.R./van de Steene/Sahu K.C., Krautter/Wichmann/Alcalá/Schmitt/Mundt/Zinnecker.

June 1993: Krautter/Wichmann/Alcalá/Schmitt/Mundt/Zinnecker, Lorenz R./Drechsel/Mayer, Kunkel/Zinnecker/Schmitt, Acker/Cuisinier/Köppen/Rolla/Stasinska/Testor, Ng/Kerschbaum/Habing/Hron/Schultheis/Blommaert, Alcalá/Krautter/Covino/Franchini/Terranegra.

July 1993: Alcalá/Krautter/Covino/Franchini/Terranegra, Covino/Pasinetti/Pastori, Greve/McKeith, Gustafsson/Asplund/Eriksson/Olofsson, Treves/Abramowicz/Falomo/Pesce, Courvoisier/Bouchet/Blecha, Karkoschka, Hubrig/Mathys/Hubeny.

August 1993: Hubrig/Mathys/Hubeny, Cacciari/Bragaglia/Fusi Pecci/Carretta, Sommer-Larsen/Christensen/Beers/Flynn.

September 1993: Gerbaldi et al. (5-004-43K), Barbieri et al. (2-007-43K), Böhringer et al. (1-023-49K), Cayrel/Nissen/Beers/Spite M./Spite F./Andersen/Nordstrom/Barbuy, Wielebinski/Koribalski/Bajaja/Dumke.

1.4-m CAT

April 1993: Neuforge/Magain/Grevesse/Noels, Artru/Gonzalez/Lanz, Baudzus/Schmidt-Kaler/Hanuschik/Hummel/Rohe, Hanuschik/Hummel, van der Bliek/Gustafsson, van Winckel/Waelkens/Waters, Mathys/Landstreet/Lanz/Manfroid/Hubrig, Magain/Zhao, Kürster/Hatzes/Cochran/Dennerl/Döbereiner.

May 1993: Kürster/Hatzes/Cochran/Dennerl/Döbereiner, Stefl/Cuypers/Hirata/Kambe, Stefl/Baade/Cuypers, van Winckel/Waelkens/Oudmaijer, Cayrel de Strobel, Mathys/Landstreet/Lanz/Manfroid/Hubrig, Schmutz, Perinotto/Corradi, Jorissen/Mayor/North.

June 1993: Mandolesi/Crane/Attolini/Palazzi, Acker/Gesicki/Szcerba/Tylenda/Stenholm/Cuisinier, Mathys/Landstreet/Lanz/Manfroid/Hubrig, Gredel, North/Glagolevskij, Lagrange-Henri/Corporon/Bouvier.

July 1993: Lagrange-Henry/Corporon/Bouvier, Zijlstra/Walsh, Kürster/Hatzes/Cochran/Dennerl/Döbereiner, Gosset, Thé/Pérez/Grady, van Winckel/Waelkens/Waters, François/Baraffe, Benvenuti/Porceddu.

August 1993: Covino/Palazzi/Penprase/Schwarz/Terranegra, Danks/Penprase/Caulet, Gustafsson/Andersen/Edvardsson/Nissen.

September 1993: Gustafsson/Andersen/Edvardsson/Nissen, North, Hanuschik/Hummel/Dietle, Poretti/Bossi/Mantegazza/Zerbi, Kürster/Hatzes/Cochran/Dennerl/Döbereiner.

1-m Photometric Telescope

April 1993: Habing et al. (7-008-51K), Courvoisier/Bouchet/Blecha, Barucci/Dotto, Kohoutek, Schneider/Weiss/Kuschnig.

May 1993: Schneider/Weiss/Kuschnig, Lagerkvist/Magnusson/Erikson, Fulchignoni/Barucci/Harris, Courvoisier/Bouchet/Blecha.

June 1993: Habing et al. (7-008-51K), Salvati/Hunt/Stanga, Richichi, Mermilliod/Claria, Liller/Alcaino/Alvarado/Wenderoth, Courvoisier/Bouchet/Blecha, Lagrange-Henri/Corporon/Bouvier, Ng/Kerschbaum/Habing/Hron/Schultheis/Blommaert.

July 1993: Ng/Kerschbaum/Habing/Hron/Schultheis/Blommaert, Epchtein et al. (9-002-49K).

August 1993: Epchtein et al. (9-002-49K).

September 1993: Barbieri et al. (2-007-43K), Debehogne/Hahn/Di Martino/Zappalà/Lagerkvist/Magnusson/de Campos/Valongo, Molinari/Liseau/Lorenzetti.

50-cm ESO Photometric Telescope

April 1993: Wolf/Mandel/Stahl/Szeifert/Zickgraf/Sterken.

May 1993: Wolf/Mandel/Stahl/Szeifert/Zickgraf/Sterken.

June 1993: Magnan/de Laverny/Mennessier, Oblak et al. (7-009-49K), Carrasco/Loyola, Lorenz/Drechsel/Mayer, Weiss/Paunzen.

July 1993: Weiss/Paunzen, Magnan/de Laverny/Mennessier, Hainaut/Detal/Hainaut-Rouelle/Pospieszalska-Surdej/Surdej, Carrasco/Loyola.

August 1993: Magnan/de Laverny/Mennessier, Carrasco/Loyola, Magnan/de Laverny/Mennessier, Oblak et al. (7-009-49K).

GPO 40-cm Astrograph

April 1993: Debehogne/López-Garcia/Machado/Caldeira/Vieira/Netto/Lagerkvist/Mourao/Protitch-Benishek/Javanshir.

May 1993: Debehogne/López-Garcia/Machado/Caldeira/Vieira/Netto, Lagerkvist, Mourao/Protitch-Benishek/Javanshir.

June 1993: Scardia.

July 1993: Ferlet et al. (9-004-51K).

August 1993: Ferlet et al. (9-004-51K).

September 1993: Ferlet et al. (9-004-51K).

1.5-m Danish Telescope

April 1993: Ardeberg/Lindgren/Lundström, Nordström B. & Andersen J. et al./Jørgensen H.E. et al./Jønch H.-Sørensen.

May 1993: Waelkens/Mayor, Jorissen/Mayor/North, Ardeberg/Lindgren/Lundström, Richtler/Hilker/Kissler, Danziger/Bouchet/Gouiffes/Lucy/Fransson/Mazzali/Della Valle, Hainaut/West, Carollo/Danziger, van der Klis/Augusteijn/Kuulkers/van Paradijs/Vaughan, Thejll P. et al.

June 1993: Thejll P. et al., Grundahl Jensen F. & Nissen P.E., Nordström B. & Andersen J. et al., Duquennoy/Mayor.

July 1993: Duquennoy/Mayor, Johnston/Picard, Tosi/Marconi/Fusi Pecci/Ferraro/Bragaglia/Greggio, Martinet/Friedli/Blecha/Pfenniger/Bratschi, Freudling/Alonso/da Costa/Wegner, Heidt.

September 1993: Mayor et al. (5-001-43K).

50-cm Danish Telescope

April 1993: Garcia J.M. et al., Jønch-Sørensen H.

May 1993: Stefl/Cuypers/Hirata/Kambe, Stefl/Baade/Cuypers, Ardeberg/Lindgren/Lundström, Andersen J. & Mathieu R.D.

June 1993: Andersen J. & Mathieu R.D., Group for Long Term Photometry of Variables.

July 1993: Group for Long Term Photometry of Variables, Sinachopoulos/van Dessel.

August 1993: Sinachopoulos/van Dessel, Group for Long Term Photometry of Variables.

September 1993: Saint-Pé/Combes M./Rigaut/Tiphène/Demailly/Tacconi-Garman, Poretti/Bossi/Mantegazza/Zerbi, Sterken/Paparo.

90-cm Dutch Telescope

April 1993: Schwarz/Corradi/van Winckel, Dutch Time.

May 1993: Dutch Time, de Winter/Thé, Turatto et al. (4-004-45K), Augusteijn/van Paradijs/van der Klis, Pottasch S.R./van de Steene/Sahu K.C., Reduzzi/Rampazzo/Sulentic/Prugniel, Kjeldsen/Frandsen/Viskum.

June 1993: Kjeldsen/Frandsen/Viskum, Oblak et al. (7-009-49K), Turatto et al. (4-004-45K), Buonanno/Piersimoni/Brocato/Straniero, Kunkel/Zinnecker/Schmitt, Stella/Buzzoni/Tavani/Mereghetti.

July 1993: Stella/Buzzoni/Tavani/Mereghetti, Dutch Time.

August 1993: van Dessel/Sinachopoulos, Schuecker/Cunow/Naumann/Ungruhe, Lagerkvist/Dahlgren/Williams/Fitzsimmons, West M.J./Schombert, Vogt/Mennickent, Oblak et al. (7-009-49K).

September 1993: Oblak et al. (7-009-49K), Augusteijn/van Paradijs/van der Klis, Turatto et al. (4-004-45K), Cetty-Véron, Beuermann/Burwitz/Schwope/Thomas, Ferrari/Bucciarelli/Massone/Koornneef/Lasker/Le Poole/Postman/Siciliano/Lattanzi/Pizzuti.

SEST

April 1993: Valtaoja, Bååth et al.

May 1993: Arnaboldi, Horellou, Wild, Mauersberger.

June 1993: Knee, Nyman, Gredel, Knee, Reipurth, Fuller, Olofsson, Lindqvist, Johansson, Aalto Bergman, Winnberg, Valtaoja, Johansson et al.

July 1993: Mauersberger, Siebenmorgen, Courvoisier, van Dishoeck, Sillanpää, Hughes, Danziger, Gredel, van Dishoeck, Reipurth, Zinnecker, Omont, Israel.

August 1993: Knee, Barsony, Vilhu, Harju, Lijeström, Gondhalekar, Olofsson, Wiklind, Rydbeck, Bergman, Nyman, Booth, Rydbeck, Valtaoja.

September 1993: Galletta, Krügel, Henkel, Danziger, Lemme, Henkel, Mauersberger, Reipurth, Cox, Omont, Montmerle.

The Recurrent Nova U Sco – a Touchstone of Nova Theories

H.W. DUERBECK[1], R. DUEMMLER[1], W.C. SEITTER[1], E.M. LEIBOWITZ[2] and M.M. SHARA[3]

[1]Astronomical Institute, Münster University, Germany

[2]Wise Observatory, Tel Aviv University, Israel

[3]Space Telescope Science Institute, Baltimore, USA

Almost 130 years ago, on May 21, 1863, N. Pogson entered the following lines in his notebook: "[A variable star] discovered by me in a hazy sky at Madras. Observed last night and again this night with a steel micrometer. Showed this – my fourteenth variable star – to Lizzy about 10 pm before observing it: also later to C. Ragoonatha Chary [the night assistant] to enable him to make pretty sure of it on the meridian." The star was at that time of magnitude 9, and fading rapidly. The entry for May 27 reads "Shown to Sir W. Denison and party. His Excellency could just discern it, but not so Lady Denison" (see Pogson 1908).

The star sank into oblivion, until Thomas (1940) found two more rises in brightness on Harvard plates taken in 1906 and 1936. Its large amplitude and long outburst intervals indicated that U Sco belonged to the small, but very interesting group of recurrent novae. Webbink (1978) analysed Ragoonatha Chary's 1863 positional measurements and was able to identify the nova in its minimum state as a star of 19th magnitude. Only two years later, another outburst was observed and followed closely by optical and UV spectroscopy (Barlow et al. 1981, Williams et al. 1981). First models for the outburst of recurrent novae were calculated. Quite unexpectedly, U Sco erupted again in 1987.

A nova outburst is successfully modelled as a thermonuclear runaway (TNR) in hydrogen-rich matter on the surface of a white dwarf of fairly high mass. The white dwarf is composed of carbon and oxygen, or oxygen, magnesium and neon, the hydrogen-rich matter is accreted from a close binary companion via an accretion disk, deposited on the surface of the white dwarf, and compressed to high densities. Depending on the mass of the white dwarf, the temperature in its upper layers, and the amount of mixing of heavy elements from the interior of the white dwarf into the hydrogen-rich layer, nuclear reactions set in sooner or later. Since the accreted layers are degenerate, the rise of temperature caused by the reactions at first does not lead to expansion and cooling. Only after the temperature has risen to many million degrees, degeneracy is lifted, and the outer layers of the object expand violently: the object undergoes a nova outburst.

To start this TNR, the density of the accreted matter in the lowermost layer must reach a critical value. If too little matter is accreted, it takes a long time, perhaps millions of years, before an outburst occurs. For explosions of recurrent novae which occur with timescales of as little as ten years, a high mass transfer rate must be invoked. There is, however, a problem: If too much mass is accreted in too short a time, it cannot cool efficiently and does not become sufficiently degenerate, the nuclear reactions set in very mildly, and no nova explosion occurs. It has been shown in the theory of nova explosions that short intervals between outbursts are only possible for white dwarfs with high masses (about 1.38 $M_\odot$), close to the Chandrasekhar limit. Such white dwarfs have small radii, the accreted matter is highly compressed, and the explosion can take place after a short time of mass transfer from the secondary, when only some 10^{-8} $M_\odot$ have been accreted (Starrfield et al. 1985, Livio 1988, Kato 1990).

Are the theoretical concepts concerning recurrent novae correct? We can test them by measuring the mass of the white dwarf. Most recurrent novae, however, have giant companions, and the light of the white dwarf and the accretion disk are difficult to trace; furthermore, orbital periods are of the order of several hundred days. T Pyx, a recurrent nova with a dwarf companion, is seen at very low inclination angle, so that its orbital period, while short, cannot be measured with sufficient accuracy.

In 1988, Bradley Schaefer found that U Sco and V394 CrA also have short periods of P = 1.2344 and P = 0.7577 days, respectively. U Sco shows deep eclipses, indicating that the orbital inclination is close to 90°. If it is possible to measure the radial velocity curves of both, the white dwarf and the cool mass transferring component, the masses of the two components can be measured, and our theoretical concepts of the TNR can be checked.

After Schaefer had published his results in 1990, we immediately applied for observing time to test the TNR theory of recurrent novae by observing U Sco. Time for spectroscopic observations was granted in 1992 and observations were carried out with EFOSC1 at the ESO 3.6-m telescope on July 1 and 3. The nights were chosen in such a way that most phases of the radial velocity curve could be covered by observa-

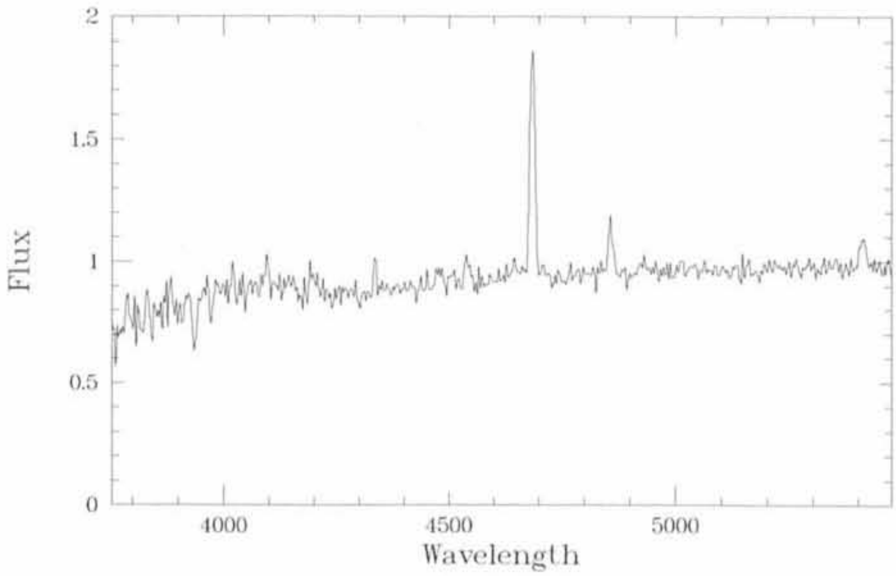

Figure 1: *Averaged spectrum of U Sco. The emission lines, formed in the disk surrounding the white dwarf, are due to ionized helium. Hydrogen lines are probably absent. The Ca II H and K lines and a few additional weak features of the cool secondary component are also seen.*

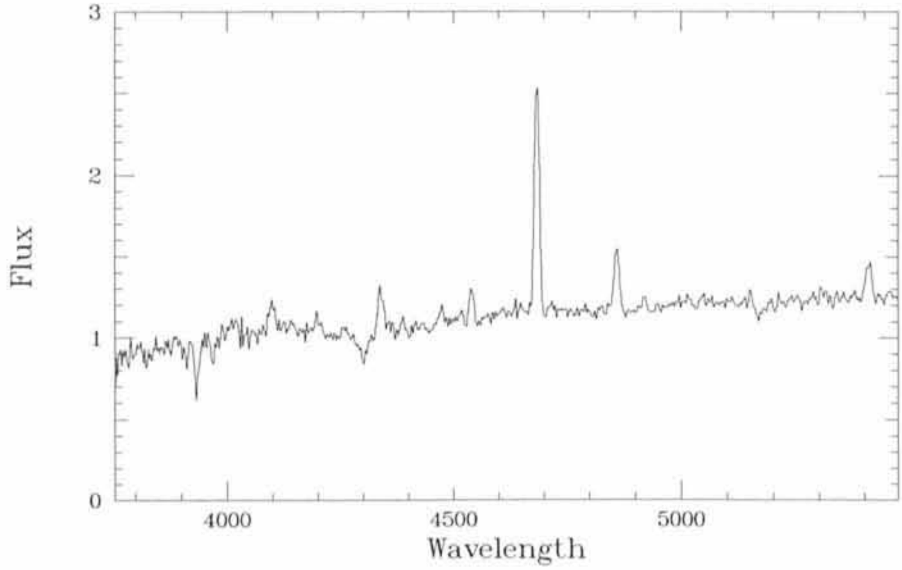

Figure 2: *Averaged spectrum of V394 CrA. The emission lines match those of U Sco quite well, the absorption lines are somewhat stronger.*

tions. Despite the poor winter skies, the first night was perfect and the second one acceptable, yielding at least a few spectra taken through gaps in the clouds. The mean spectrum of U Sco is shown in Figure 1. Most of the lines are due to He II. The strongest one is He II 468.6 nm, the others belong to the Pickering series which is shown to high series members, hydrogen is hardly visible. Features from the secondary star include the H and K lines of Ca II and a few weaker absorption lines.

It should be mentioned that the recurrent nova V394 CrA was also monitored in the two nights of July 1992. Its minimum spectrum, an almost identical twin of the U Sco spectrum, is shown in Figure 2. Only the secondary star appears slightly cooler, perhaps of type G, as indicated by its comparatively strong absorption features. The radial velocities appear to be very erratic.

While our observations were made, a preprint arrived at La Silla showing that U Sco had been observed with the Mt. Palomar 5-m telescope immediately after Schaefer's findings in 1990 and 1991. The authors, Johnston and Kulkarni (1992), found deviating properties of the system: Schaefer's period did not fit the radial velocity variations sufficiently well, so that they assumed a somewhat different period (actually, they suggested two alternative periods). Even so the hot (= white dwarf) and cool (= red dwarf) components showed radial velocity curves with considerable phase shift. The amplitudes were poorly determined (K_{WD} = 35±17 km/s, K_{RD} = 156±19 km/s) and the mass of the white dwarf, with a 3σ upper limit of 0.9 solar masses, turned out to be small. Was this the Waterloo of the TNR theory for recurrent novae?

We do not know what happened in 1990 and 1991. Maybe the nova was in a somewhat more cooperative state in July 1992. In any case, our short time base makes small uncertainties in the period unimportant, while a global solution of all radial velocity data indicates that Schaefer's period is not so bad after all: it can be used with only a small correction, to describe all existing spectroscopic observations, except two measurements discussed below. The improved period is P = 1.234518 days. The reason why the Palomar astronomers chose another period is due to two radial velocities (out of 17) which deviate to a large degree from the radial velocity curve when Schaefer's period is used. Since these values were derived from the poorest spectra of their sample, we found it acceptable to exclude them from our period analysis. Schaefer's period, slightly changed, then describes all remaining radial velocity observations including the new ones, very well. No satisfactory result can be obtained with the periods suggested by Johnston and Kulkarni.

The quality of our measurements is not better than those made at Palomar – both sets of data are quite poor, but one must keep in mind that we try to determine radial velocities of a 19th-magnitude object. The radial velocity curve derived from our measurements is shown in Figure 3. The sine fit of our data has a scatter of 74 km/s. The amplitudes are K_{WD} = 164±33 km/s, K_{RD} = 116±35 km/s. The derived masses are 1.16±0.69 $M_\odot$ for the hot and 1.64±0.83 $M_\odot$ for the cool component. The velocities of the white dwarf are

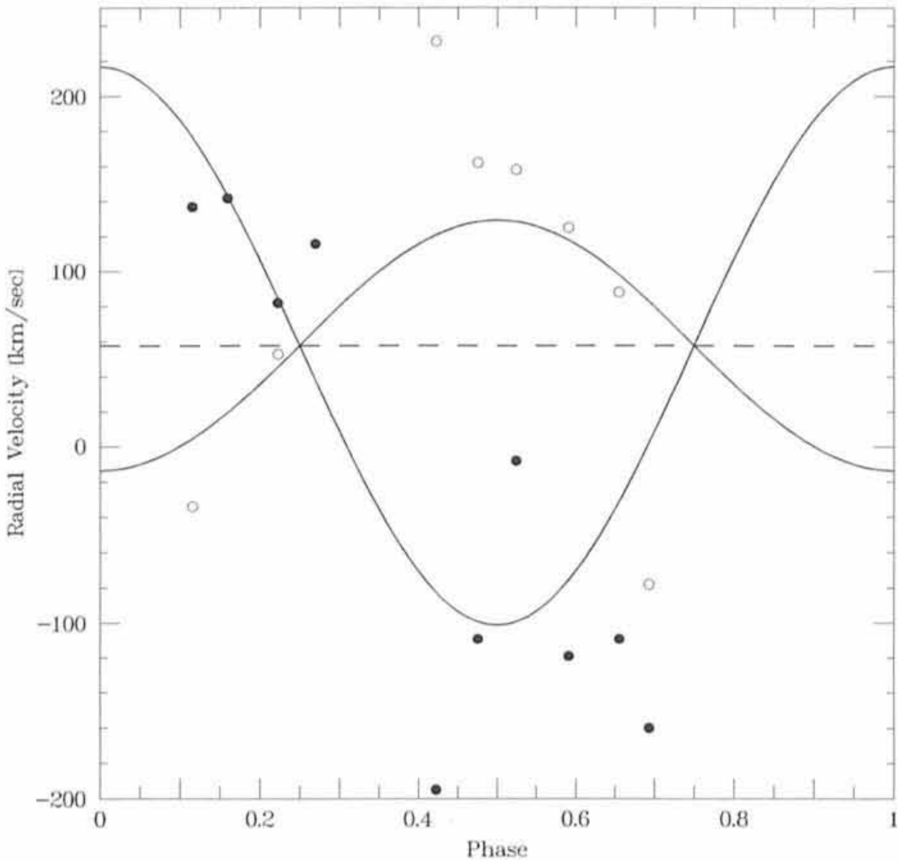

Figure 3: *New radial velocity curve of U Sco, based on CCD spectra taken with EFOSC1 at the 3.6-m telescope. Grism B150 was used, the exposure time of a single spectrum was 30 minutes.*

derived from three He II emission lines, those of the cool star from the calcium K absorption line.

The new observations are clearly compatible with the TNR theory which predicts the accreting star to be near the Chandrasekhar limit. Nevertheless, the peculiar emission line spectrum of the "hot component", formed in the accretion disk around the white dwarf, is poorly understood. Does it indicate that the accreted matter is helium-rich, or is it only the effect of high temperature? Is the secondary a normal main-sequence star of spectral type F, as indicated by its mass, its feeble impression on the total spectrum, and by the orbital elements? Can a sufficiently detailed TNR model be found which matches all the observed properties, or does one have to go back to other models, e.g. accretion disk instabilities? These questions have to be answered, and for this, additional observations are highly desirable.

It appears that theory and observation of recurrent novae are coming of age. We wonder what the state of knowledge will be after another 130 years have elapsed and VLT time will have been granted for nova research!

References

Barlow, M.J., Brodie, J.P., Brunt, C.C., Hanes, D.A., Hill, P.W., Mayo, S.K., Pringle, J.E., Ward, M.J., Watson, M.G., Whelan, J.A.J., Willis, A.J.: *MNRAS* **195**, 61 (1981).

Johnston, H.M., Kulkarni, S.R.: *ApJ* **396**, 267 (1992).

Kato, M.: *ApJ* **355**, 277 (1990).

Livio, M.: p. 323 in *The Symbiotic Phenomenon* (eds. J. Mikolajewska et al.), Dordrecht: Kluwer (1988).

Pogson, N.R.: *Mem. R.A.S.* **58**, 91 (1908).

Schaefer, B.E.: *ApJ* **355**, L39 (1990).

Starrfield, S., Sparks, W.M., Truran, J.W.: *ApJ* **291**, 136 (1985).

Thomas, H.L.: *Harvard Bull.* **912**, (1940).

Webbink, R.F.: *PASP* **90**, 57 (1978).

Williams, R.E., Sparks, W.M., Gallagher, J.S., Ney, E.P., Starrfield, S.G., Truran, J.W., *ApJ.*: **251**, 221 (1981).

Rotation of T Tauri Stars from Multi-Site Photometric Monitoring

J. BOUVIER, Laboratoire d'Astrophysique, Observatoire de Grenoble, France

1. Introduction

The present-day Sun has a very low rotational velocity: ≃ kms^{-1} at the equator. In this respect, the Sun is representative of all low-mass main-sequence stars, whose rotational velocities usually amount to less than 5 kms^{-1}. These stars have not always been such slow rotators, however. In the mid-80's, CORAVEL measurements of the rotational velocities of pre-main sequence solar-type stars, the so-called T Tauri stars with an age between 1 and 10 million years, were performed at the 1.5-m Danish telescope on La Silla and showed that their average rotation rate is about 15 kms^{-1}, i.e., nearly 10 times larger than the billion-year-old Sun. Long before the rotation rates of young stars were measured, Schatzman (1962) hypothesized that low-mass stars are braked on the main sequence, loosing angular momentum to their magnetic stellar winds. As a result, all low-mass dwarfs that have evolved onto the main sequence have lost the memory of their initial rotation rate and exhibit uniformely slow rotation by the age of the Sun.

Clues to the initial velocity distribution of solar-type stars can therefore only be obtained from the measurement of the rotation rates of very young stars, such as T Tauri stars. In turn, the rotational properties of these newly-formed stars provide constraints on the star-formation process and on the very early stellar evolution. A point of particular interest is to investigate how accretion of material from a circumstellar disk affects the rotational evolution of young stars. Approximately half of the TTS, the so-called "classical" T Tauri stars, exhibit strong mass-loss and are believed to simultaneously accrete material from a circumstellar disk at a high rate. The other half, designated as "weak-line" T Tauri stars because of their relatively weak emission-line spectrum, do not possess an accretion disk and have much weaker stellar winds (see the review on T Tauri stars by Bertout 1989). Comparison between the rotation rates of classical and weak-line T Tauri stars thus provides a way to study the impact of disk accretion and mass-loss onto their rotational evolution.

2. The "COYOTES" Campaign

Extensive measurements of spectroscopic velocities, $v\sin i$, of T Tauri stars using CORAVEL and other spectrographs have proved very powerful to derive the *statistical* rotational properties of young stars (see a review by Bouvier 1991). However, a major uncertainty arises from the unknown value of the geometric factor $\sin i$ included in the spectroscopic velocity. A more direct, but much more demanding, measurement of rotation consists in monitoring the photometric variations of young stars. T Tauri stars exhibit brightness inhomogeneities at their surface ("spots") which modulate the stellar flux as the star rotates. As a result, the light curve includes a quasi-sinusoidal component whose period is a direct measure of the star's rotational period. Rotational periods thus derived are not affected by projection effects and are usually measured with an accuracy of better than 10%.

In order to tackle the issues outlined in the Introduction, we organized an international photometric monitoring campaign on T Tauri stars (TTS) which took place between November 1990 and February 1991. This campaign was dubbed COYOTES, which stands for Coordinated Observations of Young ObjecTs from Earthbound Sites. The COYOTES campaign lasted three months. During this time the night-to-night variability of 23 TTS from the Taurus-Auriga stellar formation region was monitored in UBVRI photometry using eight telescopes in seven sites: ESO (S.Cabrit, Grenoble), Calar Alto (M. Fernandez, Madrid), La Palma (E. Martin, Canarias), Las Campanas and CTIO (J. Matthews, UBC), Catania (E. Covino, Catania), and Cananea (L. Terranegra, Mexico). Due to bad weather, no data could be collected at the last two sites. The resulting light curves span a time interval from typically 60 days, with unfortunate gaps due to non-photometric weather and/or instrumental problems, and up to 90 nights for 3 objects of the sample.

Periodic light variations were searched for in the light curves of the 23 stars using Fourier techniques. Quite

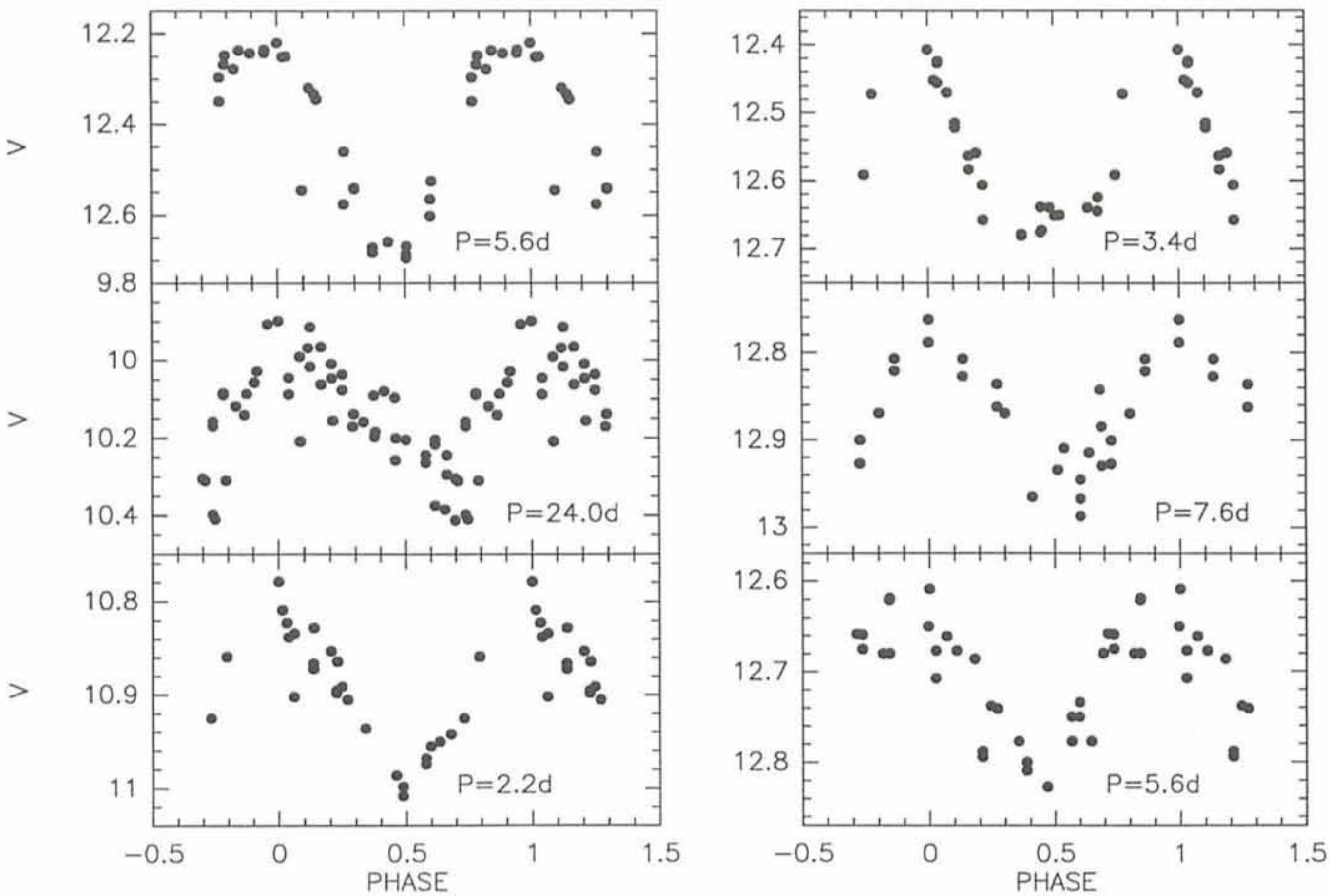

Figure 1: *Phased light curves of 6 stars from the COYOTES sample in the V-band. The photometric period is indicated in each panel. From bottom left to top right: LkCa-19, RY Tau, LkCa-7, IW Tau, DE Tau, LkCa-4.*

surprisingly, we found that *all* the 23 stars exhibit periodic light variations with periods between 1.2 and 24 days. Previous monitoring studies, spanning a time period of typically two weeks, had a detection rate of about 30%. Our much higher success rate mainly results from the much longer time period (3 months versus 2 weeks) over which we monitored the light curves of the programme stars. The phased light curves of 6 of the COYOTES stars are shown in Figure 1.

3. Cool and Hot Spots on T Tauri Stars

In 20 of the 23 programme stars, the photometric period results from the modulation of the stellar luminosity by surface spots, which directly yields the star's rotational period. The periodic light variations of the 3 remaining stars probably result from orbital motion in a binary system. The temperature and size of the spots responsible for the modulation of the stellar flux can be estimated from a model that reproduces the variation of the amplitude of modulation with wavelength from the U to I-band. Application of the spot model to the light curves of the programme stars indicates that cool spots, i.e., spots that are cooler than the stellar photosphere by about 1000 K, are responsible for the variability of weak-line TTS. These cool spots are stellar analogues of sunspots, albeit on a much larger scale since they cover typically 15% of the stellar surface compared to 0.01% for sunspots. The detection of such extended cool spots provides one of the strongest indirect evidences for the existence of kilogauss magnetic fields at the surface of T Tauri stars.

While only cool spots seem to be present at the surface of weak-line TTS, both cool and hot ($T_{spot} - T_{eff} \approx 1000$ K) spots are responsible for the flux modulation of classical TTS. The modelling of the light curves indicates that hot spots usually cover a much smaller fraction of the stellar surface than cool spots, typically a few per cent. That hot spots are exclusively found at the surface of stars which are surrounded by an accretion disk suggests that they trace the accretion shock at the stellar surface. The detection of rotational modulation by small hot spots then implies that the accretion flow is not uniformly distributed along the stellar equator, as could be expected from an axisymmetric accretion disk, but is strongly asymmetric. A possible explanation is that the accretion flow is channelled along the lines of the strong stellar magnetic field close to the stellar surface, thus resulting in localized hot accretion spots at the stellar surface.

4. The Rotational Properties of T Tauri Stars

Another clue for the interaction between the accretion disk and the star's magnetic field comes from the comparison between the rotational periods of weak-line (WTTS) and classical (CTTS) T Tauri stars. Histograms of the rotational periods of WTTS and CTTS are shown in Figure 2. These histograms include the rotational periods of 14 K7-M1 TTS from the COYOTES campaign as well as those published for 12 other K7-M1 TTS of the Taurus-Auriga cloud. Only stars with a spectral type between K7 and M1 are shown in order to deal with a homogeneous sample of 0.8-1.0 $M_\odot$ stars. The histograms show a statistically very significant difference between the rotational period distributions of WTTS and CTTS: 9 out of 11 WTTS have periods ranging from 1.2 to 6 days, while 13 out of 15 CTTS have periods between 6 and 12 days. The mean rotational period is 4.1 ± 1.7 d for WTTS, and 7.6 ± 2.1 d for CTTS. Hence, WTTS rotate faster than CTTS by nearly a factor of 2 on average.

This is a surprising result on several grounds. First, extensive measurements of the spectroscopic rotational velocities, *v*sin*i*, of many T Tauri stars performed in the 80's failed to reveal any significant difference between the rotation rates of WTTS and CTTS. Presumably, both measurement uncertainties and the unknown value of sin*i* conspired to hide the relatively subtle difference revealed by the COYOTES campaign. Second, while photometric monitoring demonstrates that CTTS rotate more slowly than WTTS, one would naively expect the opposite on theoretical grounds since CTTS accrete material from their rapidly rotating circumstellar disk, which ought to spin the star up, while WTTS do not possess accretion disks.

A possible explanation for the faster rotation rates of WTTS compared to CTTS is that the former are slightly older than the latter, though the two stellar groups are commonly believed to have similar ages. This belief mainly rests on their similar location in the H-R diagram and their similar lithium abundances. Still, these arguments are more suggestive than conclusive. On the one hand, it is not easy to locate classical T Tauri stars in the HR diagram due to the strong non-photospheric UV and IR excesses they exhibit. On the other hand, interpretation of lithium abundances of pre-main-sequence stars is somewhat uncertain due to the poor knowledge we have of the lithium depletion timescale at this stage of stellar evolution. Both WTTS and CTTS are contracting onto their pre-main-sequence evolutionary tracks toward the ZAMS. Therefore, if we assume that WTTS are slightly older than CTTS, their faster rotation rate would naturally result from their smaller radii (assuming no angular momentum loss). The observed difference of a factor of 2 between the rotation of WTTS and CTTS would then imply an age difference of a few 10^6 yrs, much smaller than the contraction timescale to the main sequence (a few 10^7 yrs). This hypothesis, however, is unlikely. If correct, it would imply that pre-main-sequence stars are continuously accelerated as they contract towards the main sequence, thus reaching the ZAMS with a rotational velocity in the range from about 40 to 150 km s^{-1}. While approximately half of ZAMS solar-mass stars do have velocities in this range (Stauffer 1991 and references therein), the other half have velocities less than 10-20 km s^{-1}, which cannot be explained in the framework of this hypothesis. Therefore, the results of the COYOTES campaign provide independent support to the coevality of CTTS and WTTS.

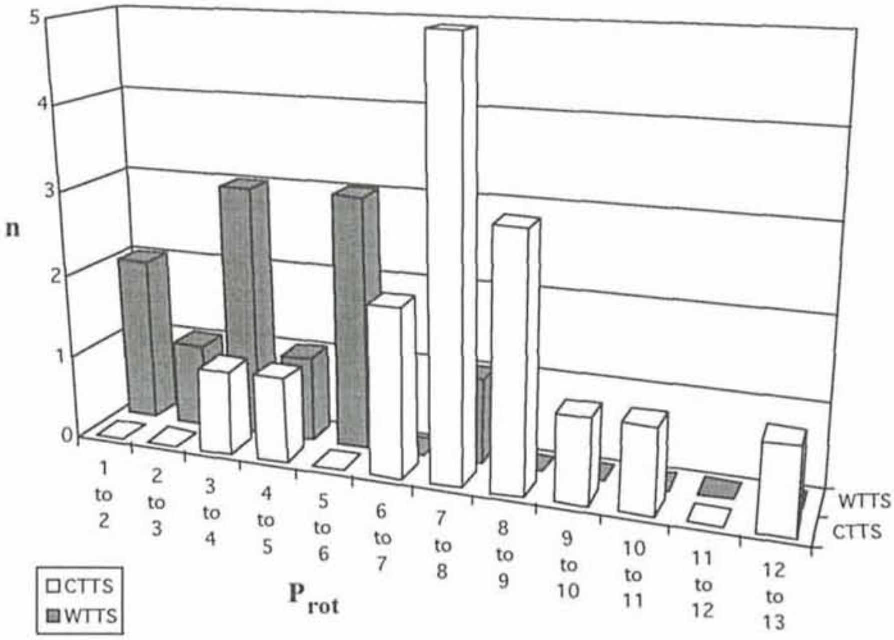

Figure 2: *Histograms of the rotational periods of weak-line (grey) and classical (white) T Tauri stars. A Kolmogorov-Smirnov test shows that the 2 distributions are different at the 99.9 % level, indicating that WTTS rotate faster than CTTS.*

What is then the origin of the different rotation rates between WTTS and CTTS? A paradoxical possibility is that accretion of circumstellar material leads to the braking of the central star rather than to its acceleration. Rotational braking due to accretion of circumstellar material is not a new idea. It was originally proposed by Ghosh and Lamb in 1979 to explain why some strongly magnetized, compact objects spin down while accreting material from a nearby companion. The deceleration of the accreting object is described as resulting from the interaction of the accretion flow with the strong star's magnetic field, which leads to a transfer of angular momentum from the star to the accretion disk. TTS are not pulsars; their magnetic field is much weaker than that of white dwarfs and neutron stars. Still, kilogauss fields appear to be sufficient to disrupt the inner regions of their accretion disk up to a distance of several radii from the star, thus channelling the accretion flow along the field lines and, incidentally, producing the hot accretion spots revealed by photometric monitoring. Models analogous to the Ghosh and Lamb model for compact objects have started to be developed for T Tauri stars (e.g., Königl 1991) and show that the disk may indeed be disrupted up to a large enough distance from the star (beyond the disk's co-rotation radius) so that angular momentum flows from the star to the disk, thus effectively braking the central star. By demonstrating that CTTS do rotate more slowly than WTTS, the results of the COYOTES campaign provide one of the strongest evidences for the interaction of the accretion flow with the stellar magnetic field and lend support to the recently developed models that describe the magnetospheric coupling between the central star and the disk.

5. Towards an Understanding of the Rotational Evolution of Young Stars

The hypothesis that young stars are braked by their accretion disks opens new perspectives to understand their subsequent rotational evolution to the zero-age main sequence (ZAMS). The observation that approximately half of the solar-type ZAMS stars have rotational velocities less than 20 km s^{-1} while the other half have velocities in the range from 40 to 150 km s^{-1} has remained a challenge to theoretical models for the last few years. The major difficulty was to understand how the relatively small dispersion of rotation rates observed among solar-mass T Tauri stars (from $\simeq$ 5 to 30 km s^{-1}) could result in such a wide range of velocities at the ZAMS (from $\simeq$ 5 to 150 km s^{-1}), 3 10^7 yrs later. The proposed interpretation of the COYOTES results may considerably alleviate this difficulty. In the framework of our hypothesis, WTTS do not possess accretion disks and are therefore continuously accelerated as they contract towards the main sequence. According to pre-main sequence evolution models, they will then end up onto the ZAMS with rotational velocities between 40 and 150 km s^{-1}, as observed for half of ZAMS, solar-type stars. CTTS, in contrast, are braked down to low velocities up to the point where they disperse their disk. The disk survival time is estimated to be of the order of 10^7 yr at most, i.e., the star is still some 2 10^7 yr away from the ZAMS. From thereon, having lost its disk, the star will spin up as would a WTTS. However, if the star was braked down to a velocity of a few km s^{-1} at the end of the accretion phase, it will still reach the ZAMS with a velocity of less than 20 km s^{-1}, thus accounting for the other half of ZAMS stars observed to have small velocities.

Admittedly, the above description of how CTTS evolve into slowly rotating ZAMS stars while WTTS are the progenitors of rapidly rotating ZAMS dwarfs may be a little over-optimistic. Many issues have to be addressed more quantitatively. For instance, are CTTS really braked by their disks down to small enough velocities, i.e., a few km s^{-1} at most, so that they reach the ZAMS with a *v*sin*i* of less than 20 km s^{-1}? The answer to this and other pending questions awaits further observational and theoretical work. Other campaigns such as COYOTES I will have to determine the rotational periods of stars with an age intermediate between T Tauri stars and ZAMS dwarfs, which will allow one to trace observationally the evolution of angular momentum of solar-type stars prior to the main sequence. Observations will also have to provide better estimates of both the strength and surface coverage of magnetic fields in T Tauri stars and bring clues to the field structure (dipole vs. multipole?). Helped by these new constraints, theoreticians will have to develop more realistic models of the interaction between the accretion flow and the star's magnetic field, thus enabling more accurate predictions as to the impact of disk accretion onto the angular momentum evolution of young stars.

6. Conclusion

The unexpected results obtained from the COYOTES I campaign clearly illustrate how powerful coordinated observations of T Tauri stars are, even from such a site as La Silla where performing (relatively) accurate photometry of Taurus stars (Dec. ≃ +15°) with the bright moon not very far from the target stars is (almost) an art. At the time this contribution is being written, COYOTES II has been completed. It took place during the winter 1992–1993 and involved the same participants as COYOTES I plus a few more. The results are under analysis. A complete description and analysis of COYOTES I results are being published in two papers in A&A.

References

Bertout C. 1989, *ARA&A* **27**, 351.

Bouvier J. 1991, in: *Angular Momentum Evolution of Young Stars*, ed. S. Catalano and J. Stauffer, p. 41.

Ghosh P., Lamb F.K. 1979, *ApJ* **234**, 296.

Königl A. 1991, *ApJ* **370**, L39.

Schatzman E. 1962, *Ann. d'Ap.* **25**, 18.

Stauffer J. 1991, in: *Angular Momentum Evolution of Young Stars*, ed. S. Catalano and J. Stauffer, p. 117.

TY CrA: a Pre-Main-Sequence Binary

A.M. LAGRANGE, J. BOUVIER, P. CORPORON, Observatoire de Grenoble, France

The southern young star TY CrA, embedded in the reflection nebulae NGC 6726/7, has a strong far-IR excess which is attributed to circumstellar cold grains, larger than the usual interstellar grains, cf. Cruz-Gonzales et al. [1984] and Bibo et al. [1992]. Photometric variability has been found by Kardopolov et al. [1981], and the photometric curve is known to be the one of an eclipsing binary system, with a 2.888777-day period.

Spectroscopic observations of this object have been performed in the period 1990–1992 with the CES and the 1.4-metre CAT at La Silla. Lines of CA II K, Ca II triplet, Mg II, Ti II, Hα, He I, O I and Na I were investigated (Lagrange et al. [1993] and we show in Figure 1 some of the spectra which were obtained.

The three main results are the following:

- Contrary to what is generally observed for Herbig stars, no strong emission is seen in any of the investigated lines. This had already been noticed by Finkenzeller and Mundt [1984] for the Hα line. However, it is still possible that this line, as well as the Ca II line, do have absorption that is partly filled by emission. Moreover, we detected for the first time transient, blue-shifted emission in the O I triplet lines.
- Narrow absorption lines are observed with FWHM ≤ 8 km s^{-1} in the CA II K, Ca II triplet, Ti II, Na I, O I, as well as cores in the Hα and He I lines. The Na I line additionally exhibits a broad absorption profile.
- The narrow absorption lines are periodically variable in velocity; this is shown in Figure 2, where a 2.888777d phase diagram has been constructed for the radial velocities of all the narrow lines. The radial velocity period is the same as the photometric period previously reported by Kardopolov et al. [1981].

Our data thus provide the first direct evidence that TY CrA is a spectroscopic binary. As the radial velocity variations of *all* the narrow lines can be phased together, we can conclude that all these lines have a common origin. In contrast, the broad components of the Na I lines exhibit radial velocity variations that are anti-correlated with those of the narrow component. This then argues for a different origin.

From Figure 2, we get a radial velocity semi-amplitude for the primary of ≃ 75 km s^{-1}. Assuming an eccentricity of 0 and sin*i* = 1 since it is an eclipsing system, and knowing the 2.888777-day period, we derive a semi-major axis of 4.56 $R_\odot$ for this component. For a mass ranging between 4 and 7$M_\odot$ for the B7 primary star, Kepler's third law implies a mass between 1.8 and 2.5 $M_\odot$ for the secondary, and a total semi-major axis between 15.4 and 18.1 $R_\odot$. This range of mass for the second component corresponds to spectral type A. Other observations will now be performed to further investigate the spectral types of both components.

The observations described above show that TY CrA is a spectroscopic binary. To our knowledge, this is the first spectroscopic binary observed among the Ae–Be Herbig stars. The origin of the narrow components, however, remains puzzling. If they are of photospheric origin, it would imply a spectral type B7 for the primary (somewhat earlier than B8-9 as previously reported) with $v \cdot sin(i) \leq$

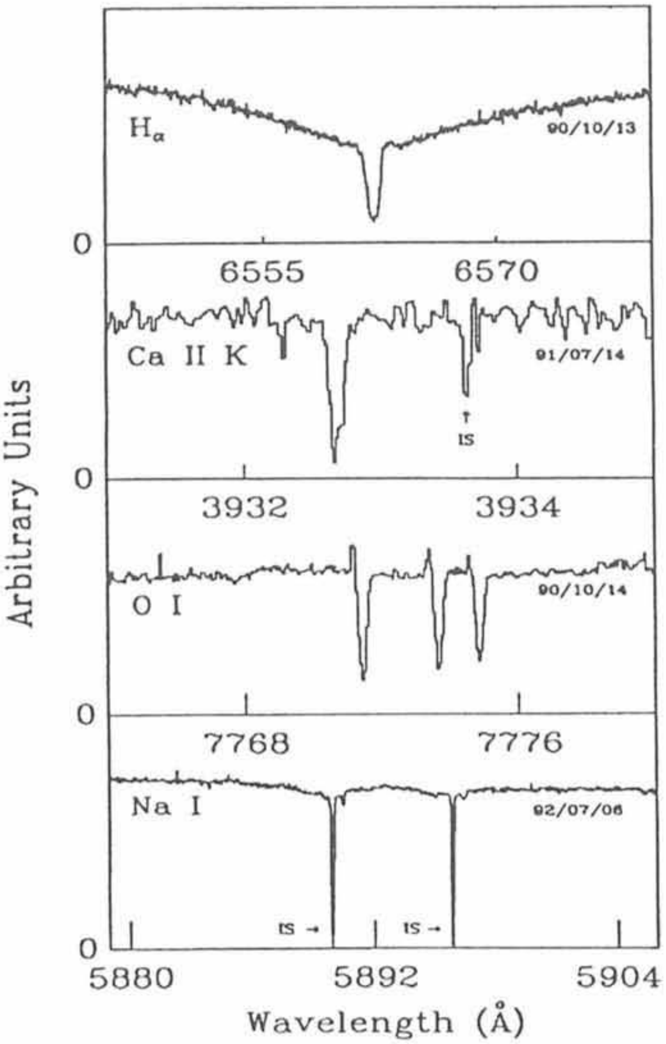

Figure 1: *Examples of high-resolution spectra of TY CrA with lines of Hα, Ca II K, O I, Na I. Narrow absorption lines are observed, and there is a narrow core at the bottom of the Hα line; see the text. They are all variable in velocity except those of IS origin (indicated with an arrow). Note the narrow absorption feature and the broader absorption in the Na I line.* ◀

Figure 2: *Heliocentric velocities of all observed narrow lines (FWHM ≤ 50 km s^{-1}), folded in phase with a period of 2.888777 days.* ▼

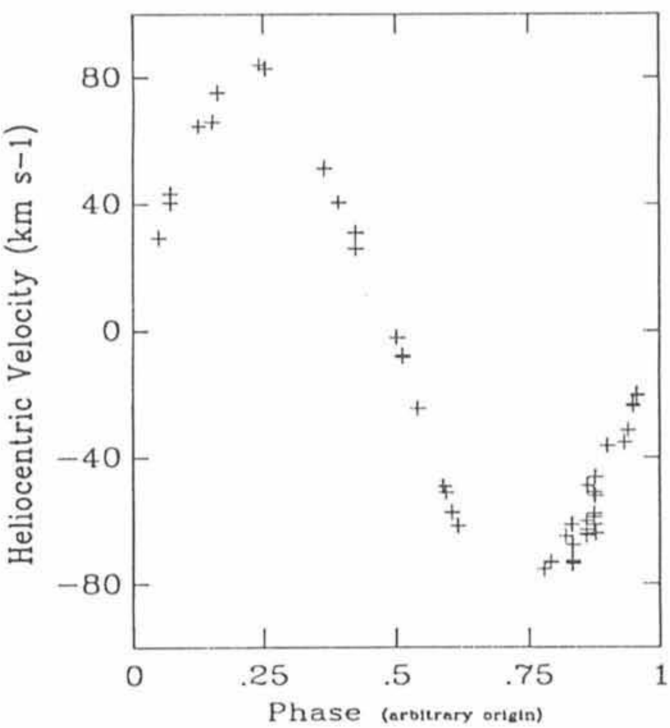

8 km s^{-1}. Since we are dealing with an eclipsing binary system, this means that the true rotational velocity of this B7 star is close to this value: but such a value does not fit with the rotational velocity expected for a 3 $R_\odot$ object, if the rotational and 2.9-day orbital motions are synchronized (55 km s^{-1}).

Another possibility is that the narrow lines originate in a circumstellar shell (CS) that surrounds the primary component. In fact, these narrow lines are very similar to the ones observed for the A-type main-sequence star βPictoris, which are clearly due to CS gas. TY CrA's spectrum is more similar to that of βPictoris than to those of usual Herbig stars. This may indicate that this star is more evolved than the latter objects, perhaps very near the end of its pre-Main-Sequence evolution. Further observations are needed to pursue the investigation of this possibility.

References

[1992] Bibo E.A., The P.S. and Dawanas D.N., 1992, *A&A* **260**, 293.

[1984] Cruz-Gonzalez I., McBreen B.P. and Fazio G.G., 1984, *ApJ* **279**, 679.

[1984] Finkenzeller, U., and Mundt, R., 1984, *A & AS* **55**, 109.

[1981] Kardopolov V.I., Sahanionok V.V. and Philipjew G.K., 1981, *Perem. Zvezdy*, **21**, 589.

[1993] Lagrange A.M., Corporon P., Bouvier J., 1993, *A&A*, in press.

Atomic Processes and Excitation in Planetary Nebulae

X.-W. LIU, Beijing Observatory, P.R. China,
and J. DANZIGER, ESO

Introduction

Owing to their relatively simple geometry and physical conditions, Planetary Nebulae (PNe) are potentially an ideal laboratory to study various atomic processes important in gaseous nebulae. O III Bowen fluorescence lines, excited by the ultraviolet pumping of the $2p^2\ ^3P_2$–$2p3d\ ^3P^o_2$ line of O III at 303.799 Å by the He II Lyα line at 303.780 Å (Bowen 1934, 1935), are observed in a variety of astrophysical sources, as diverse as PNe, Seyfert galaxies, the Sun, and X-ray binary and burster sources (Schachter et al. 1989, 1990, 1991; Sternberg et al. 1988 and the references therein). These lines are interesting because they provide a powerful diagnostic probe of the physical environment in which they appear. Charge transfer (CT hereafter) of O^{3+} ions in collisions with hydrogen atoms, $O^{3+} + H^0 \rightarrow O^{2+} + H^+$ populates excited states of O^{2+} (Dalgarno, Heil and Butler 1981, DHB hereafter), and con-

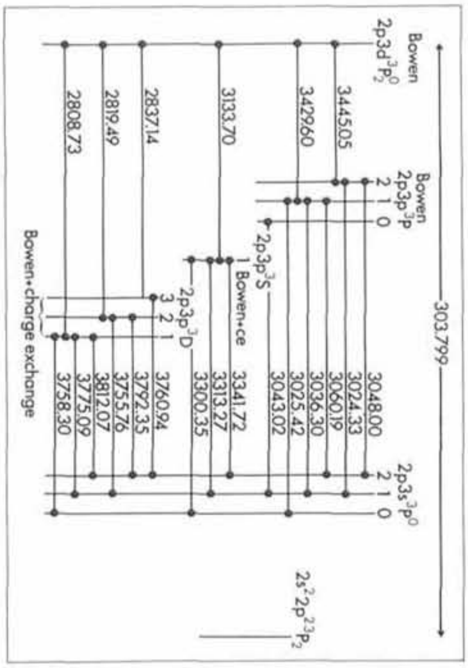

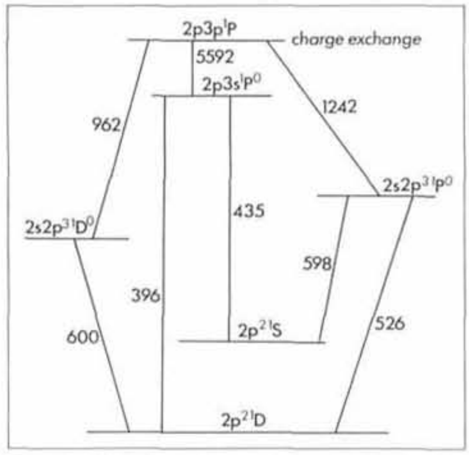

Figure 1: *We show the energy level diagrams for most of the relevant transitions in the optical domain arising from Bowen fluorescence and charge exchange mechanisms.*

tributes significantly to the Bowen cascade from the ^3D state in some planetary nebulae. CT also populates the singlet state 2p3p ^1P which provides an allowed transition at 5592 Å (DHB; Dalgarno and Sternberg 1982). Figure 1 provides an abbreviated description of the relevant energy levels. Charge transfer is an important process in determining the ionization equilibrium and now is a standard ingredient in models of gaseous nebulae.

Since 1986, we have systematically observed the OIII Bowen fluorescence and CT lines in a number of high-excitation PNe. Sample spectra of NGC 3242 are plotted in Figure 2. From these data we have obtained a number of interesting results which are summarized below. In addition, we will address the important problem of electron temperature fluctuations in PNe. Details of these results have been given elsewhere (Liu and Danziger 1993a, b; Liu, Danziger and Murdin 1993). Interested readers are referred to those papers.

The Bowen Fluorescence Line Ratios and Evidence for Departure from Pure LS Coupling

The relative intensities of the Bowen fluorescence lines depend only on the radiative transition probabilities, and measurements of these lines give a direct verification of these quantities. The radiative transition probabilities of OIII have been calculated by Saraph and Seaton (1980, hereafter SS) and by Luo et al. (1989, hereafter LPSSY). In these approaches LS coupling is assumed. Calculations of OIII transition probabilities within the scheme of intermediate coupling are presented by Kastner, Behring and Bhatia (1983, hereafter KBB) and by Kastner and Bhatia (1990, hereafter KB).

Our measurements in the λλ3100–4000 wavelength region at resolutions and S/N greater than previously used show:

(1) The observed ratios λ3428/λ3444, λ3299/λ3341, λ3312/λ3341, λ3791/λ3755 and λ3774/λ3757, where each of these pairs of lines in the ratio decay from the same upper level and belong to the same multiplet; thus their ratios depend only on the assumed coupling scheme, and deviate from the predictions of pure LS coupling and are in better agreement with those using intermediate coupling calculated by KBB and KB. Echelle observations of NGC 7009 between λλ3750–3800 with a resolving power as high as 40,000 strengthen the conclusion that the discrepancies are not due to blending effects from unidentified lines.

(2) The observed ratio I(λ3133)/I(λ3444 + λ3428) is best reproduced using the transition probabilities from LPSSY and is in disagreement with that predicted by KB. Although the three lines decay from the same upper level, the λ3133 belongs to a multiplet other than that of the λ3444 and λ3428. Therefore, this ratio depends not only on the coupling scheme but also on transition probabilities for the multiplet. Similarly, the observed ratio I(λ3299 + λ3312 + λ3341)/I(λ3133), after the contribution from CT to the λ3299, λ3312 and λ3341 has been corrected, is in best agreement with that predicted by LPSSY. However, there is weak evidence that even in the calculations of LPSSY, the role of depopulation of the 2p3p ^3S, ^3D levels by cascades has been overestimated by about 5–10%. It appears that the results given by LPSSY represent the best available calculations of OIII transition probabilities for these permitted lines.

The Efficiency of the Bowen Fluorescence Mechanism

The fraction of HeII photons that are absorbed by the O^{2+} ions and converted to the Bowen fluorescence lines may depend on a number of characteristics of the nebula, including the optical depth of the HeII Lyα, the geometry and the thermal and ionizational structure of the nebulae. Photoionization of the residual H^0 and He^0 in the He^{2+} zone as well as dust absorption can also destroy the HeII Lyα photons.

The efficiency, R, of the Bowen fluorescence mechanism (BFM hereafter) quantifies the fraction of all those HeII Lyα photons created following recombination of He^{2+} ions and electrons which are converted to Bowen fluorescence lines. The value of R can be derived by comparing a Bowen fluorescence line (e.g. OIIIλ3133) and a HeII recombination line (e.g. HeIIλ4686). The efficiency of the BFM is an important quantity because it provides a unique probe to study the radiative transfer problem of the (extremely optically thick) HeII Lyα line. Calculations of R in model PNe and Seyfert galaxies (Weymann and Williams 1969, Harrington 1972, Kallman and McCray 1980) show that R ≈ 0.5, and is insensitive to the input parameters, such as temperature, ionizing source and the resulting ionizing structure.

Measurements of R in PNe are presented by Barker (1978) and Likkel and

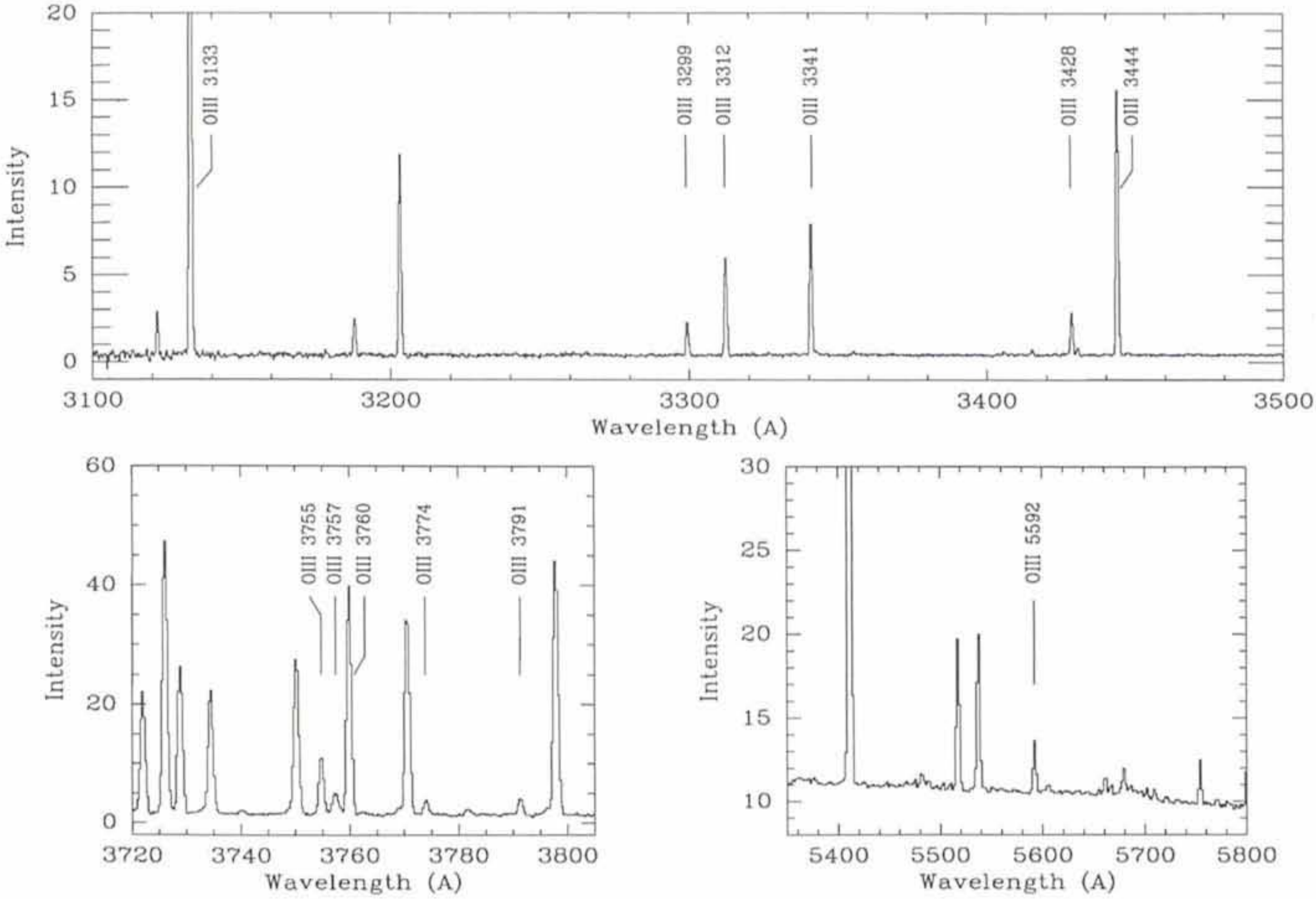

Figure 2: *Integrated spectra of NGC 3242 showing all the O III Bowen fluorescence and charge transfer lines discussed in the paper. The spectra in the blue and UV regions were secured at La Palma in January 1987, using INT 2.5-m + IDS + IPCS and with a spectral resolution of 0.72 Å in FWHM. The one in the yellow region was obtained at ESO-La Silla in January 1991, using ESO/MPI 2.2-m + B&C + CCD. The observed intensities of λ3299, λ3791 and λ5592 relative to Hβ are 0.026, 0.0024 and 0.00064, respectively.*

Aller (1986, hereafter LA). From our new high quality observations, we have derived accurate values of R in 14 PNe, and a wide range is apparent. These new measurements are analysed together with those presented by Barker (1978) and LA. Some new understanding of the Bowen fluorescence efficiencies has been achieved through the correlation of accurately determined efficiencies with other characteristic parameters of the nebulae. It is found that when the expansion velocity of O^{2+} exceeds 28 km/s, the efficiency drops abruptly, a result supported by quantitative considerations. We show that there is a good linear positive correlation between the Bowen efficiencies and the fractional abundances of singly ionized helium and doubly ionized oxygen, as well as a remarkable anticorrelation between the Bowen efficiencies and the electron temperature as first noted by LA. The difference in R between PNe with different morphology types or excited by stars with different spectral characteristics as suggested by LA is however not observed.

Obviously, the observations agree only marginally with modelling calculations and there are a number of results not accommodated by the currently available theoretical predictions. To interpret these results, calculations of the efficiency of Bowen conversion based on detailed modelling, taking into account both the thermal and ionization structure of individual nebulae are necessary.

Rate Coefficients for CT Reaction $O^{3+} + H^0 \rightarrow O^{2+} + H^+$

As described in section 1, the CT reaction between O^{3+} and H^0 is a significant source of the excitation of the O III multiplet λ3760 emitted from the ^3D state. Rate coefficients of this process have been calculated by DHB, Gargaud et al. (1989, GMO hereafter) and by Roueff and Dalgarno (1988, RD hereafter). In the calculations of DHB and GMO neither the fine-structure levels of the ground term of O IV 2p $^2P_{1/2,3/2}$ nor those of the product O III are taken into account. Dalgarno and Sternberg (1982) suggest that the CT excitation of the O III 2p3p ^3D_J(J = 1,2,3) levels tends to equalize the fine-structure populations and they assume that the rate coefficients into the individual fine-structure levels of ^3D are equal. This suggestion is not supported by the calculations of RD where the individual fine-structure levels of both the initial O^{3+} ion and the product O^{2+} have been taken into account. They find that the cross-sections increase approximately with the statistical weights of the fine-structure levels, i.e. 2J + 1.

By observing the lines excited only by the BFM and the pure CT line λ5592, we are able to decouple these two processes, which in turn enables for the first time accurate measurement of the relative CT rate coefficient k(2p3p ^3D_J)/ k(2p3p ^1P) (J = 1, 2 and 3).

Lines of the multiplets containing λ3760 as well as the λ5592 are generally quite weak and may be contaminated by excitation from processes other than the BFM and CT. One of the possible mechanisms is excitation by dielectronic and radiative recombination. To estimate the contribution from this process, we make use of the O IIIλ3261, λ3265 and λ3267 lines of multiplet

$2p3p\ ^3D_3 - 2p3d\ ^3F^o_4$. This multiplet has been identified for the first time and measured in most objects studied here. Due to the large orbital angular momentum of the upper levels, these lines are very likely excited only by radiative and dielectronic recombination. This is confirmed by the close agreement found between the ionic abundances of O^{3+} derived from this multiplet with those from the UV collisionally excited lines OIV]λλ1403, 1409 in objects for which measurements of both the UV and the optical lines are available. Another possible mechanism which might excite the lines studied here is fluorescent absorption of stellar UV radiation. However, we show that this process is completely negligible for lines we are interested in.

The derived values of $k(2p3p\ ^3D_J)/k(2p3p\ ^1P)$ are found to be sensitive to the adopted transition probabilities. This is particularly true for the $^3D_3$ level mainly excited by the BFM and in objects of relatively low excitation. CT is found to be more efficient in objects of higher excitation class. When the transition probabilities from LPSSY are adopted, the values of the above ratio found from measurements of different objects have the smallest scatter, giving $k(2p3p\ ^3D_J)/k(2p3p\ ^1P) = 1.44 \pm 0.17$, 1.10 ± 0.13 and 1.03 ± 0.32 for J = 1, 2 and 3, respectively. These values lie somewhere between the predictions of 1.40 and 0.98, independent of J, by DHB and by GMO, respectively, and support the suggestion by Dalgarno and Sternberg (1982) that the charge transfer reaction tends to equalize the fine-structure populations, giving an equal rate coefficient for the three fine-structure levels of 2p3p ^3D. They are certainly inconsistent with the theoretical predictions of RD who find $k(2p3p\ ^3D_J) = 1.4$, 2.2 and 3.1 for J = 1, 2 and 3, respectively, i.e. $k(2p3p\ ^3D_J)$ increases approximately with 2J + 1. It seems to us that $k(2p3p\ ^3D_J)/k(2p3p\ ^1P) = 1.20$, independent of J, would be a good value to adopt for the moment and should be accurate to about 30%.

Stronger conclusions on the CT rate coefficients than those reached in this work are frustrated by the uncertainties in the available atomic data. Again, more accurate calculations of O^{2+} transition probabilities, especially taking into account the deviation from pure LS coupling are highly desirable.

Nebular Continuum Emission and Evidence for Temperature Fluctuations

As a by-product of the observations carried out above, we have obtained accurate measurements of the Balmer discontinuity of nebular continuum emission. A spectrum showing the Balmer discontinuity in NGC 3242 is given in Figure 3. The most important application of measured Balmer discontinuities is that they provide information on the electron temperature. Using this method, Peimbert (1971) derived electron temperatures in three planetary nebulae and for several regions in the Orion nebula and found that the temperatures derived in this way were systematically lower than those found from forbidden lines. He attributes this difference to temperature fluctuations in the nebulae and uses their difference to make first-order corrections for the effect of temperature fluctuations on abundance determinations. The physical idea is that the nebular continuum emission originates from recombination processes and weights preferentially low-temperature regions whereas the forbidden lines are excited by electron collisions and weight preferentially high-temperature regions. Thus if there are temperature fluctuations, the electron temperature derived from the Balmer discontinuity, T_e(Bal), will be lower than that derived from the [OIII] nebular to auroral line ratio I(λ4959 + λ5007)/I(λ4363), T_e([OIII]na). On the other hand, Barker (1978, 1979) derived electron temperatures from observations of the Balmer discontinuity for a number of PN's but found general agreement with those parameters from forbidden lines.

From the new measurements of the Balmer discontinuity, we have derived T_e(Bal) in fourteen PNe. These, together with those presented by Peimbert (1971) and by Barker (1978) are compared to T_e([OIII]na). In total there are 34 objects, covering a wide range of excitation class and electron temperature. The data clearly show that T_e(Bal) tends to be lower than T_e([OIII]na) for the same objects, with the former on the average about 1500 K lower than the latter, which corresponds to a temperature fluctuation parameter $t^2 = 0.029$ as defined by Peimbert (1967). There are however, a few objects for which T_e(Bal) is considerably lower than T_e([OIII]na), leading to values of t^2 as large as 0.10. Excluding these extreme cases, we recommend that $t^2 = 0.030$ may be used as a representative value for most PNe. This value has the effect that composition determinations of PNe assuming a homogeneous temperature may underestimate the metal abundance by about 0.1 dex.

The observed large temperature fluctuations cannot be reconciled with the current models of PNe (cf. Harrington et al., 1982) and some additional mechanisms are required to explain the observations. At the moment, two possibilities can be envisaged. One is that there is an additional source of energy input to the nebulae other than the photoionization, e.g. shock waves produced by stellar winds (Peimbert et al., 1991). Large temperature fluctuations can also be produced if the PNe are very inhomogeneous in chemical composition, such as suggested by the models of NGC 4361 constructed by Torres-Peimbert et al. (1990). Further evidence for an additional heating mechanism other than the photoionization in at least some planetary nebulae is provided by new observa-

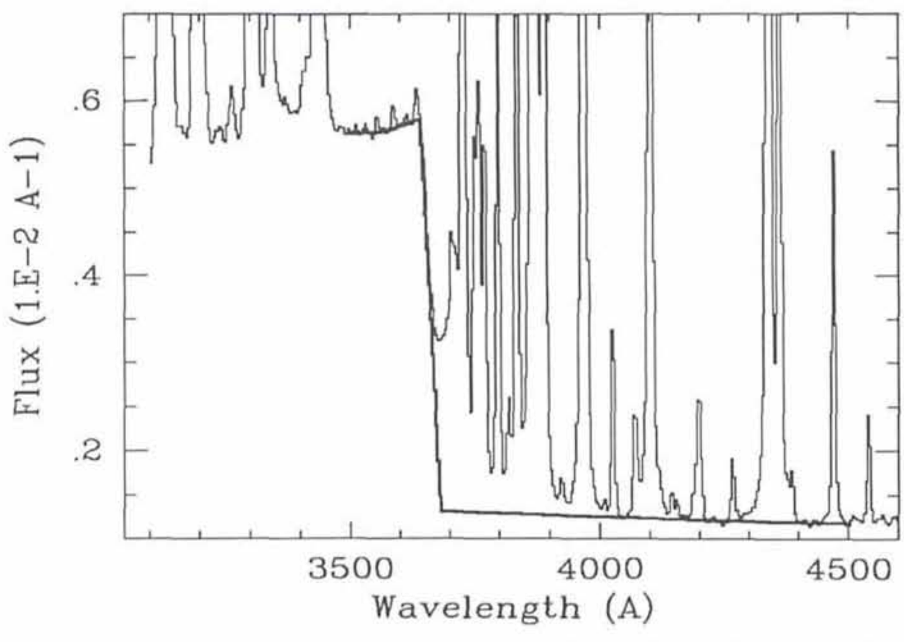

Figure 3: *Integrated spectrum of NGC 3242 showing the Balmer discontinuity at λ3645. The observation was carried out in February 1991 using ESO/MPI 2.2-m + B&C = CCD. The thick line overplotted is a spline fit to the estimated continuum (nebular plus stellar).*

tions in X-ray carried out with ROSAT. Kreysing et al. (1992) report detection of extended X-ray emission from six planetary nebulae. It appears that these objects tend to have exceptional large temperature fluctuation and belong to a special group in which some unknown process (e.g. shock heating) is playing an important role. This category includes objects such as NGC 2392, NGC 4361, NGC 6543 and J320. Further investigation is required to clarify the problem. It is worth noting that the type of work described above can be accomplished on modest sized telescopes provided there is adequate UV throughput of the system.

References

Barker, T., 1978, *Ap.J.*, **219**, 914.
Barker, T., 1979, *Ap.J.*, **227**, 863.
Bowen, I. S., 1934, *Pub. A. S. P.*, **46**, 146.
Bowen, I. S., 1935, *Ap.J.*, **81**, 1.
Dalgarno, A., Heil, T. G. and Butler, S. E., 1981, *Ap.J.*, **245**, 793 (DHB).
Dalgarno, A. and Sternberg, A., 1982, *M.N.R.A.S.*, **200**, 77P.
Gargaud, M., McCarroll, R. and Opradolce, I., 1989, *Astr. Ap.*, **208**, 251 (GMO).
Harrington, J. P., 1972, *Ap.J.*, **176**, 127.
Harrington, J. P., Seaton, M. J., Adams, S. and Lutz, J. H., 1982, *M.N.R.A.S.*, **199**, 517.
Kallman, T. and McCray, R., 1980, *Ap.J.*, **242**, 615.
Kastner, S. O., Behring, W. E. and Bhatia, A. K., 1983, *Ap.J. (Supplement)*, **53**, 129 (KBB).
Kastner, S. O., and Bhatia, A. K., 1990, *Ap.J.*, **362**, 745 (KB).
Kreysing, H. C., Diesch, C., Zweigle, J., Staubert, R., Grewing, M. and Hasinger, G., 1992, *Astr.Ap.*, **264**, 623.
Likkel, L. and Aller, L. H., 1986, *Ap.J.*, **301**, 825 (LA).
Liu, X. W. and Danziger, I. J., 1993a, *M.N.R.A.S.*, in press.
Liu, X. W. and Danziger, I. J., 1993b, *M.N.R.A.S.*, in press.
Liu, X. W. and Danziger, I. J. and Murdin, P., 1993, *M.N.R.A.S.*, in press.
Luo, D., Pradhan, A. K. Saraph, H. E., Storey, P. J. and Yu Yan, 1989, J. Phys. B., **22**, 389 (LPSSY).
Peimbert, M., 1967, *Ap.J.*, **150**, 825.
Peimbert, M., 1971, *Bol. Observ. de Tonantzintla Y Tacubaya*, **6**, 29.
Peimbert, M., Sarmiento, A. and Fierro, J., 1991, *Pub. A.S.P.*, **103**, 815.
Roueff, E. and Dalgarno, A., 1988, *Phys. Rev.*, A **38**, 93 (RD).
Saraph, H. E. and Seaton, M. J., 1980, *M.N.R.A.S.*, **193**, 617 (SS).
Schachter, J., Filippenko, A. V., and Kahn, S. M., 1989, *Ap.J.*, **340**, 1049.
Schachter, J., Filippenko, A. V., and Kahn, S. M., 1990, *Ap.J.*, **362**, 74.
Schachter, J., Filippenko, A. V., Kahn, S. M. and Paerels, F. B. S., 1991, *Ap.J.*, **373**, 633.
Sternberg, A., Dalgarno, A. and Roueff, E., 1988, *Comments Astrophys.*, **13**, 29.
Torres-Peimbert, S., Peimbert, M. and Peña, M., 1990, *Astr.Ap.*, **233**, 540.
Weymann, R. J. and Williams, R. E., 1969, *Ap.J.*, **157**, 1201.

Two New Catalogues of Small Magellanic Cloud Members Coming Soon

M. AZZOPARDI, ESO and Observatoire de Marseille, France

Within the framework of our studies of the stellar populations of the Small Magellanic Cloud (SMC) two extensive surveys – one for carbon stars and one for point-source Hα emission-line objects – were undertaken in the early eighties. For these surveys we introduced an observing technique which turned out to be very efficient for the detection of the SMC OB and blue supergiant stars (Azzopardi and Vigneau 1975), as well as for the identification of the Magellanic Cloud Wolf-Rayet stars (Azzopardi and Breysacher 1979, 1980). Briefly, the surveys combined a IIa-O emulsion with a suitable interference filter in order to restrict the instrumental spectral range to a selected useful spectral domain, according to the type of object to be detected. By reducing the sky background, the interference filter allowed longer exposures hence reaching fainter stars. Furthermore, since the resulting spectra on the plates were very short, the number of overlaps was kept low enough to make the survey of very crowded SMC regions possible.

Due to the relative faintness of the objects we have detected, which are generally located in very crowded fields, accurate positions and clear finding charts are absolutely necessary to facilitate further observations. For this purpose, the equatorial coordinates (equinox 2000.0) of the objects of interest, in both surveys, were inferred from those of several secondary astrometric reference stars. The positions of these stars were themselves computed with reference to the right ascension and the declination of the stars listed in the Perth catalogue and appearing on the ESO Schmidt telescope plate No. 6266. The transformation of very accurate x-, y-coordinates into equatorial coordinates, for all the stars, was done using special astrometry routines written at ESO by R. West. The objects listed in both catalogues were identified on individual finding charts of 2.25 arcmin square. These have been extracted from scans of a glass copy of the Schmidt red plate No. 6266, processed at the ESO Sky Atlas Laboratory by B. Dumoulin using an improved unsharp masking technique in order to reduce the density range of the deep original plate while keeping the fine details of the image. The plate has been scanned by J. Marchal at Nice Observatory with a PDS 1010A microdensitometer linked to a VAX 785 computer. Extensive photographic work has been done by M. Gerbal and H.H. Heyer when preparing each set of finding charts.

SMC Carbon Star Survey

Earlier detections of carbon stars in the Magellanic Clouds were carried out by Blanco, McCarthy and Blanco (1980) and Blanco and McCarthy (1983). Their survey, in the near infrared spectral domain, of 37 SMC sample regions with the Cerro Tololo Inter-American Observatory (CTIO) 4-m telescope equipped with low-dispersion transmission gratings (grisms) resulted in the identification of 860 carbon stars in the Small Cloud. From the carbon star-count isopleths, based on the sample region surface densities found for these stars, Blanco and McCarthy (1983) estimated the total number of the SMC carbon stars to be 2900.

In the mean time, during the 1981, 1983 and 1984 Magellanic Cloud observing periods, an extensive spectral survey for field carbon stars in the SMC was carried out by B.E. Westerlund, J. Breysacher and the author, in order to get the best possible picture of the distribution of these stars. Adopting the Sanduleak and Philip (1977) survey technique in searching for carbon stars (identification of their pronounced C_2 Swan bands at 4735 Å and especially at 5165 Å), we used the ESO 3.6-m telescope equipped with the large-field triplet adaptor (0.78 degree circular field)

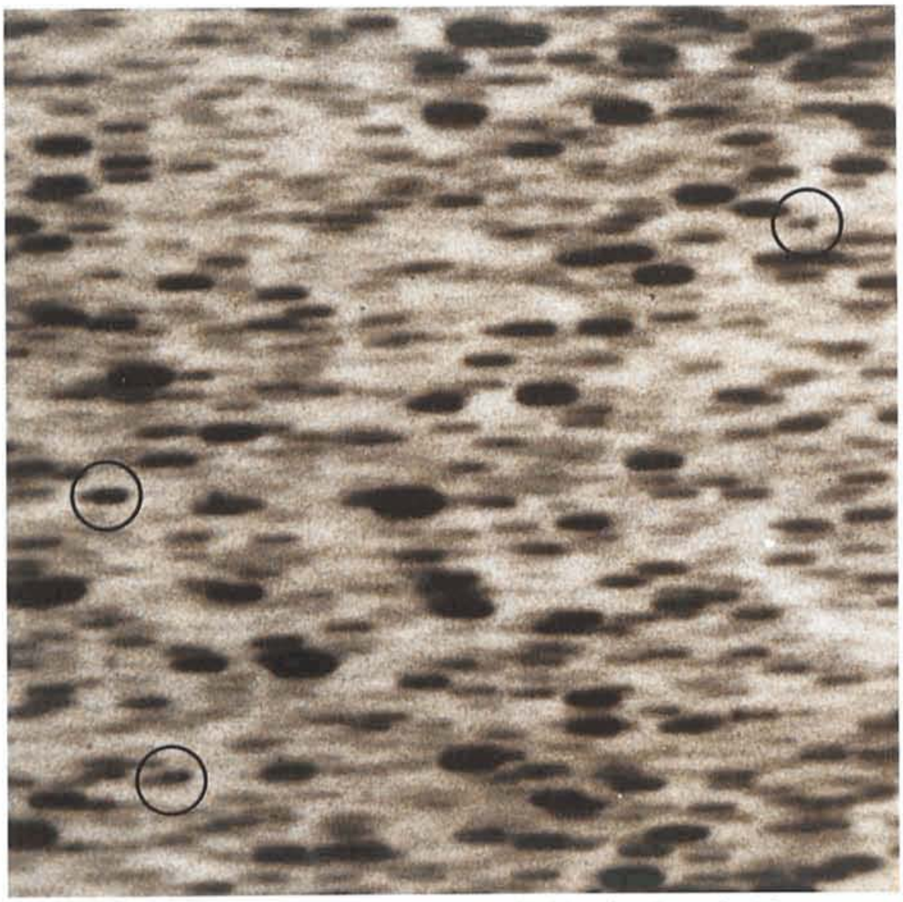

Figure 1: *Crowded field in the southern region of the SMC bar. Small part of a 1-hour exposure ESO grism plate obtained on IIIa-J emulsion through a Schott GG435 filter. The spectra of some newly identified carbon stars are marked with circles.*

and a Hoag grism yielding a dispersion of 2200 Å/mm. The restricted useful range (4350–5300 Å) was obtained, in that case, by combining a IIIa-J emulsion with a Schott GG435 filter (for more information see the paper by Breysacher and Lequeux 1983). 28 plates for 13 partially overlapping fields, which together cover the main body of the SMC, were secured during three observing runs, by J. Breysacher from the outset of the project, and then by myself.

Both 60-min- and 5-min-exposure grism plates were systematically surveyed with a binocular microscope: three fields were first searched for carbon stars by B.E. Westerlund and the author to work out the plate survey procedure and determine the specific spectral features to be measured (Westerlund, Azzopardi and Breysacher 1986), then all plate material was carefully scrutinized and processed by E. Rebeirot at the Marseille Observatory. The spectra of the identified carbon stars were scanned individually, in the density mode, on our deepest exposure plates, using the microdensitometer PDS 1010A of the Laboratoire d'Astronomie Spatiale (LAS) de Marseille; density to intensity transformation, image processing and data reduction were performed as explained by Westerlund et al. (1986). This provided a magnitude, a colour equivalent and two measurements of the strength (equivalent width and depth) of the C_2 band at 5165 Å.

This survey resulted in the identification of 1707 field carbon stars found in the main body of the SMC. A comparison of the near-infrared carbon star survey by Blanco and associates with our survey work, for the fields in common, leads to the conclusion that the detection of those objects in the SMC is reasonably complete. At present, the degree of completeness achieved in the recognition of field carbon stars in the Small Cloud makes possible the study of its large-scale structure and kinematics, as shown, for instance, by the works of Hardy, Suntzeff and Azzopardi (1989), and Azzopardi and Rebeirot (1991). An important result inferred from those studies is that the SMC carbon stars, like the planetary nebulae, form an intermediate-age or old stellar population on the average, lying in an almost elliptical system with no concentration, more especially in the so-called SMC wing (region of the young clusters NGC456, 460 and 465). Consequently, the overall carbon star surface distribution, that resembles the distribution of the red light (de Vaucouleurs and Freeman 1973), is markedly different from that of Population I objects. In addition, subsequent medium resolution spectroscopy of some carbon stars listed in our catalogue, remarkable for their magnitudes and/or colours, led to the discrimination of natural groups of stars, and among other things, to the discovery of a sample of very faint carbon stars ($-3.0 < M_{bol} \leq -1.7$), which are the faintest ever found in a galaxy (Westerlund, Azzopardi, Breysacher and Rebeirot 1991, 1992), except for the galactic bulge (Westerlund, Lequeux, Azzopardi and Rebeirot, 1991).

In order to facilitate further studies, a paper by Rebeirot, Azzopardi and Westerlund (1993) entitled "Carbon Stars in the Small Magellanic Cloud – II. Catalogue of 1707 Objects with Identifications and Spectrophotometry" will appear in the next February issue (Vol. **97**, No. 3) of *Astronomy and Astrophysics Supplement Series*. In this paper accurate positions and finding charts for all the carbon stars we have detected on our grism plates are provided. Also magnitudes, colours, and carbon abundance measurements are given for most of them, as well as cross identifications for all stars previously identified by other authors.

SMC Hα Emission-Line Object Survey

Hα emission-line objects in the SMC have been identified mainly by Henize (1956) and Lindsay (1961). Since no more recent systematic detection for point-source Hα emission-line objects existed, a new extensive objective-prism survey for this kind of object was undertaken by the author in 1982.

This survey for Hα emission-line objects in the SMC was performed with the CTIO Curtis Schmidt telescope when the author was a CNRS/NSF scholarship visitor in the Department of Astronomy of the University of Texas at Austin (Azzopardi and Meyssonnier 1988). Observations were carried out using the 10-degree objective-prism (420 Å/mm dispersion at Hα) in combination with a 110-Å bandwidth interference filter centred at 6565 Å. Exposures of 30 min, 1, 2 and 4 hours on hypersensitized IIIa-F plates allowed us to identify objects λλ 6548–6583 [N II] lines up to a limiting magnitude $m_{pg} \sim 18$ (for stellar continuum), some 2 to 3 magnitudes fainter than those from previous detections.

Hα emission-line objects have been searched for by N. Meyssonnier at the Marseille Observatory, who carefully surveyed all the plates with a binocular microscope; slitless spectra of the objects of interest were classified according to the intensity of the continuum, and the shape and strength of the Hα line. This, added to the presence and appearance of the [N II] lines, led to the discrimination of the Hα emission-line stars from the emission nebulae, and facilitates the identification of planetary nebulae. Furthermore, the detected objects were also scrutinized on the grism plates used for the carbon star survey. This allowed us to confirm the nature of the emission nebulae through the λλ 4959–5007 [O II] lines (for instance selecting the Very Low Excitation objects (VLE) among the planetary nebula candidates), and to establish the emission nature of very faint stars by the observation of a weak continuum underlying the Hβ line.

This survey resulted in the identification of 1898 Hα emission-line objects in the central regions of the Small Cloud, almost quadrupling the number of those found, in the same area, by the previous objective-prism surveys. Among the 178 emission nebulae we have detected, 62 are planetary nebulae (PN) and 81 compact/very small H II regions, the remaining nebulae being bubbles, loops and bright parts of large H II regions or filaments. 15 planetary nebulae (14 confirmed by our subsequent medium-resolution slit spectroscopy) and 25 compact H II regions are newly identified objects. Note that the total number of PN/VLE objects already found in the Small Cloud is about 75 – taking into account those beyond the boundaries of our survey – some 65 % only of the estimated total SMC PN population (116 objects), according to Boroson and Liebert (1989). Three B[e] supergiants (S6, S18 and N82) out of the four presently known in the SMC – S65 is outside the boundaries of our survey – (see Azzopardi, Breysacher and Muratorio 1981; Zickgraf 1986, 1989; Heydari-Malayeri 1990) and the VV Cephei star N55 (Walker 1983) were found again (Henize's identification numbers are given). In addition to the VV Cephei star, 28 other late-type star candidates with emission in the Hα line have been detected. The emission nature of five of them has been confirmed by our subsequent slit spectroscopy, one being a proven symbiotic star independently found by Morgan (1992) (star SMC3 from his Table 2).

The surface distribution of the Hα emission-line stars (Meyssonnier and Azzopardi 1991) resembles the overall distribution of the most luminous blue SMC stars (Azzopardi and Vigneau 1977). That of the small nebulae displays a similar pattern in spite of the smaller sample. It is difficult to draw any definitive conclusion about the surface distribution of the identified SMC planetary nebulae (Meyssonnier and Azzopardi 1991) on account of their restricted number. However, it is only reasonable to postulate that their overall distribution might have the same pattern as that of the carbon stars.

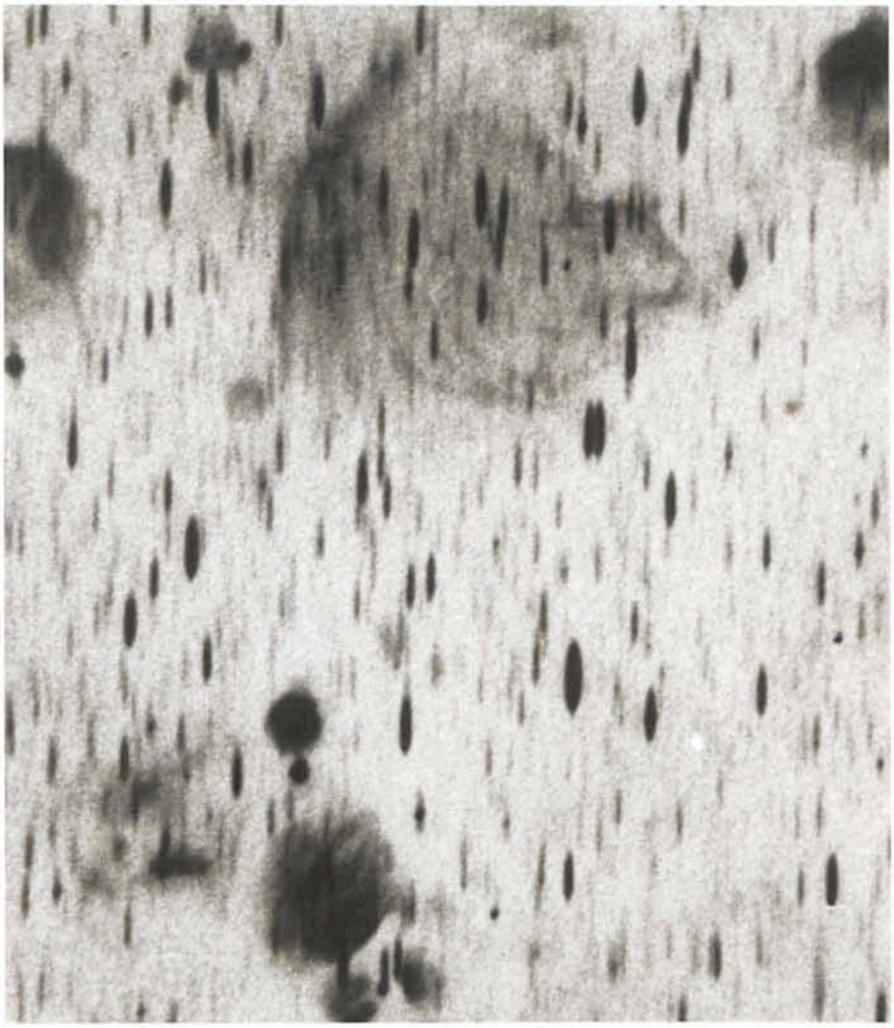

Figure 2: *Field in the southern region of the SMC bar. Part of the 4-hour exposure CTIO Curtis-Schmidt objective-prism plate (420 Å/mm dispersion at Hα)* obtained on IIIa-F emulsion through a 110-Å bandwidth interference filter centred at 6565 Å. Several objects show up strongly due to the emission from Hα and/or [N II] lines.

The identification of the Hα emission-line objects has been a very long task. Now completed, this work will be submitted soon for publication to *Astronomy and Astrophysics Journal.* It is expected that the "New Catalogue of Hα-Emission-Line Stars and Small Nebulae in the Small Magellanic Cloud" by Meyssonnier and Azzopardi will appear by the end of this year.

New Slitless Spectroscopic Surveys in Progress

From the experience we gained from low to very low objective-prism and -grism spectroscopy, we are now using the ESO Faint Object Spectrograph and Camera in the field spectroscopy mode (slitless) at the Cassegrain foci of both ESO 3.6-m and 2.2-m telescopes (EFOSC and EFOSC2, respectively) in order to carry out very deep surveys in selected regions of the Magellanic Clouds. We aim to detect very faint field carbon stars or planetary nebulae as well as Be stars in the centre of young globular clusters (Azzopardi 1993).

Thanks to its flexibility and versatility, an EFOSC-type instrument is especially well adapted, in selecting the best spectral dispersion and domain, to identify the typical spectral feature(s) of the type of object to be detected. For instance, when performing surveys with spectral dispersions lower than ~500 Å/mm we use preferably prisms instead of grisms in order to avoid the disturbing images due to the different grating orders (mainly the direct image or "zero" order). Also, on account of the dispersion achieved, we used 100–150 Å bandwidth to broad-band (~1000 Å) interference filters. Although the field of view of the

(continued on page 34)

Paranal at Sunset

This picture was taken in late October 1992, just before sunset. It shows the new, characteristic profile of the Paranal mountain, after the removal of the uppermost 28 metres of the peak. The huge VLT platform stands out against the transparent evening sky. In the foreground and some hundred metres lower is the VLT Base Camp. The photo was taken with a Hasselblad camera with a 50-mm lens on Kodak Ektachrome 100 film. Photographer: H. Zodet, ESO.

EFOSC CCD camera is restricted to a few (~20) square arcminutes, this survey technique is very efficient to identify objects showing up strongly through either their emission-lines or molecular bands. Concurrently, a semi-automatic procedure has been worked out by G. Muratorio in the MIDAS environment (Muratorio and Azzopardi 1993) to select through an impersonal mode, and more rapidly than by visual examination, the objects of interest.

References

Azzopardi M., 1993, Survey of Carbon Stars and Emission Objects. In: Baschek B., Klare G., Lequeux J. (eds.) Proc. Heidelberg Conference, New Aspects of Magellanic Cloud Research. Springer-Verlag, Heidelberg, p. 86.

Azzopardi M., Breysacher J., 1979, *A&A* **75**, 120.

Azzopardi M., Breysacher J., 1980, *A&A* **39**, 19.

Azzopardi M., Breysacher J., Muratorio G., 1981, *A&A* **95**, 191.

Azzopardi M., Meyssonnier N., 1988, A Curtis Schmidt Survey of Hα-Emission Objects in the Small Magellanic Cloud. In: Blanco V., Phillips M.M. (eds.) Proc. CTIO 25th Anniversary Symp., Progress and Opportunities in Southern Hemisphere Optical Astronomy. Brigham Young University, p. 386.

Azzopardi M., Rebeirot E., 1991, Large Scale Structure and Kinematics of the MCs from Carbon Star Studies. In: Haynes R., Milne D. (eds.) Proc. IAU Symp. 148, The Magellanic Clouds. Kluwer, Dordrecht, p. 71.

Azzopardi M., Vigneau J., 1975, *A&A* **22**, 285.

Azzopardi M., Vigneau J., 1977, *A&A* **56**, 151.

Blanco V.M., McCarthy M.F., Blanco B.M., 1980, *ApJ* **242**, 938.

Blanco V.M., McCarthy M.F., 1983, *AJ* **88**, 1442.

Boroson T.A., Liebert J., 1989, *ApJ* **339**, 244.

Breysacher J., Lequeux J., 1983, *The Messenger* **33**, 21.

de Vaucouleurs G., Freeman K.C., 1972, *Vistas in Astronomy* **14**, 163.

Hardy E., Suntzeff N.B., Azzopardi M., 1989, *ApJ* **344**, 210.

Henize K.G., 1956, *ApJS* **2**, 315.

Heydari-Malayeri M., 1990, *A&A* **234**, 233.

Lindsay E.M., 1961, *AJ* **66**, 169.

Meyssonnier N., Azzopardi M., 1991, A New Survey for Hα-Emission-Line Stars and Related Objects in the SMC. In: Haynes R., Milne D. (eds.) Proc. IAU Symp. 148, The Magellanic Clouds. Kluwer, Dordrecht, p. 196.

Morgan D.H., 1992, *MNRAS* **258**, 639.

Muratorio G., Azzopardi M., 1993, Detection of Faint Hα Emission-Line Objects and Carbon Stars in the Magellanic Clouds. In: Baschek B., Klare G., Lequeux J. (eds.) Proc. Heidelberg Conference, New Aspects of Magellanic Cloud Research. Springer-Verlag, Heidelberg, p. 96.

Rebeirot E., Azzopardi M., Westerlund B.E. 1993, *A&AS* **97**, 603.

Sanduleak N., Philip A.G.D., 1977 *Publ. Warner and Swasey Obs.* **2**, 105.

Walker A.R., 1983, *MNRAS* **203**, 25.

Westerlund B.E., Azzopardi M., Breysacher J., 1986, *A&AS* **65**, 79.

Westerlund B.E., Azzopardi M., Breysacher J., Rebeirot E., 1991, *A&AS* **91**, 425.

Westerlund B.E., Azzopardi M., Breysacher J., Rebeirot E., 1992, *A&A* **260**, L4.

Westerlund B.E., Lequeux J., Azzopardi M., Rebeirot E., 1991, *A&A* **244**, 367.

Zickgraf F.J., Wolf B., Stahl O., Leitherer C., Appenzeller I., 1986, *A&A* **163**, 119.

Zickgraf F.J., Wolf B., Stahl O., Humphreys R.M., 1989, *A&A* **220**, 206.

Study of the Shapley Supercluster

S. BARDELLI [1,4], R. SCARAMELLA [2], G. VETTOLANI [3], G. ZAMORANI [4,3], E. ZUCCA [1,3], C.A. COLLINS [5] and H.T. MACGILLIVRAY [6]

[1] Dipartimento di Astronomia, Università di Bologna, Italy; [2] Osservatorio Astronomico di Roma, Monteporzio Catone, Italy; [3] Istituto di Radioastronomia/CNR, Bologna, Italy; [4] Osservatorio Astronomico, Bologna, Italy; [5] Physics Department, University of Durham, United Kingdom; [6] Royal Observatory, Edinburgh, United Kingdom

1. Introduction

Superclusters (SC's) are the largest physical structures we know of today, and they constitute a very powerful probe for cosmology and extragalactic research. Indeed, some of the important questions which may be answered by studying superclusters concern the formation of galaxies and of galaxy clusters and related astrophysical problems. For example, biasing processes and efficiency of galaxy formation, the large-scale dynamics, power spectra of primordial density fluctuations, trends of M/L with size, and interactions and feedbacks on galaxies from a rich environment can all be investigated through the study of superclusters.

Superclusters are relatively rare objects and therefore are, on average, at large distance from us. This fact makes it difficult to collect the amount of different data which is necessary to perform a detailed analysis of their intrinsic properties. Therefore, a great opportunity is given if one is able to study a not too far but very rich SC. Fortunately, these are the characteristics of the SC discovered by Scaramella et al. (1989), which comprises about 25 rich Abell clusters over ≈ 300 square degrees, located at a distance of ~ 140 h^{-1} Mpc in the Centaurus region. The extreme richness of this SC in terms of galaxies brighter than 17th magnitude is such that its core was already noted in 1930 by Shapley, who reported an excess of counts over ~ 2.2 square degrees. Hence the name of Shapley Supercluster (or Concentration, hereafter SSC).

The SSC is by far the richest (Vettolani et al., 1990) and most interesting SC within 0.1c from us (Zucca et al., 1993). In fact, this concentration appears exceptional also by studying the surface distribution of optical galaxies (Raychaudhury, 1989; Raychaudhury et al., 1991) and by analysing the spatial distribution of IRAS galaxies (Allen et al., 1990). The SSC is also prominent in the X-ray band (Lahav et al., 1989). Indeed, this region contains 6 of the 46 X-ray brightest clusters of the sky at $|b^{II}|>20°$ (Edge et al., 1990), i.e. 13 % of the X-ray brightest clusters reside in only 1.4 % of the sky.

The SSC is also likely to be an important player in explaining the peculiar motion of the Local Group with respect to the Cosmic Microwave Background frame. In fact, Scaramella et al. (1989, 1991) pointed out that the SSC may be responsible for a significant fraction (≲30 %) of the Local Group peculiar motion, adding its dynamical pull on the LG to that from a closer overdensity of galaxies at ~40 h^{-1} Mpc. The latter overdensity of galaxies, dubbed "Great Attractor", was suggested to be the source of the Local Group acceleration (Lynden-Bell et al., 1988; Lynden-Bell et al., 1989; Faber&Burstein, 1988; Dressler, 1988). The suggestions of Scaramella et al. (1989, 1991), on the contrary, implied a significantly larger

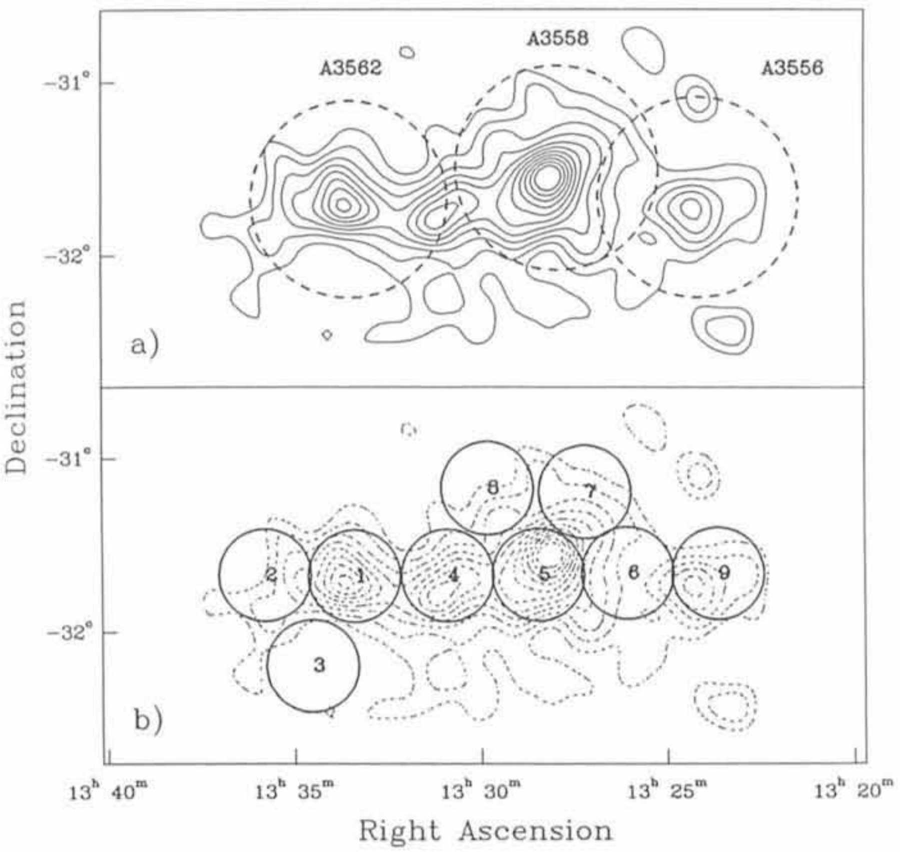

Figure 1: *a) Isodensity contours of the core of the SSC in an area of* $\sim 3.^{\circ}5 \times 2^{\circ}$. *The figure refers to galaxies with* $b_J \leq 19.5$ *and binned in 1 arcmin × 1 arcmin bins; the data have been smoothed with a Gaussian with a FWHM of 6 arcmin. For the three Abell clusters of the core circles of one Abell radius have been drawn (dashed curves); the poor cluster SC 1329-314 is the peak between the clusters A3558 and A3562. b) The same as Figure 1a, with superimposed the nine OPTOPUS fields observed in March 1991.*

coherence scale for the peculiar velocity flow, a fact which seems to be supported by recent findings (Willick, 1990; Mathewson et al., 1992). Also, Tully et al. (1992) suggested that these two "attractors" could be part of a single elongated planar structure, extending for $\sim 450\,h^{-1}$ Mpc.

The astronomical interest of the SSC is therefore evident, and we are carrying on a long-term study of the SSC in order to describe its dynamical state and to determine its mass and its luminosity. Our project consists of redshift determinations (with the ESO telescopes at La Silla) for galaxies both in the clusters and in the intra-cluster field of the SSC, and of X-ray observations (ROSAT) of the hot gas in some of its clusters.

In this paper we report the current status of this project and our future plans.

2. Analysis of the Bi-Dimensional Distribution of Galaxies

The photometric data used in our analysis derive from the COSMOS/UKST galaxy catalogue of the southern sky (Yentis et al., 1992) obtained from automated scans of the UKST-J plates by the COSMOS machine. Our sample consists of all galaxies brighter than $b_J = 20$ in seven plates (382, 383, 443, 444, 445, 509 and 510), for which the catalogue lists accurate coordinates (α and δ), b_J magnitudes, major diameters, ellipticities and position angles.

The core of the SSC, formed by A3556, A3558, A3562 and SC 1329-314, is entirely contained in the plate 444. Figure 1a shows the isodensity contour map of the galaxies in this region. The radii of the dashed circles superimposed on the three Abell clusters correspond to $1.5\,h^{-1}$ Mpc (i.e. one Abell radius). The centre of the cluster SC 1329−314 coincides with the density enhancement between A3562 and A3558. This figure, in which the contours of each cluster smoothly join with those of the adjacent clusters, suggests the possibility that all these clusters may be interacting and may be part of a single dynamical structure. In order to better assess the dynamical status of this complex we need information about the three-dimensional distribution of galaxies in this region.

3. Analysis of the Three-Dimensional Distribution of Galaxies

In order to obtain three-dimensional information for the core of the SSC, we have covered it with a number of fields (shown in Figure 1b) observed with the

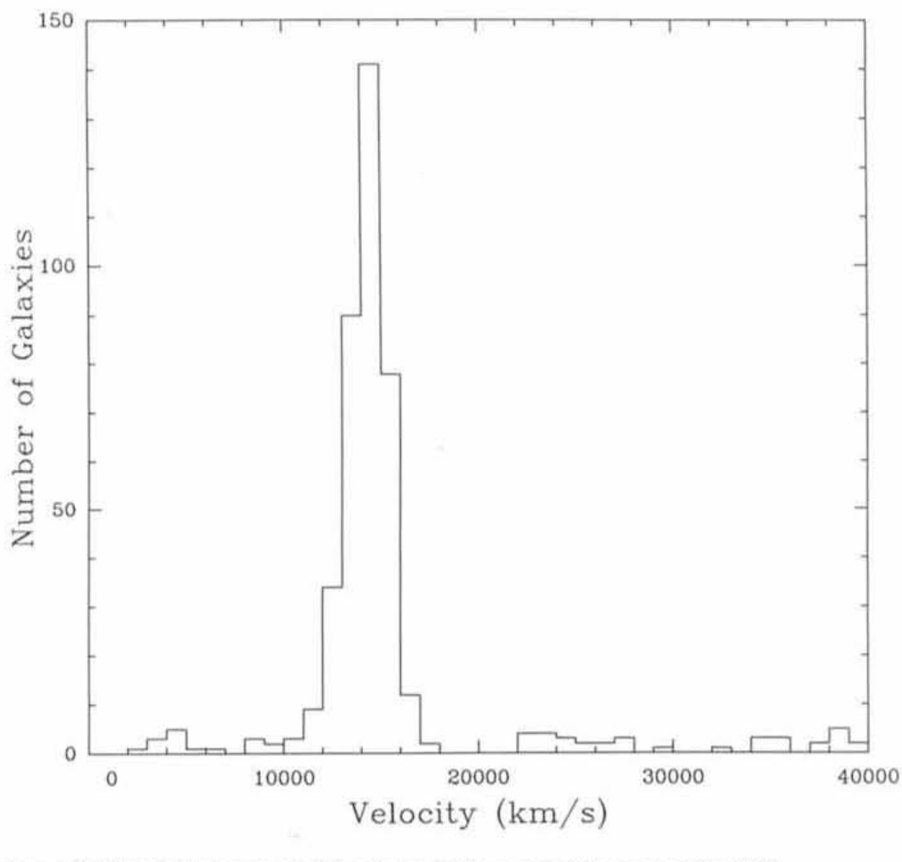

Figure 2: *Velocity histogram of 446 galaxies in the region of the core of the SSC.*

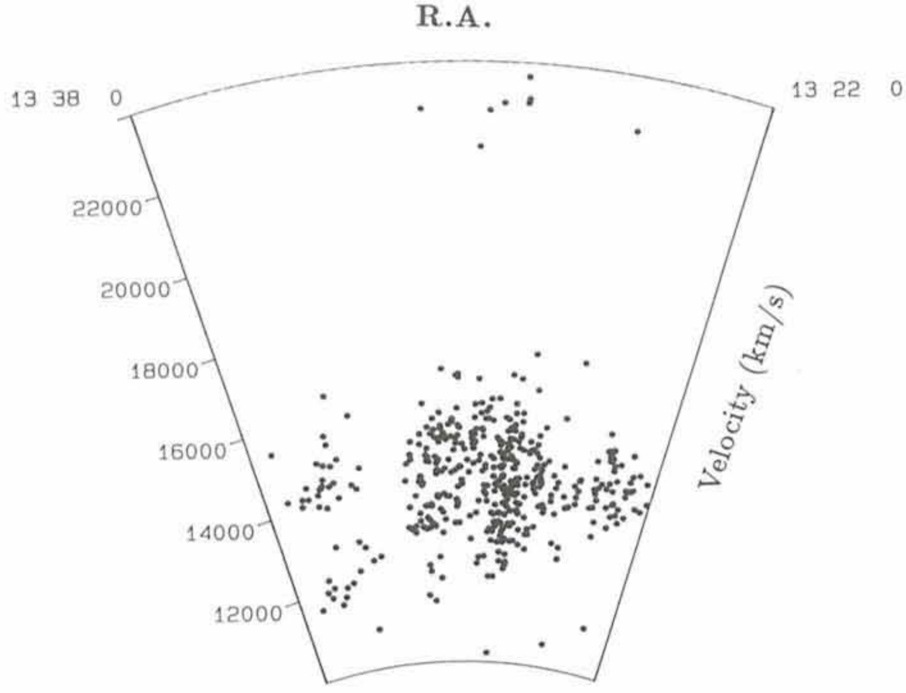

Figure 3: *Wedge diagram of our sample in the velocity range 10,000–24,000 km/s. The coordinate range is* $13^h22^m < \alpha < 13^h38^m$ *and* $-32°35' < \delta < -30°35'$.

ence of a void of about 4,000 km/s, just behind the peak. No galaxy is seen in the velocity range 18,000–22,000 km/s, where ~ 10 galaxies would be expected on the basis of a uniform distribution. This number has been computed by integrating the galaxy luminosity function with the magnitude limit corresponding to our data.

Figure 3 is a wedge diagram of this sample, in the velocity range 10,000–24,000 km/s. The "hole" on the left of the diagram is due to the absence of data in field #1, corresponding to the core of A3562. From this figure it is clear that the clusters and the galaxis between them form a single structure, as already indicated by the contour map in Figure 1a.

We have determined the mean and the dispersion of the velocities for the clusters in this region. However, the interpretation of these data is not straightforward because of the presence, outside the core of A3558, of a number of sub-condensations, some of which are clearly visible in Figure 3. A quantitative

OPTOPUS multifiber spectrograph (Lund, 1986) at the 3.6-m ESO telescope at La Silla. Two different observations were planned for three of these fields (#1, 4 and 5), because of their high density of galaxies. These observations were performed in March 1991; unfortunately field #1 could not be observed because of bad weather. For the same reason, the next observing run was completely lost also (April 1992), during which we had planned to extend the coverage of this area and to observe the concentration A3528-A3530-A3532, which is also part of the SSC.

We used the ESO grating #15 (300 lines/mm and blaze angle of 4°18′) which gives a dispersion of 174 Å/mm in the wavelength range from 3700 to 6024 Å. The detector was the Tektronix 512×512 CCD with a pixel size of 27 μm corresponding to 4.5 Å. Five out of the 50 OPTOPUS fibers were dedicated to sky measurements, while the remaining 45 fibers were dedicated to the galaxies. We have obtained a total of 421 spectra: 81 spectra (~19 %) were not useful for redshift determination, while 29 objects (~7 %) turned out to be stars, leaving us with a sample of 311 new galaxy redshifts. These data, added to the 135 redshifts already present in literature for A3558, lead to a three-dimensional sample of 446 galaxies.

In Figure 2 we show the velocity histogramm of this sample: notice that, in addition to the outstanding peak centred at v ~ 14,200 km/s which corresponds to the core of the SSC, this histogram suggests the possible pres-

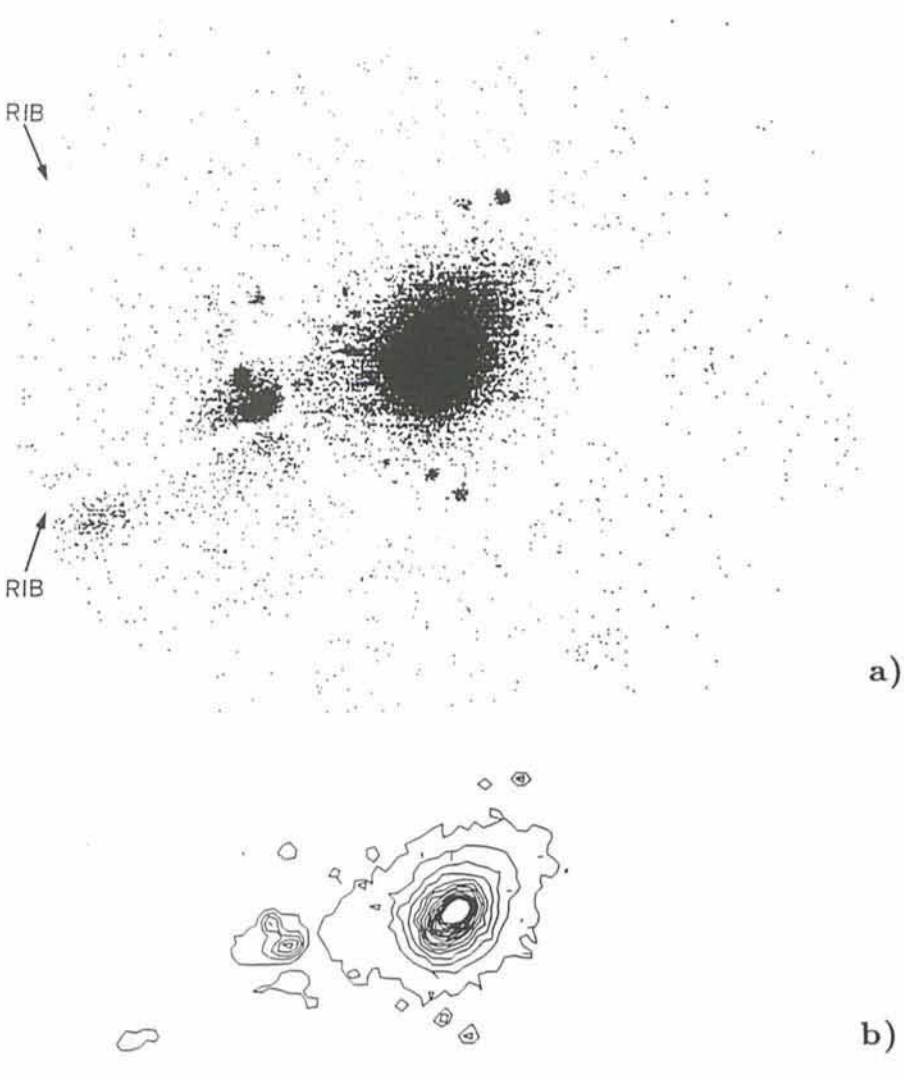

Figure 4: *a) X-ray image of the clusters A3558 obtained with the PSPC camera of the ROSAT satellite. The image is partially disturbed by the ribs of the PSPC camera. b) The same as Figure 4a represented with isophotes.*

analysis of these data will be presented elsewhere (Bardelli et al., in preparation). On a qualitative basis, we can here conclude that Figures 1 and 3 suggest that the massive cluster A3558 could be accreting galaxies from its nearby clusters; probably, this is the beginning of a merging process. Further redshift data about these clusters will enable us to calculate the masses of A3558 and A3562, in order to estimate the time scale of this merging.

4. Future Work

A3558 is the richest ACO cluster (the only one with richness class 4) and is placed in the core of the SSC; moreover, it is probably attracting its surrounding clusters. For this reason it is important to determine its mass and its dynamical state. For this purpose, we have observed it in the X-ray wavelength with the ROSAT satellite: Figure 4 is the image of this cluster obtained with the PSPC camera, in the range 0.1–2.4 KeV, with an exposure time of ~ 30,000 seconds. Similar observations for the cluster A3528 (the central cluster of the concentration A3528-A3530-A3532, see Zucca et al., 1993) are scheduled for the next ROSAT observing period.

In the context of further optical observations, our next run at the 3.6-m ESO telescope will be in February 1993. In this run we will extend the coverage of the core of the SSC and we will observe the A3528-A3530-A3532 structure, in addition to the observation of the field #1 (A3562). These data will allow an estimate of the mass of these clusters.

In order to study the mass distribution of the whole complex and to estimate the overdensity of galaxies outside clusters, we are also planning to map the whole SSC with a regular grid of MEFOS fields, observing all galaxies with $17 < b_J < 18$.

References

Allen, D.A., Norris, R.P. Staveley-Smith, L., Meadows, V.S., and Roche, P.F., 1990, *Nat.* **343**, 45.
Dressler, A., 1988, *Ap.J.* **329**, 519.
Edge, A.C., Stewart, G.C., Fabian, A.C., and Arnaud, K.A., 1990, *M.N.R.A.S.* **245**, 559.
Faber, S.M., and Burstein, D., 1988, in *Large-Scale Motions in the Universe*, proc. of the Pontifical Academic of Science Study Week #27, V.C. Rubin and G.V. Coyne eds., Princeton University, Princeton, p. 115.
Lahav, O., Edge, A.C., Fabian, A.C., and Putney, A., 1989, *M.N.R.A.S.* **238**, 881.
Lund, G., 1986, *OPTOPUS – ESO Operating Manual No. 6.*
Lynden-Bell D., Faber, S.M., Burstein, D., Davies, R.L., Dressler, A., Terlevich, R.J., and Wegner, G., 1988, *Ap.J.* **326**, 19.
Mathewson, D.S., Ford, V.L., and Buchhorn, M., 1992, *Ap.J. (Lett.)* **389**, L5.
Lynden-Bell., D., Lahav, O., and Burstein, D., 1989, *M.N.R.A.S.* **241**, 325.
Raychaudhury, S., 1989, *Nat.* **342**, 251.
Raychaudhury, S., Fabian, A.C., Edge, A.C., Jones, C., and Forman, W., 1991, *M.N.R.A.S.* **248**, 101.
Scaramella, R., Baiesi-Pillastrini, G., Chincarini, G., Vettolani, G., and Zamorani, G., 1989, *Nat.* **338**, 562.
Scaramella, R., Baiesi-Pillastrini, G., Chincarini, G., Vettolani, G., and Zamorani, G., 1991, in *Large-Scale Motions* (Rio Workshop 1989), Latham, D.W. e da Costa, L. (eds.), *A.S.P. Conf. Ser.* **15**, 13.
Shapley, H., 1930, *Harvard Obs. Bull.* **874**, 9.
Tully, B.R., Scaramella, R., Vettolani, G., and Zamorani, G., 1992, *Ap.J.* **388**, 9.
Vettolani, G., Chincarini, G., Scaramella, R., and Zamorani, G., 1990, *A.J.* **99**, 1709.
Willick, J.K., 1990, *Ap.J. (Lett.)* **351**, L5.
Yentis, D.J., Cruddace, R.G., Gursky, H., Stuart, B.V., Wallin, J.F., MacGillivray, H.T., and Collins, C.A., 1992, in *Digitized Optical Sky Surveys*, H.T. MacGillivray and E.B. Thomson eds., Kluwer Academic Publishers, The Netherlands, p. 67.
Zucca, E., Zamorani, G., Scaramella, R., and Vettolani, G., 1993, *Ap.J.* in press.

HIGH-RESOLUTION IMAGING WITH THE NTT:

The Starburst Galaxy NGC 1808

B. KORIBALSKI, Max-Planck-Institut für Radioastronomie, Bonn, Germany
R.-J. DETTMAR[1], Radioastronomisches Institut der Universität Bonn, Germany

1. Introduction

NGC 1808 is a beautiful spiral galaxy located in the southern sky at a distance of more than 10 Mpc. The peculiarity of its nuclear region has first been mentioned by Morgan (1958) who identified numerous, extremely brilliant, small nuclei in the central region which he called "hot spots". A real-colour image of this most interesting and unusual central region has been presented in *The Messenger* by Véron-Cetty & Véron (1983). This image nicely demonstrates the presence of several very blue "hot spots", corresponding to bright H II regions, and of a reddish nucleus which shows spectroscopic evidence for the presence of Seyfert activity (Véron-Cetty & Véron 1985).

An additional peculiarity of this complex central region was noted in 1968 by Burbidge & Burbidge. They found that NGC 1808 "contains an unusual amount of dust [in the disk] and some curious dust lanes which look almost radial in form". These prominent dust filaments which seem to emerge from the nuclear region are best seen on optical short exposures of NGC 1808, e.g., those given by Laustsen et al. (1987) or Tarenghi (1990) in a previous issue of *The Messenger*. Whereas in 1970 Arp & Bertola already speculated "that these lanes represent the passage of compact bodies outwards from the nucleus", we now have observational evidence that they are indeed connected with the outflow of neutral and ionized gas into the halo of NGC 1808 (Koribalski et al. 1992a, Phillips 1992). Also new is the discovery of a fast rotating torus of cold gas very near to the centre which has been revealed using HI absorption measurements against the extended radio continuum emission (Koribalski et al. 1992b).

The far-infrared (FIR) luminosity of NGC 1808 is with ≈ 2 10^{10} $L_\odot$ quite high, similar to NGC 253 and M 82.

Here, we want to present high-resolution Hα observations of NGC 1808 which have been kindly made available by Sandro D'Odorico from ESO (thanks a lot!). These new data may very well help answering the question how the various phenomena observed in NGC 1808 are related to each other.

2. Observations

Over the last couple of years the starburst galaxy NGC 1808 has been observed in detail with the Very Large

[1] Present address: Space Telescope Science Institute*, Baltimore, MD, USA (*affiliated with ESA).

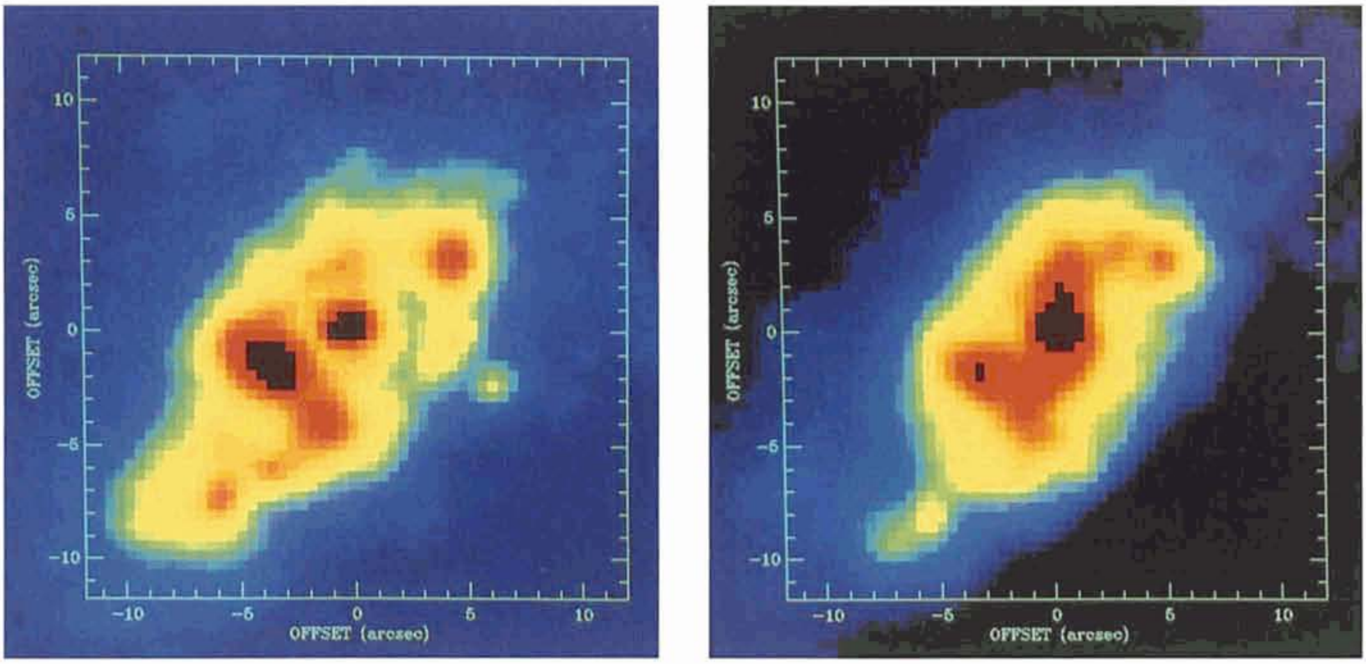

Figure 1: *Displayed here is the nuclear region of the starburst galaxy NGC 1808. (North is to the top and east to the left.) (a) The Hα+[NII] emission at λ 6570 Å. Numerous "hot spots" (= bright HII regions) seem to be distributed along a ring of radius 8". The nucleus at position (0,0), which is slightly offset from the ring centre, shows signs of nuclear activity. (b) The I-band continuum emission at λ 9137 Å. Due to the altered relative intensities of the bright condensations, their distribution appears quite different compared with the above image. Especially peculiar is the "hot spot" 5" SE of the nucleus, which is not very prominent in the continuum image, but has about the same brightness as the nucleus in the Hα+[NII] line emission.*

Array (VLA) in the radio continuum and HI λ 21-cm emission line (Koribalski et al. 1992a, b) in order to study the overall gas dynamics in the disk and a possible large-scale flow of matter from the disk into the halo, as suggested by the structure of the dust filaments in the nuclear region of this galaxy. A very valuable addition to these data sets were the above-mentioned optical observations obtained with the 3.5-m NTT during commissioning time for EMMI, the ESO Multi Mode Instrument, in October 1991 (for a description of EMMI see *The Messenger* **61**, p. 51). Both long-slit spectroscopy in the red near Hα and direct imaging (Hα- and I-filter) were carried out. The observing parameters are summarized in Table 1. The data reduction was carried out with the MIDAS software package.

3. Results

In this preliminary report we will concentrate on two peculiar features in the distribution of Hα emission which might be of interest for understanding the relation between starburst nuclei and the kinematics of the host galaxy on larger scales. The Hα-image obtained with EMMI shows

(1) a "mini-spiral" or nuclear ring describing the distribution of "hot spots" in the central region of NGC 1808 and

(2) a linear structure of bright HII regions on kpc scales. This is correlated with a ridge of neutral hydrogen (HI) gas and continuum emission in the disk.

3.1. The "hot spot" region

In Figure 1 we show the colour coded intensity distribution in the central region for emission lines and stellar continuum. Figure 1a displays the light distribution of the Hα+[NII] emission lines. The pure line emission has been obtained by subtracting the scaled I-band continuum image (Fig. 1b) from the narrow-band Hα-image. One can distinguish a number of bright components, the so-called "hot spots", which are distributed over an area of about 1 kpc (20"). They seem to lie along a "mini-spiral" or nuclear ring of radius 400 pc and inclination 60° (≈ the disk inclination). Its centre is slightly offset from the nucleus (= position 0,0). The continuum image (Fig. 1b) reveals a slightly different structure, with the nucleus being much more prominent (see also Fig. 2b, dotted line) than in the Hα image.

The most accurate position of the nucleus, which is identical with the brightest component at several wavelengths, has been determined at λ 6 cm with α, δ (1950) = $05^h05^m58^s\!.56$, $-37°36'36''\!.3$ (Saikia et al. 1990). The other compact radio components observed at λ 6 cm do not correlate with any of the "hot spots" and are probably supernova remnants.

With the Hα spectrum taken at a position angle of PA = 145° (roughly along the major axis) we are able to get some insight into the central gas kinematics. Figure 2a displays the "hot spot" region as in Figure 1a but now the x-axis is oriented along the slit (y ≈ 0). The other plots of Figure 2 show the fit parameters of the Hα line along the slit: (b) the relative intensity profile, (c) the position-velocity diagram, and (d) the line width FWHM, not corrected for instrumental broadening. The dotted line in Figure 2b is just for comparison and shows the I-band emission on an enhanced scale.

The rotation curve obtained from this spectrum (Fig. 2c; not corrected for the inclination) reveals a systemic velocity of about v_{sys} = 985 km s^{-1} at the location of the nucleus. It is very symmetric in the inner ±4"–5" where radial velocities of v_{sys}±115 km s^{-1} are measured. Further out we derive extrema of +130 km s^{-1} and –180 km s^{-1} at about 10" NW and 12" SE from the nucleus, respectively. The two "hot spots" on the SE side of the continuum (in Fig. 2b the two peaks to the left) cause an additional component which is responsible for the asymmetry of the rotation curve at this slit position. The rotation curves obtained by Burbidge & Burbidge (1968) and Véron-Cetty & Véron (1985) do not resolve this inner region.

The width of the Hα line (Fig. 2d) has an interesting radial dependence which is directly related to the rotation curve and the nuclear environment. In the

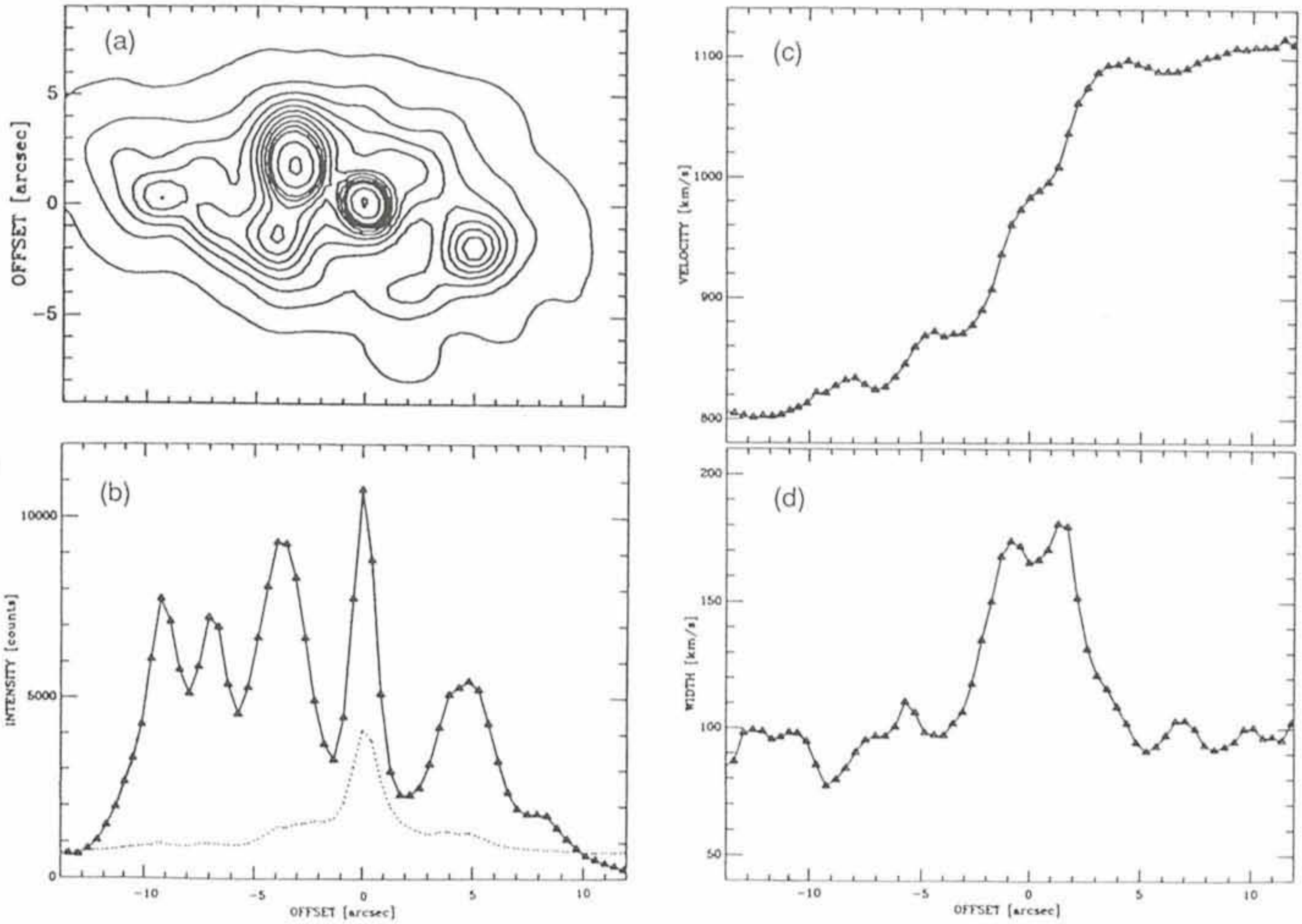

Figure 2: *(a) The "hot spot" region of NGC 1808 as in Figure 1a but with the x-axis oriented along the slit (PA = 145°) where the Hα spectrum was obtained. Further displayed are (b) the relative intensity profile of the Hα line emission (solid curve) and continuum emission (dotted curve), (c) the position-velocity diagram, and (d) the width (FWHM) of the Hα line.*

same range where the rotation curve is symmetric, the width of the Hα line starts to increase from 100 km s^{-1} to unusually large values, reaching about 180 km s^{-1} near the nucleus, and slightly less at the nucleus itself. The enormous line width at the position of the nucleus as well as the observed asymmetric line profiles and increasing [N II]/Hα ratios (which will be discussed elsewhere) are hinting at nuclear activity as had already been suggested by Véron-Cetty & Véron (1985).

3.2. The bar

We will now concentrate on the disk of NGC 1808 which has an optical extent of 7′.2×4′.1 along PA = 133° (B_{25}, de Vaucouleurs et al. 1976). The direct image of NGC 1808 obtained in the red channel of EMMI is already displayed in the ESO Annual Report 1990 (p. 56–57). Our Figure 3 shows the Hα+[N II] line emission from the disk of NGC 1808 which is mainly confined to a thin line of numerous bright H II regions and reveals only a small amount of diffuse emission.

The alignment of the H II regions from –60″ SE to +60″ NW of the nucleus and the correspondence of this linear structure with a ridge in the H I distribution as well as the elongation of the radio continuum distribution in the same direction strongly suggests the presence of a *bar*. The linear dimension of the bar is ≈ 6 kpc at a position angle of PA = 155° which is about 20° offset from the PA of the disk. The ratio of bar to disk length is roughly D_{bar}/D_{25} = 0.3. Beyond ±3 kpc the H II regions bend in opposite directions following the galactic rotation, which is also observed in the distribution of neutral hydrogen gas.

Table 1. *Observing Parameters*

Telescope	3.5-m New Technology Telescope
Observer	S. D'Odorico (ESO)
Date	1990, October 23/24
Instrument	ESO Multi Mode Instrument
Type of CCD chip	1024^2 THX Thompson
Observing mode:	
(A) Long-slit spectroscopy	
Slit-length, slit-width, PA	6′, 1″.2, 145°
Grating, dispersion	#6, 28Å/mm
Resolution	1.2 Å ≙ 55 km s^{-1}
Integration time	Hα-spectrum: 30 min
(B) Direct imaging	
Field dimensions	7′.5×7′.5 (– > 0″.44/pixel)
Filters (number, centre, width)	#596 (Hα), 6570 Å, 72 Å #656 (I), 9137 Å, 194 Å
Integration time	Hα-image: 5 and 10 min I-image: 10 min
Resolution	≈ 3 pixels

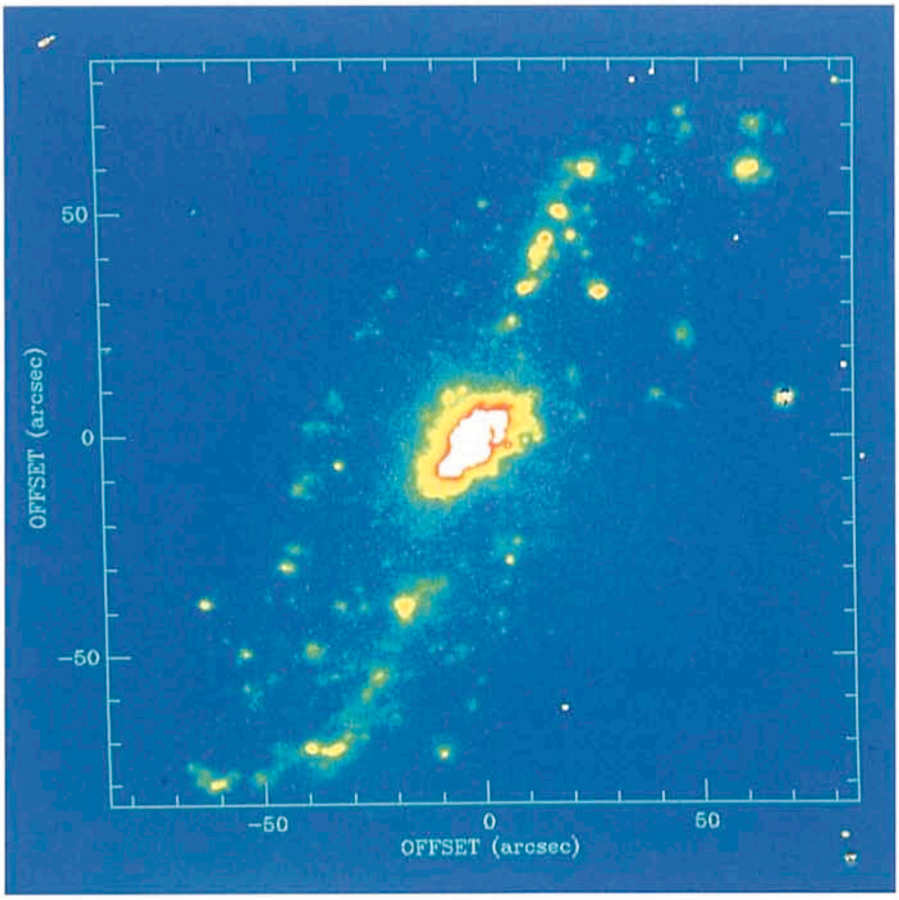

Figure 3: *The disk of NGC 1808. The Hα+[NII] line emission is mainly observed along a line at PA = 155°. This linear structure extends roughly 3 kpc to both sides of the nucleus and further out bends in opposite directions following the galactic rotation. (North is to the top and east to the left).*

To determine the velocities in and around the bar it is now necessary to obtain further spectra at various position angles.

4. The Scenario

The question arises, what is the physical connection of the different features described above. In the following we describe a scenario which tries to answer this question.

The clue to the scenario is *the bar*. The presence of a bar potential strongly influences the gas flow in the disk and the nuclear region of a galaxy. Galactic disks are very sensitive to m=2 resonances, and it is therefore expected from stellar dynamical studies that bars can easily be excited by gravitational interaction (e.g. Athanassoula 1990). The warp of the outer spiral arms in NGC 1808 (see Koribalski et al. 1992a) could be the result of a recent tidal interaction with the neighbour galaxy NGC 1792, located at a projected distance of about 130 kpc. The bar in NGC 1808, which is not seen in the visual light, is clearly detected in optical emission lines and less pronounced in the neutral hydrogen and radio continuum emission. The curved dust lanes in the disk of NGC 1808 (see Laustsen et al. 1987) could correspond to shocks induced by this 6 kpc bar.

According to Combes & Gerin (1985) a bar causes molecular clouds inside corotation to stream towards the centre and to accumulate at the Inner Lindblad Resonance (ILR). The crowd of clouds at this specific radius is often observed as a nuclear ring. In NGC 1808 the resonance location is denoted by a ring or spiral of "hot spots" (Fig. 1) enveloped by a fast rotating torus of cold gas (Koribalski et al. 1992b). A similar scenario is for example found in the barred galaxy NGC 2903 (Jackson et al. 1991).

CO measurements obtained with the SEST show a high concentration of molecular gas in the central area (Dahlem et al. 1990). The FIR/CO(1–0) luminosity ratio which is often used as a measure of massive-star formation efficiency is about 20 $L_\odot/M_\odot$. Due to the low resolution of the data we have no information about the molecular gas distribution in the bar.

Finally, the observed *outflow* of neutral and ionized gas from the central starburst region into the halo of the galaxy NGC 1808 (Koribalski et al. 1992a, Phillips 1992) might be the consequence of the accretion of cold gas near the centre, at the location of the ILR(s). Reaching the nuclear region, it will be heated and, due to the gas pressure of supernovae and winds, ejected along the rotation axis of the galaxy. The radial dust filaments emerging from the central region of NGC 1808 to at least 3 kpc above the plane clearly show the large energetics involved in this process.

References

Arp, H., & Bertola, F. 1970, *Astrophysical Letters* **6**, 65.
Athanassoula, E. 1990, in IAU Coll. 124 "Paired and interacting galaxies", eds. J.W. Sulentic & W.C. Keel, NASA CP 3098, pp. 505.
Burbidge, E.M., & Burbidge, G.R. 1968, *ApJ* **151**, 99.
Combes, F., & Gerin, M. 1985, *A&A* **150**, 327.
Dahlem, M., Aalto, S., Kein, U., et al. 1990, *A&A* **240**, 237.
Jackson, J.M., Eckart, A., Cameron, M., et al. 1991, *ApJ* **375**, 105.
Koribalski, B., Dahlem, M., Mebold, U., Brinks, E. 1992a, *A&A*, in press.
Koribalski, B., Dahlem, M., Mebold, U., Brinks, E. 1992a, *A&A*, in press.
Koribalski, B., Dickey, J.M., Mebold, U. 1992b, *ApJ Letters*, in press.
Laustsen, S., Madsen, C., West, R.M. 1987, *"Exploring the Southern Sky"*, Springer Verlag, page 30/31.
Morgan, W.W. 1958, *PASP* **70**, 364.
Phillips, A. 1992, *AJ* (submitted).
Saikia, D.J., Unger, S.W., Pedlar, A., et al. 1990, *MNRAS* **245**, 397.
de Vaucouleurs, G., de Vaucouleurs, A., Corwin Jr., H.G. 1976, Second Reference Catalogue of Bright Galaxies, University of Texas Press, Austin and London.
Véron-Cetty, M.-P., & Véron, P. 1983, *The Messenger* **34**, 22.
Véron-Cetty, M.-P., & Véron, P. 1985, *A&A* **145**, 425.
Tarenghi, M. 1990, *The Messenger* **59**, 17.

New ESO Preprints

(December 1992 – February 1993)

Scientific Preprints

887. E.J. Wampler et al.: The Absorption Spectrum of QSO 2116-358 *Astronomy and Astrophysics*.
888. F. Matteucci et al.: Constraints on the Nucleosynthesis of Cu and Zn from Models of Chemical Evolution of the Galaxy. *Astronomy and Astrophysics*.
889. Xiao-wei Liu et al.: Observations of the Bowen Fluorescence Mechanism and Charge Transfer in Planetary Nebulae II. *Monthly Notices of the Royal Astronomical Society*.

890. M.-H. Ulrich et al.: The Time Variability of the UV Continuum and of Lyα in 3C273. *The Astrophysical Journal.*

891. I. J. Danziger et al.: Gradients of Metal Line Indices in a Sample of Early Type Galaxies.
C. M. Carollo and I. J. Danziger: Line-Strength Gradients and Dynamics of NGC 2663 and NGC 5018.
F. Matteucci: Chemical Evolution of Elliptical Galaxies with Dark Matter.
Presented at the ESO/EIPC Workshop "Structure, Dynamics and Chemical Evolution of Early-Type Galaxies", Elba, 25 – 30 May 1992.

892. O. Hainaut et al.: Imaging of Very Distant Comets: Experience and Future Expectations.
R. M. West: Summary and Discussion of Observations.
Contributions to the Proceedings of the "Workshop on the Activity in Distant Comets."

893. P. François and F. Matteucci: On the Abundance Spread in Solar Neighbourhood Stars. *Astronomy and Astrophysics.*

894. P. Bouchet and I. J. Danziger: Infrared Photometry and Spectrophotometry of SN 1987 A: II. November 1987 to March 1991 Observations. *Astronomy and Astrophysics.*

895. P. Møller and S. J. Warren: Emission from a Damped Lyα Absorber at Z = 2.81. *Astronomy and Astrophysics.*

896. M. A. Prieto et al.: The Extended Nebulosity in the Radio Galaxy 3C227. *Monthly Notices of the Royal Astronomical Society.*

897. C. N. Tadhunter et al.: Optical Spectroscopy of a Complete Sample of Southern 2 Jy Radio Sources. *Monthly Notices of the Royal Astronomical Society.*

898. J. Surdej et al.: Gravitational Lensing Statistics Based on a Large Sample of Highly Luminous Quasars.

899. J. M. Beckers: On the Relation Between Scintillation and Seeing Observations of Extended Objects. Published as a Letter to the Editor of *Solar Physics.*

900. M. A. Albrecht: Archiving Data from Ground-based Observatories. Presented at Astronomical Data Analysis Software & Systems (ADASS '92), Boston, November 1992.

901. M. Della Valle and H. Duerbeck: The Space Density of Classical Novae in the Galactic Disk. *Astronomy and Astrophysics.*

902. R. L. M. Corradi and H. E. Schwarz: The Bipolar Outflow of He 2-36. *Astronomy and Astrophysics.*

903. P. Artymowicz et al.: Star Trapping and Metallicity Enrichment in Quasars and AGN's. *The Astrophysical Journal.*

904. Xiao-wei Liu and J. Danziger: Electron Temperature Determination from Nebular Continuum Emission in Planetary Nebulae and the Importance of Temperature Fluctuations. *Monthly Notices of the Royal Astronomical Society.*

905. A. Jorissen et al.: S Stars: Infrared Colors, Technetium, and Binarity. *Astronomy and Astrophysics.*

906. Bo Reipurth and S. Heathcote: Observational Aspects of Herbig-Haro Jets. Invited review presented at the Astrophysical Jets symposium held at the Space Telescope Science Institute in Baltimore on 12 – 14 May 1992.

907. P. Molaro et al.: Interstellar Ca II and Na I in the SN 1987A Field: I. Foreground and Intermediate Velocity Gas.
G. Vladilo et al.: Interstellar Ca II and Na I in the SN 1987A Field: II. LMC Gas. *Astronomy and Astrophysics.*

908. J. K. Kotilainen et al.: CCD Imaging of Seyfert Galaxies: Deconvolution of the Nuclear and Stellar Components. *Monthly Notices of the Royal Astronomical Society.*

Technical Preprint

50. M. Faucherre et al.: The VLT Interferometer: Current Status and Expectations for the Next 20 Years. Proceedings of an ESA Colloquium on Targets for Space-Based Interferometry, Beaulieu, France, 13 – 16 October 1992.

ESO Proceedings "HIGH-RESOLUTION IMAGING BY INTERFEROMETRY II"

In the September 1992 issue of *The Messenger* we announced the imminent availability of the above-mentioned proceedings. As a matter of fact, they were delivered only at the end of February 1993. We apologize for this delay, which could not be anticipated at the time the September issue of *The Messenger* went to press.

Delivery of the proceedings had originally been promised by the printer for August 1992. In early September more than half of the pages had been printed and a large number of the printing sheets had already been mounted and corrected. Then, in mid-September, the printer had to leave his old premises and move into new ones. At the same time, the staff who had been working on the proceedings left the printer.

It was then that the printer completely lost control of the production process. Part of the original manuscripts disappeared, some of the printed sheets as well. New, corrected sheets were printed without our corrections having been carried out. The quality of many of the illustrations was such that we could not accept them. When they were printed again, the result was hardly better. In addition, progress was extremely slow.

Now the proceedings have been delivered, and, apart from some minor imperfections and a number of "weak" illustrations, the quality is satisfactory.

We are sorry that this all could happen and apologize again, especially to those who have already ordered and paid the proceedings and whose patience has been put to a severe test.

K. K.

IRAC2 Observations of the Spiral Galaxy NGC 2997

D. Block[1,2], P. GROSBØL[3], A. MONETI[3], P. PATSIS[3]

[1]Visiting Astronomer, European Southern Observatory; [2]Witwatersrand University, South Africa; [3]European Southern Observatory

The galaxy NGC 2997 is one of the beautiful, grand-design, spiral galaxies in the southern sky. It is classified as Sc(s)I in the Revised Shapley-Ames Catalog (Sandage and Tammann, 1981) and has a D_{25} diameter of 8.3 arcmin. Blue images show very regular inner arms with clear dust lanes while the arms bifurcate (break up) in the outer parts (see Fig. 1). Its inclination angle of $\approx 40^\circ$ is well suited for both morphological and dynamical studies. With a linear scale of $1'' \approx 50$ pc on the sky (H_o = 80 km/s/Mpc), it is possible to analyse not only general features but also the finer details such as the material lying between the spiral arms and the bulge.

These characteristics make NGC 2997 a perfect candidate for a detailed study of grand-design spiral structure in disk galaxies. Two important ingredients in making dynamic models of galaxies are their rotation curve and accurate surface photometry maps. Wheras the rotation curve gives the overall potential or mass distribution, maps are required

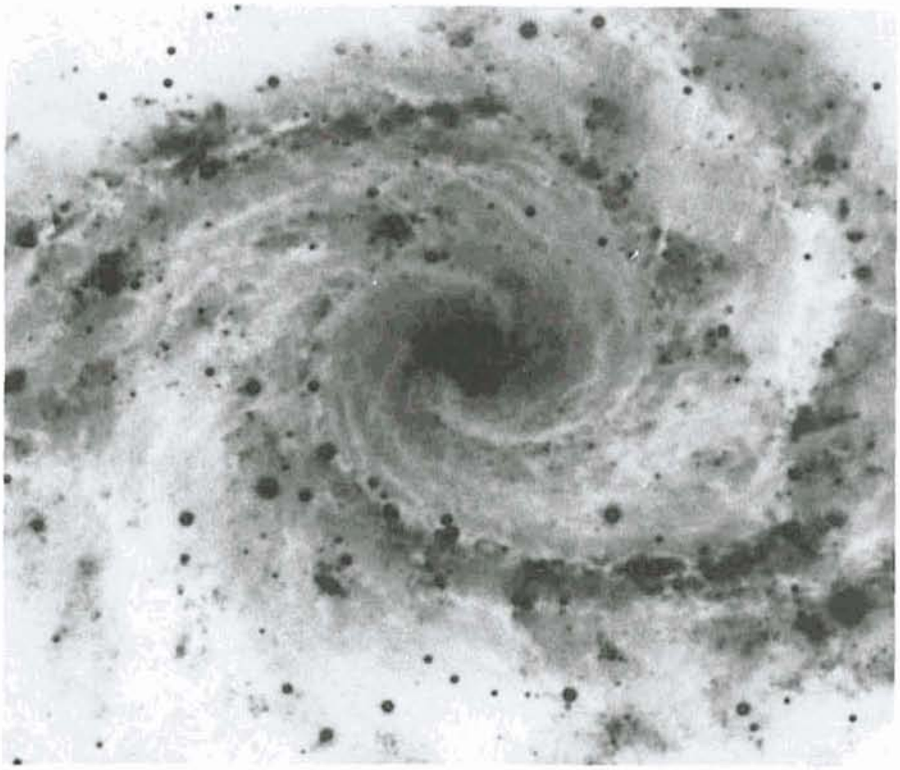

Figure 1: *A 90-minute blue exposure (GG385+IIIa-J) of NGC 2997 made by S. Laustsen at the 3.6-m prime focus in 1977.*

Figure 2: *Single 3-minute image in K′ of a field just south of the centre of NGC 2997. The image was sky subtracted and flat field corrected. No cleaning was applied so that bad pixels and stars in the sky exposure can readily be seen.*

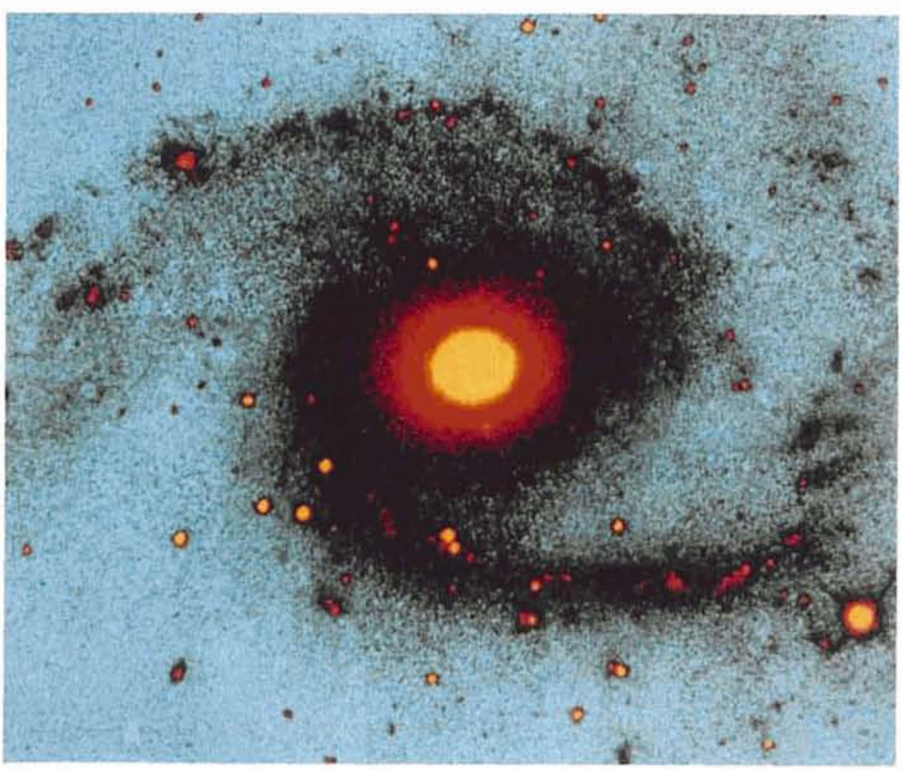

Figure 3: *Mosaic of NGC 2997 in K′ consisting of 6 fields each with a total of 15 minutes exposure taken at the 2.2-m with IRAC2.*

to describe the detailed distribution of matter in the disk such as spiral perturbations. The light distribution on images in the visual wavelength range is difficult to interpret as tracer of mass due to significant population and dust effects. New large-format infrared detectors like the 256 × 256 NICMOS3 array in the IRAC2 instrument (Moorwood et al., 1992) provide an opportunity to observe in the K′ band (2.1 μ) where such effects are much less important. This can give a radical change in the morphology of the galaxy (Block and Wainscoat, 1991).

A large mosaic in K′ covering the main spiral structure of NGC 2997 with six 2′ × 2′ fields was observed in January 1993. A single sky-corrected 3-minute exposure of a field just south of the centre is given in Figure 2. The full mosaic was composed of five exposures of each field with interleaved sky frames giving a total integration time of 15 minutes on the galaxy. The reduction, stacking and composition of the mosaic was done with MIDAS. The final 621 × 435 pixel map of NGC 2997 in K′ is shown in Figure 3 with a scale of 0.5″ per pixel. It reaches a surface brightness of 17.1 mag/arcsec^2 with a signal-to-noise ratio of 10. The slight offset between some of the individual fields is caused by a change in sky brightness during the observations and can first be fully removed when a better model for the relative contributions from sky and telescope to the background is available.

NGC 2997 has a much smoother appearance in K′ than in blue light. The strong dust lanes in the inner parts have disappeared and the Population I objects in the arms are much less prominent. The azimuthal profile to the inner arms is still so sharp that it suggests a strong and possibly non-linear density perturbation in the disk. The northern interarm region is significantly brighter than its southern counterpart while the peak amplitude of the southern arm is stronger. Note also that the arms are much weaker in K′ than in blue outside point where they bifurcate. These features will be compared with a detailed dynamic model of the galaxy including a density wave perturbation of its disk.

References

Block, D.L. and Wainscoat, R.J., 1991: *Nature,* **353**, 48.

Moorwood, A., Finger G., Biereichel, P., Delabre, B., Van Dijsseldonk, A., Huster, G., Lizon, J.-L., Meyer, M., Gemperlein, H., and Moneti, A., 1992, *The Messenger,* **69**, 61.

Sandage, A. and Tammann, G.A., 1981, "A Revised Shapley-Ames Catalog of Bright Galaxies", *Carnegie Inst. Wash. Pub.* **635**, Washington, D.C.

Prototype of the FORS Multiple-Object Spectroscopy Unit Under Test

K.-H. DUENSING, R. HARKE, H. NICKLAS, H. RENZIEHAUSEN,
Universitäts-Sternwarte Göttingen, Germany
H. BÖHNHARDT, H.-J. HESS, S. KIESEWETTER, W. MITSCH,
Universitäts-Sternwarte München, Germany

Two Focal Reducer and Spectrograph Instruments (FORS) are foreseen for the Cassegrain foci of the VLT telescope units 1 and 3. The FORS instruments will provide imaging, spectroscopy, polarimetry and spectropolarimetry observing modes in the 330 to 1100 nm wavelength options. A detailed description of the FORS instruments is given by I. Appenzeller and G. Rupprecht in *The Messenger* No. **67**, pp. 18–21, 1992.

The slit unit of the instrument is a crucial device for the quality of the spectroscopic observations with FORS. It is the instrument part located in the Cassegrain focus of the VLT in front of the optical train (collimator, grisms, filters, camera) of the instrument. Besides a long-slit mask the FORS slit unit will contain the multiple-object spectroscopy unit (MOS) for simultaneous spectroscopy of up to 19 different objects in the telescope field of view. The MOS unit will also be used to generate a strip mask for the polarimetric imaging mode. Consequently, the full-size MOS unit will consist of a row of 19 pairs of opposite slitlets. During multiple-object spectroscopy each pair of opposite slitlets will form a 22 arcsec long slit of adjustable width. The slits can be moved independently in one direction in the VLT Cassegrain focus surface. In order to match best an observer selected constellation of objects in the field of view by the MOS unit slit pattern, a combination of linear positioning of the slits and instrument rotation around the optical axis will be used. When switching FORS to imaging mode, the slitlets will move to their park positions and clear up the Cassegrain focal plane.

Since the mechanical properties and the accurate positioning of the slitlets are very important issues for the multiple-object spectroscopy and the polarimetric observations with FORS, a prototype of the most critical parts of the MOS unit was manufactured in the course of the on-going final design work for the FORS contract between ESO and the VIC consortium (Landessternwarte Heidelberg, Universitäts-Sternwarte Göttingen, Universitäts-Sternwarte München). Coming from the mechanical workshops in Göttingen the MOS prototype (Fig. 1) arrived in München in December 1992 for the electronics installation and for performance tests.

The central part of the MOS prototype consists of 6 slitlets arranged in two opposite rows in the 208×208 mm wide focal area (Fig. 2). By adequate linear positioning of a pair of opposite slitlets, a single slit of a user-defined width can be formed and positioned at a suitable location in the focal area. The 12-mm length of the individual slits corresponds to 22.5 arcsec in the FORS field of view at the VLT. The slitblade itself is carried by a 250-mm-long support arm which is movable over the full length of the instruments's field of view. On both sides of the focal area the guiding and drive system for the movable slitlets is mounted to a very stiff rectangular platform of about 1 m length which provides a reference for measurements of the MOS prototype with micron range accuracy (Fig. 1). In order to allow for the simulation of the different orientations of FORS with respect to gravity (i.e. the telescope elevation and the rotation of the Cassegrain adaptor around the opti-

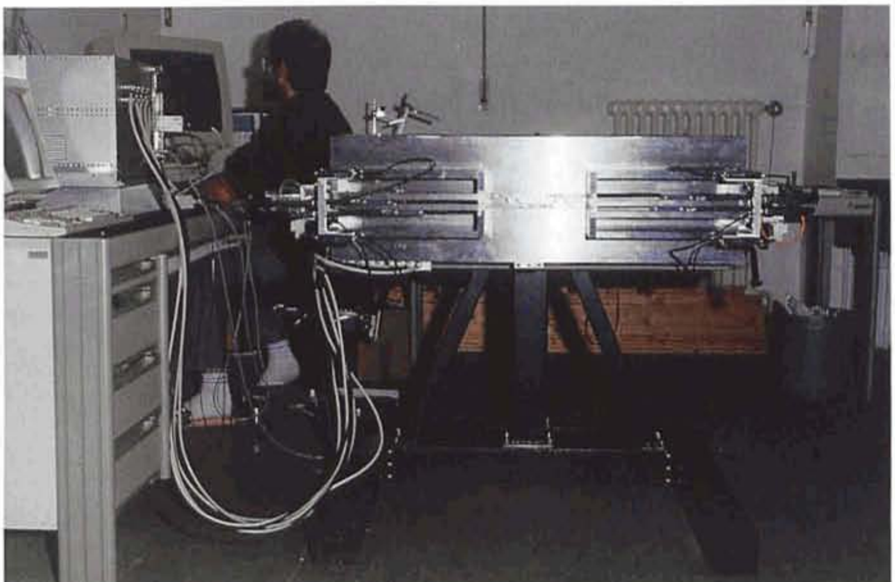

Figure 1: *The MOS unit prototype in its support stand. The MOS unit is pointing to a horizontal position. The rack for the control electronics stands on the desk on the left-hand side of the MOS prototype. The tests are operated by a HP workstation in the background of the laboratory. (Photo by M. Pfeiffer, USM.)*

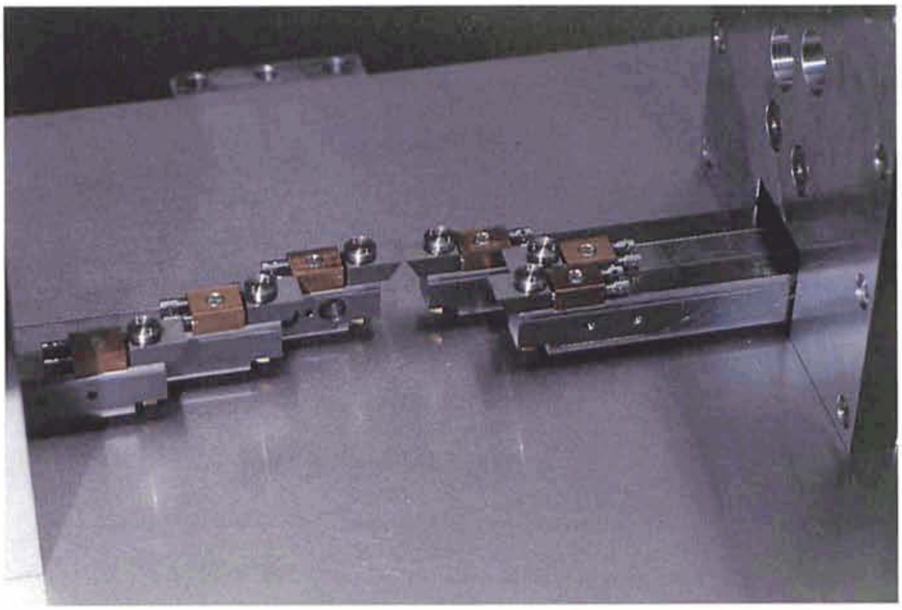

Figure 2: *View of the focal area of the MOS unit prototype with its 6 slitlets. The upper slitlet pair is forming a narrow slit while the slitlets of the two other pairs are in wide separation. (Photo by M. Pfeiffer, USM.)*

cal telescope axis), the prototype is attached to a support stand with two rotation axes (Fig. 1). The control electronics of the prototype is installed in a separate rack. During the tests the prototype is controlled by a VME based local control unit prototype with motor test software running under VXWORKS.

The MOS prototype will be used to check the design principles of the MOS unit by practical tests, to verify mechanical specifications and to identify necessary design modifications. The tests have already been started with measurements of the mechanical bending of the slitlet carrier arms and guiding system and of the accuracy of the slitlet positioning. In a second step a reliability test will be performed which simulates 10 years of MOS unit operations by a comparable number of reconfigurations of the slitlets in a one-month prototype test period (it is assumed that during spectroscopic observations with FORS the slitlets will be reconfigured typically once every 30 minutes). Finally, tests with colliding slitlet pairs shall verify the manufacturing quality and safety of the slitblades in the case of unfavourable malfunctions of the unit control.

LITE: the Large Imaging Telescope

L. VIGROUX[1], V. DE LAPPARENT[2], Y. MELLIER[3], J. RICH[4], H.J. BREUER[5], H. LORENZ[6], S. MARX[7]

[1]DAPNIA, Service d'Astrophysique, CEN Saclay, France; [2]CNRS, Institut d'Astrophysique de Paris, France; [3]Observatoire Midi-Pyrénées, Toulouse, France; [4]DAPNIA, Service de Physique des Particules, CEN Saclay, France; [5]Sonneberg Observatory, Germany; [6]Astrophysical Institute Potsdam, Germany; [7]Tautenburg Observatory, Germany

It was realized very early in the development of the ESO 16-metre equivalent Very Large Telescope (VLT) that wide-field imaging would be too complicated and costly to be implemented on the VLT itself and should therefore be done with a smaller telescope.

Accompanying imaging observations are essential for the optimal use of the VLT. Let us take an example. For large-scale structure studies, the VLT allows to measure redshifts in a 30-arcmin field of view of galaxies of magnitude 23 or even fainter. They are too faint to be reliably detected on Schmidt plates, so the input observation catalogue must be obtained from deep CCD imaging. In this example, outstanding image quality is needed to make a clear separation between faint galaxies and stars. The VLT will have in its imaging mode a 7-arcmin field and is not useable for obtaining such images. The best compromise is a middle-size telescope of about 2.5 m diameter and equipped with a wide-field CCD camera.

These considerations led the French astronomical community to propose the construction of such a special telescope. The definition of this project, now referred to as the Large Imaging Telescope (LITE), started in spring 1992 with the establishment of a consortium of several French laboratories, including Observatoire de Meudon, Institut d'Astrophysique de Paris, Observatoire Midi-Pyrénées, Observatoire de Besançon, Observatoire de Marseille, and led by the Department of Astrophysics and Particle Physics in Saclay. At the same time, a German group from Sonneberg Observatory, Tautenburg Observatory and the Institute of Astrophysics in Potsdam were working on a project of a second-generation Schmidt telescope to pursue the type of research which has long been done at these institutes. Richard West and Ray Wilson of ESO, who were aware of both projects, acted as the go-betweens of the two groups who, in a meeting held at the ESO headquarters in Garching in December 1992, decided to join their efforts. The telescope is the responsibility of the German group, whereas the CCD camera and its acquisition system will be designed and constructed in France.

While this project was originally designed for observations of mainly cosmological interest, it has the technical capabilities to cover a much broader range of astrophysical problems. The consortium is now working on several programmes.

Galactic structure study will take advantage of the deep images obtained for extragalactic purposes, with the addition of the observations of selected galactic fields, in particular in the thick disk region. The main emphasis is the study of the low-mass star luminosity function. On a 10-year time scale, we also can detect the proper motions of a large number of faint stars and we expect that the combined information will improve our knowledge of the structure and evolution of our Galaxy. These fields will be monitored to detect and analyse the variable stars, and to obtain a catalogue fainter than was already existing. By-products of these analyses will be a large-scale extinction map and the study of Galactic Cirrus at a scale smaller than the IRAS resolution.

Programmes on nearby galaxies will include the determination of colour gradients of early-type galaxies, the analysis of which is now limited by the poor statistic of the available samples. The LITE survey will be an invaluable tool to study the relationship between the environment and the galaxy morphology and luminosity distribution, a related topic being the search for very low surface brightness galaxies. These domains are still open. For example our present knowledge of the morphology density relation is based on the Dressler sample that contains only 6000 galaxies. With LITE, we may be able to study this relation on a sample larger by a factor of at least 10. A systematic search for starburst galaxies is also planned using slitless low-resolution spectroscopy. It will allow to investigate their spatial distribution, their luminosity function, their evolutionary stage, and the significance of triggering mechanisms. This survey will also be a new opportunity for examining the existence of primordial galaxies at low redshift.

LITE will offer an efficient way of mapping the large-scale galaxy distribution out to redshifts of 0.6–0.8. The existing faint catalogues over significant areas of the sky were obtained from digitization of photographic plates, yielding a limiting magnitude of $m_B \sim 22$. However, the non-linearity and coarse spatial resolution of the photographic emulsion call into question the reliability of galaxy catalogues at the plate limit. LITE will provide the necessary galaxy catalogue for performing deep redshift surveys to $m_B \sim 22-23$ over several tens of square degrees of the sky using multi-fiber VLT instruments such as FUEGOS. These redshift surveys are needed for understanding the nature of the intercepted over- and under-densities of galaxies in the existing narrow pencil-beam probes, and for putting reliable limits on the typical and largest size for the large-scale structures.

From the galaxy catalogue, LITE will be able to detect clusters of galaxies by correlation analysis up to redshifts of 1.0. Coupled with redshift measurements on the VLT (FUEGOS and FORS), the cluster catalogue will provide a unique sample for studying cluster dynamics, their evolutionary stages, their content in dark matter, and their relationship with the large-scale structures. Moreover, LITE will be in operation at the same time as the new generation of X-ray satellites, AXAF and XMM. We can therefore foresee large coordinated programmes on distant clusters.

From the large galaxy catalogue, we also plan an unprecedented search for gravitational distortions by large-scale structures. In analogy with the gravitational lensing effect by dark matter halos in clusters of galaxies, dark matter distributed over larger scales would lead to a significant number of distorted images of faint background galaxies. A statistical detection of alignments of faint galaxies could be obtained in spite of their intrinsic morphological variations thanks to the large number of objects in the sample. Given the performances of LITE, the detection of large structures of dark matter will be optimal in the redshift range 0.2–0.4 using source galaxies in the 0.5–0.8 range.

A very deep photometric survey to $m_B \sim 26$ is also planned for deriving new constraints on galaxy evolution over cosmological time scales. Multicolour counts of objects per magnitude interval in a catalogue more than an order of magnitude larger than the existing samples will put new constraints on the merging processes recently suggested as a major clue to recent galaxy evolution. The excellent resolution of the images obtained with LITE will provide direct estimates of the rate of occurrence of close pairs and merging systems and its dependence on redshift. Along these lines, the galaxy redshift survey at brighter magnitudes will put constraints on the influence of the environment on the evolution of galaxies, and will allow to measure the slope of the galaxy luminosity at the faint end, a crucial parameter in the evolutionary models.

Low-resolution spectroscopy of the large number of compact objects detected with LITE will yield a complete and homogeneous catalogue of QSOs. The absence of the biases present in existing catalogues and resulting from the multi-colour selection procedure, will allow a new examination of the QSO luminosity function and the apparent redshift cut-off in their distribution (at ~ 3). The homogeneity of the catalogue will also greatly benefit the understanding of the QSO-AGN connexion. Using the high quality images we will be able to study the environment of low redshift QSOs and their relationship to the large-scale galaxy distribution. Acquisition of the spectra with the VLT (FUEGOS and/or FORS) for the selected candidates will allow to probe the distribution and properties of known absorbers along the QSO's line of sight (galaxies surrounded by large envelopes, etc. ...). New types of absorbers may also be discovered (metal enriched intergalactic clouds for example). Combination of spectroscopy and high-quality imaging will provide for the first time a firm basis for a model describing the formation and evolution of halos around galaxies. New cases of lensed QSOs will also be found, and monitoring the variability of the images will put constraints on the value of the Hubble constant.

LITE will be used to detect distant supernovae. in 100 square degrees, we

PARTICIPANTS IN THE LITE PROJECT

Participants from France

CEA/DSM/DAPNIA/Service d'Astrophysique: Laurent Vigroux (Principal Investigator), M. Arnaud, O. Boulade, M. Cassé, C. Cesarsky, M. Lachièze-Rey.
CEA/DSM/DAPNIA/Service de Physique des Particules: P. Bareyre, E. Lesquoy, C. Magneville, J. Rich, M. Spiro, S. Zylberach.
CEA/DSM/DAPNIA/Service d'Etude des Détecteurs: Philippe Lavocat (Project Manager).
Institut d'Astrophysique de Paris: V. de Lapparent (Chairperson of the Science Team), B. Guiderdoni, D. Kunth, B. Rocca-Volmerange.
Observatoire Midi-Pyrénées: Y. Mellier (Project Scientist), B. Fort, G. Mathez, J. P. Picat, G. Soucail.
Observatoire de Besançon: O. Bienaymé, A. Robin.
Observatoire de Paris: C. Catala, P. Felenbok, J. Léorat, G. Mamon, D. Rouan.
Observatoire de Marseille: M. Azzopardi, A. Bosma, G. Comte.
Université de Montpellier: A. Mazure.
Observatoire de Nice-Côte d'Azur: E. Slezak.
Ecole Normale Supérieure: P. Boissé.

Participants from Germany

Astrophysical Institute Potsdam: H. Lorenz, G. Richter, S. Saar.
Sonneberg Observatory: H.-J. Breuer, P. Kroll.
Tautenburg Observatory: U. Laux, S. Marx.

will be able to discover 40 supernovae up to a redshift of 0.5 each week. The advantage of LITE for this search is of course its very good image quality and photometric performances which will help to detect supernovae as faint as $m_V = 23$ embedded in distant galaxies. The redshift determination will be done with the VLT.

Another domain will be the continuation of the brown dwarf research by microlensing effects on stars in the Magellanic Clouds. The two existing experiments are based on a 40-cm telescope and a 4-million-pixel CCD camera for the French MACHO instrument at ESO, and a 1.20-m telescope and a double 4-million-pixel CCD camera for the Australian-American instrument at Mont Stromlo. LITE will provide a gain by a factor 10 compared to these instruments.

Three types of observational programmes are considered: (1) a multicolour astrometric and photometric survey in individual fields selected according to Galactic structure and stellar programme, (2) a multicolour and slitless, low-resolution spectroscopic survey of typically 100 square degrees for cosmological observations and supernova research, and (3) observations in front of the Magellanic Clouds for detection of brown dwarfs. All of these programmes require very good image quality.

The scientific requirements call for LITE being a telescope of 2.5 m diameter with a mean image quality, including seeing, of 0.8 arcsec (or better) over a field of 1.5 degree (or more). This can only be achieved with good sampling of the image PSF by the CCDs. For a typical pixel pitch of 15 microns, 0.3 arcsec pixels are achieved with 10 m focal length; this corresponds to an f/4 aperture ratio. We first designed a quasi-Ritchey Chretien system with a Gascoigne corrector, but we finally adopted a new optical concept worked out at the Tautenburg Observatory, with the assistance of Ray Wilson from ESO. It is a modified version of the 3-mirror Paul-Baker telescope which provides a plane focal surface at the "prime focus" location, behind the secondary mirror. A preliminary design study has shown that for a telescope with 2.5 m diameter and focal ratio f/4, an image quality of 0.4 arcsec can be obtained at the edge of a 2.5-degree field, and significantly better towards the centre. Compared to the initial Cassegrain solution, this design has two important advantages, the absence of chromatic aberrations, because there are only reflecting mirrors, and a very easy baffling system to suppress straylight.

As a baseline, the CCD camera will be organized around thin, backside illuminated Thomson CCDs, each with 2048 x 2048 pixels and 15 micron length. These CCDs are being developed for the VLT, and the thick version should become available in 1993 and the thin one in 1994. The three-side buttability allows to make strips of 2 CCD widths. A 1-square degree surface can be covered with 36 CCDs. Readout time of the whole array will be as low as 30 seconds, thanks to a parallel acquisition system. Cryogenic temperatures will be provided by a closed cycle cooler in order to simplify the operations.

The natural site for this telescope is near the VLT, in the Paranal area, where it may take advantage of the excellent seeing and the large number of photometric nights as compared to the other Chilean sites. Discussions will take place with ESO to study this possibility.

The definition phase of the project will be undertaken in 1993. We must still settle the details of the German-French collaboration, work out the relationships between the consortium and ESO, and obtain funding. The actual start of the project is expected in 1994 and the beginning of the observations in 1999. In the present status of the project, nothing has been absolutely fixed and new groups are welcome to join. If you are interested, please do not hesitate to contact us. We expect to make a first presentation of the project at the IAU Symposium on Wide Field Imaging in Potsdam next August.

Projects similar to ours are under development, in particular the Sloan Digital Sky Survey (SDSS) in the USA. We wish to emphasize the differences between our project and the SDSS. The main goal of the SDSS is to make a survey over a large fraction of the entire sky ($\sim \pi$ steradians), both in photometry and in spectroscopy, and with the same telescope. However, the use of the SDSS 2.5-m telescope for spectroscopic measurements will naturally limit the observations to moderately faint galaxies only. The necessity of the all sky survey pushes towards the largest possible field, but at the detriment of image quality, and to a transit instrument which simplifies the operations.

In our case, the spectroscopic observations are planned with the much larger VLT, which, of course, can reach much deeper. Due to the increasing number of objects at fainter magnitudes, we cannot expect to cover a large fraction of the sky. On the contrary, we shall only be able to obtain images significantly deeper than the SDSS by limiting the sky coverage. For LITE, the priority of optimization is then image quality first, and field of view second. In addition, the pointing mode of operation is more suitable for very deep imaging than a transit mode. While many scientific areas are common to both instruments, the trade-offs are different, and the scientific programmes will be different too.

We believe that the combination of the VLT and LITE will offer a unique capability of probing the deep sky and will become a prominent instrument for future cosmological studies.

The ESO Red Sky Survey – a Tool for Galactic and Cosmological Studies

M. NAUMANN, R. UNGRUHE and W. C. SEITTER,
Astronomisches Institut der Universität Münster, Germany

Motivation

The ESO/SERC R-Survey of the southern sky is the observational contribution of ESO to the first complete sky survey south of −17.°5 declination. The other part, the ESO/SERC J-Survey, was observed in Australia. The ESO-Schmidt telescope at La Silla produced 606 photographic red plates covering some 15,000 square degrees of the sky, the UK Schmidt Telescope in Coonabarabran, Australia, took the corresponding blue/green J-plates. Sky coverage of the same order of magnitude is still far beyond the range of

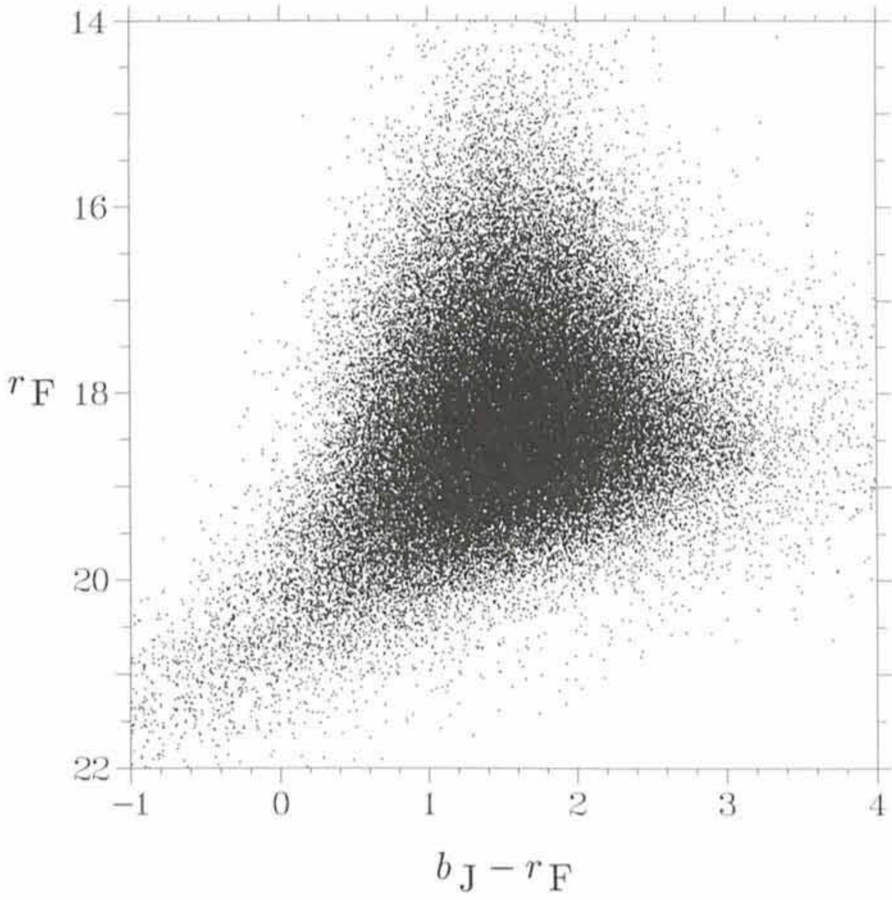

Figure 1: *The colour-magnitude diagram of 84,000 galaxies from 6 ESO/SERC R-plates.*

CCDs, which were not even introduced into astronomy when the atlas project started in the early 1970s, and wide-field telescopes specially designed for CCD imaging are only in the planning stage. Nobody knows the time scales on which an equivalent or deeper CCD survey can be realized, and a photographic atlas is still a singular tool for large-scale studies.

The Sky Atlas Laboratory at ESO-Garching, as before in Geneva, took the responsibility of producing and editing both parts of the ESO/SERC Atlas, including the laborious tasks of quality controls, partially re-evaluating the original photographs as well as checking every single one of almost 200,000 glass or film copies of the atlas fields, to ensure highest quality before they were distributed to hundreds of institutions around the world.

The J-atlas, the observational contribution of the UK, was digitized at two UK institutions: at the Institute of Astronomy in Cambridge with the APM machine and at the Royal Observatory Edinburgh with the COSMOS machine. Thus, it seemed appropriate to have the R-atlas digitized in an ESO member country.

The Astronomical Institue of Münster University (AIM) took up the challenge. We needed the atlas for our work, and there were some ulterior motives. One was getting an additional PDS 2020GMplus microdensitometer (thanks to the Federal Ministry of Science and Technology of Germany) for the time-consuming task of scanning. Both PDS machines were equipped with powerful new amplifiers, developed and constructed at AIM (the "plus" to the original name indicates this addition), which permit us to use the double-slit machines to the mechanical limit of their scanning speed of 200 mm s^{-1}. Another one is our contribution to ROSAT source identification. While Edinburgh has provided ROSAT headquarters at the Max-Planck-Institut für Extraterrestrische Physik in Garching with catalogues from the J-plates, AIM provides R-catalogues. Last not least, the data base resulting from the R-atlas is a tribute to the two people who created the red atlas: to Hans-Emil Schuster, who dedicated many years on La Silla to the tedious and responsible task of taking the plates – as earlier for the ESO Quick Blue Survey (QBS) – while training his assistants to perfection, and to Richard West who, together with his able helpers, produced the complete atlases at ESO headquarters – as he now edits the new three-colour POSS II/ESO Survey.

Digitization, Data Reduction and Catalogues

The area chosen by us for digitization, data reduction and interpretation covers 216 plates. It encompasses almost 5000 square degrees of the sky between declinations $-17\overset{\circ}{.}5$ and $-82\overset{\circ}{.}5$ and right ascensions 20^h30^m to 5^h30^m. Outside this area, star densities become too high for proper automatic detection and evaluation of single objects. 1.5 years were invested for scanning and basic reductions. The step size of 15 μm and the aperture of 20 μm × 20 μm yield a positional accuracy of $0\overset{''}{.}3$. Due to the double slit and the high density range of our amplifier (its effective limit is determined by photon statistics rather than by sensitivity) we are able to measure system magnitudes $14 \leq m \leq 21$ with an accuracy of about $0\overset{m}{.}1$ in the middle range, and $0\overset{m}{.}2$ in the very bright and very faint ranges. For magnitude corrections on individual plates (center-edge sensitivity variations) internal methods are used; for the determination of catalogue zero points, standard sequences are measured with the Dutch 0.90-m telescope at La Silla and, in collaboration with the University of South Africa, Pretoria, with the 1.0-m telescope of the South African Astronomical Observatory (SAAO).

The galaxy catalogue lists 7.1 million galaxies down to magnitude $m = 21$, the star catalogue almost 20 million stars to the same limit. The catalogues will literally broaden – and hopefully deepen – our views in observational cosmology as well as in stellar statistics.

Project History

In 1986, we started the Münster Redshift Project (MRSP) by measuring direct atlas plates as the indispensible counterparts of objective prism plates, used for the determination of redshifts. At this time the red survey was not yet complete and we chose J-plates for the start. The first 400 square degrees were used to develop scanning techniques and reduction algorithms and to introduce and implement methods in stellar statistics and observational cosmology. The low dispersion objective prism plates (reciprocal linear dispersion of 246 nm/mm at Hγ) were taken with the UK Schmidt telescope.

Redshift measurements from objective prism plates need reliable zero points. This induced us to add astrometry to our programme and to use plate transformations from direct to objective prism plates to define reference positions. To date more than 120,000 galaxy redshifts have been measured in 12 fields and are presently used for cos-

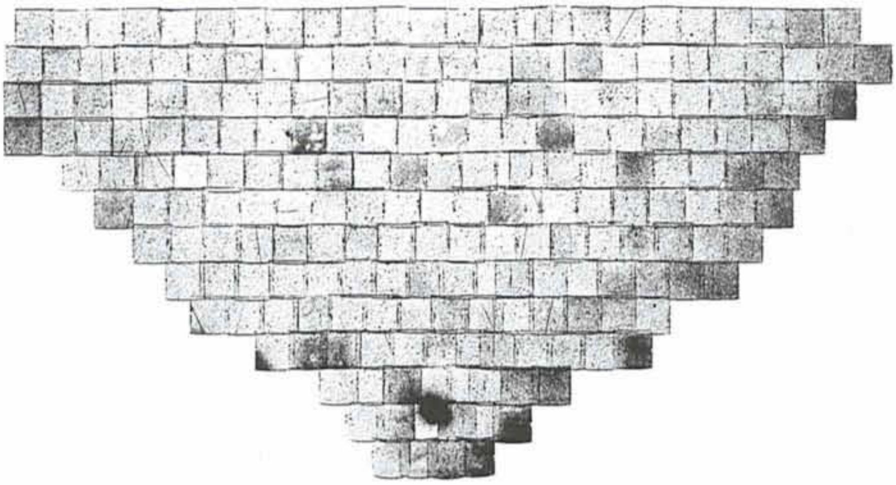

Figure 2: *The distribution of artifacts found on 216 plates of the ESO/SERC-R-Atlas. The individual plates are clearly outlined by the plate frames, which are scanned but rejected as artifacts by the software. The increase of artifacts towards the Milky Way region is due to the increasing numbers of rejected overlaps.*

mological investigations. Colour information is an important additional tool.

Astrometry from Schmidt plates also provides us with statistical proper motions in the Milky Way and in neighbouring galaxies. Using for the first epoch ESO QBS plates and for the second epoch ESO Schmidt plates, taken 15 years later specifically for the project, the absolute proper motion of the LMC was determined and other Local Group galaxies are now investigated. Astrometry is a useful tool for the interpretation of stellar colour-magnitude diagrams.

Magnitude Calibrations

Magnitudes are obtained in a lengthy process: each measured isophotal and aperture magnitude is subjected to transformations, corrections and calibrations, amounting to 8 steps for galaxies and 6 steps for stars. The overlap regions of the 216 fields are used to adjust all plates to a common zero point. CCD sequences, distributed over the whole area, are needed to transform the plate magnitudes into an international system.

All hypersensitized Schmidt plates have a tendency to loose sensitivity towards the plate edges. This effect, together with that of vignetting, must be corrected. Desensitization is severe for J-plates, especially the older ones, taken before UK astronomers became aware of the effect and found partial remedies. Although the effect is smaller on R-plates, it cannot be neglected. The best way, short of having tens of calibration sequences over each plate (which would require a dedicated 1-m telescope on La Silla for several years) are magnitude corrections based on the comparison of galaxy numbers per unit area in the central part of the plate and at the edges. Galaxy counts on several plates near the SGP as a function of local photographic background densities yield a good average correction curve for the magnitudes. The quality of this curve is tested by comparing the results in the regions of large plate overlaps.

Magnitudes from the J- and R-plates are labelled b_J and r_F, the symbols indicating the blue and red passbands and the photographic emulsions Kodak IIIa-J and Kodak IIIa-F (for the atlas used in combination with filters). About 70% of all objects brighter then $r_F = 20$, i.e. 35,000 stars on the average R-plate, and more than 11,000 galaxies are sufficiently well matched with their J-counterparts to yield the colour index $b_J - r_F$.

Colours and Magnitudes

Colours of stars and galaxies hold information on intrinsic and extrinsic parameters, such as stellar temperatures and dust absorption, galaxy populations and cosmological effects. Colour-magnitude diagrams of field stars comprise objects at largely different distances, representing two or three different stellar populations – halo, thin disk and possibly thick disk. With the aid of astrometry, we can interpret colour-magnitude diagrams of stars with measured proper motions $\mu > 0''.1\ yr^{-1}$. This helps us to find good starting parameters for simulations, used to explain the colour-magnitude diagrams of all stars. Preliminary results support the presence of a thick disk.

Colour-magnitude diagrams of galaxies include mixtures of morphological types with different dust content, at all inclination angles, in a range of redshifts and affected by evolution. The colour-magnitude diagram in Figure 1 shows 84,000 galaxies with all these characteristics and can only be explained by comparison with simulations.

Tracing the effects of galaxy evolution for magnitudes $r_F \approx 20$ with large statistical samples may lend credulity to the conclusions drawn from the much smaller samples available so far. The comparison of colour distributions of intrinsically faint and bright galaxies may yield constraints for the timescales of formation and evolution of massive and of low-mass galaxies.

For fluctuation analysis in cosmology, using galaxy counts-in-cells in three dimensions, magnitude measurements of the same objects in different spectral ranges may help to smooth the effects of magnitude errors. These must be small when larger scales are to be reached. Large-scale fluctuation analysis needs large survey volumes of equal extent in all spatial dimensions and is thus a task which can well be achieved by photographic surveys with their large sky coverage, and with z-values from objective prism plates – provided the magnitudes can be improved.

Colours are of interest for objects which we identify as quasar candidates on the basis of their objective prism spectra. Almost 12,000 candidates have been found so far. On the basis of earlier measurements, we expect to find usable redshifts for about 75% of the candidates. In spite of our bias towards Lyman α quasars, the colour distribution of this sample will be of interest for comparison with quasar surveys where the objects are selected by colour.

Colours are also of technical help. Together with the morphological types of galaxies, determined automatically within the MRSP down to $b_J = 19.5$, colour information can aid in determining the mixture of galaxy types in various samples and thus the K-corrections to be applied. This avoids systematic errors due to global K-corrections and yields more reliable luminosities and distances.

Finally, one might mention the possibilities of having an independent check on results from cosmological investigations using b_J magnitudes. Controversial conclusions, such as the ones drawn from galaxy counts $N(_J)$ within the APM Project may be independently supported or rejected with $N(r_F)$ counts. For large samples of galaxies, angular correlation functions $w(\theta)$ will be determined on the basis of r_F magnitudes and comparisons will be possible of results from essentially the same volume of space and from data which were ob-

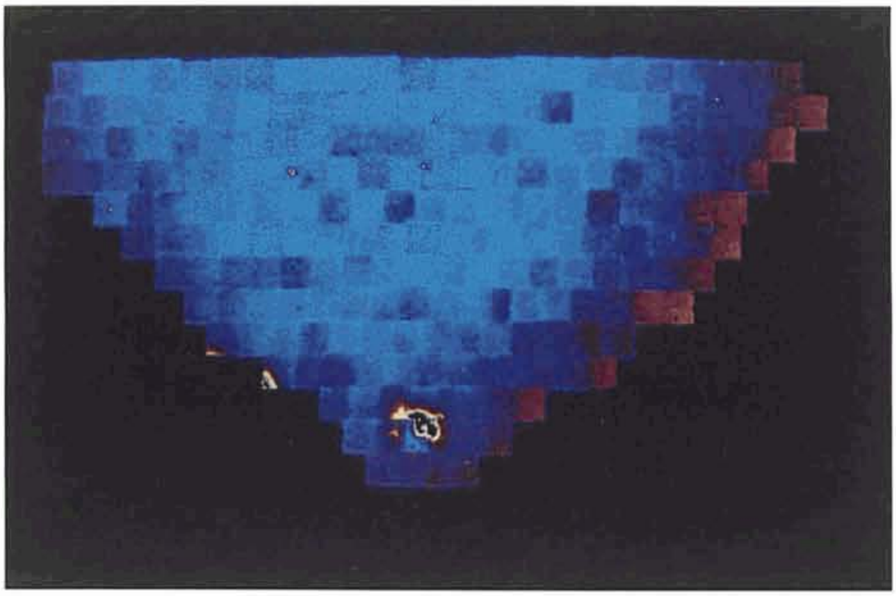

Figure 3: *The distribution of stars on 216 plates of the ESO/SERC-R-Atlas. It shows strong density gradients towards the Milky Way, which are indicated by increasingly redder colours. Aside from this gradient and some plate-to-plate variations, which are due to the fact that zero points and limiting magnitudes have not yet been adjusted, the distribution is quite smooth. The extremely crowded regions of the SMC and LMC are seen in the lower centre and to the lower east. The brightest white spot is the Sculptor dwarf galaxy, its nearest neighbour the Fornax dwarf galaxy.*

tained with very similar techniques – except that the different passbands may introduce different selection criteria and measuring errors.

Artifacts

Leaving the realm of cosmology and coming literally down to earth, we may look at the artifacts found on the survey plates, as displayed in Figure 2. There is no doubt that most artifacts are man-made. Aside from dust, which is unavoidable even in a relatively clean measuring environment, and satellite trails, found abundantly, a large source for artifacts are blended stellar images which no doubt owe their existence to the imperfection of imaging and image analysis techniques – aside from the earth's atmosphere. The number of artifacts increases towards the Milky Way fields, in the vicinity of the SMC, seen in the lower middle of the total field, as well as in the LMC which just touches some fields on the eastern side. Other dense regions, such as star clusters and clusters of galaxies, are not so obvious. Surprisingly, the plate edges are well delineated by artifacts. Because of the generally small overlap regions of the plates, all scans have been made over somewhat larger regions than covered by useful data, just to be sure not to loose information. Cutting the edges properly is then a software process which lists the plate frames as artifacts.

Stars

Figure 3 shows the distribution of stars. The most striking feature is the rapid steepening of the density gradient towards the Milky Way region at the eastern and western edges of the total field, apparent fromt the dramatic change in colour in this false colour presentation. Noticeable changes in star density across even short distances are indicated by colour changes within individual plates. In addition, each as yet uncalibrated plate has its own zero point and magnitude limit, leading to systematically enhanced or reduced numbers of objects, as is indicated by different hues in the central part of the field. They will disappear after proper plate calibration, which is possible as soon as all CCD standards are obtained. Nevertheless, the overall impression even of the uncalibrated plates is one of a smooth stellar background with no trace of large-scale structures.

Galaxies

The galaxies whose distribution provides an observational stepping stone for cosmology, are shown in Figure 4. Again, the magnitudes are uncalibrated and the plates have different magnitude limits. Because the galaxy number densities show no systematic gradients over large areas, the patchiness can be removed – just for viewing purposes – by presenting each one of 10^4 bins per plate normalized to the mean number density over a given plate. At the low resolution of the image shown here, the general pattern is not affected by this procedure. Quantitative analysis, of course, has to wait for proper plate calibration.

It is rewarding to see that the distributions of stars and galaxies are quite different – as is expected. It gives us

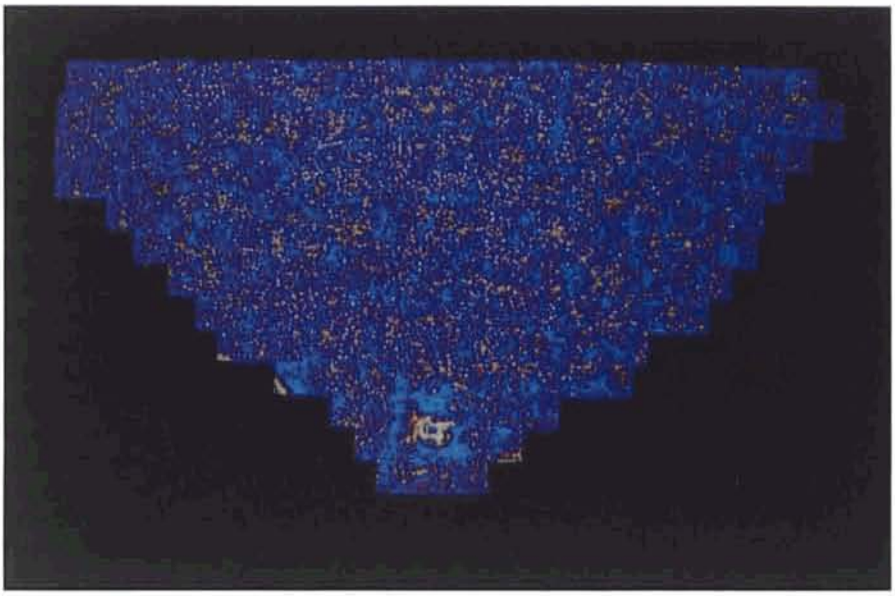

Figure 4: *The distribution of galaxies on 216 plates of the ESO/SERC-R-Atlas. The intricate pattern known from other galaxy surveys is clearly seen. A small percentage of blended stellar images in the rich regions of the SMC and LMC shows up as misidentified galaxies. The apparent decline of contrast towards the Milky Way region is an artifact due to increasing numbers of misclassified overlapping stars and the normalization procedure described in the text.*

some confidence that the tricky process of star/galaxy separation works well. Visual checks of our method suggest that the automatic star/galaxy separation yields errors smaller than 10% at reasonably high galactic latitudes.

An automized comparison of the data from the R-plates with those from the J-plates has the advantage that the classification of all objects can be checked. Although the quality of the procedures is not tested by the comparison, the reliability with which the procedures work on the same object at different brightness levels and on plates taken under different observing conditions will become apparent. Another test is the comparison between automatically determined morphological types of galaxies on R- and J-plates. Its outcome will be more difficult to interpret because of additional physical effects. It will be interesting to see whether a colour dependence of morphological classification can be quantified.

The Stage and the Plot

Dwelling on basic details, such as removing artifacts and struggling with photographic magnitudes, while results from the red survey are still in the making, reminds us of showing a stage in daytime.

Nothing looks glamorous and the actors are still rehearsing. We hope, however, that the scenery promises to become a worthy background for a great production. The plot will be presented in the version offered by the ESO/SERC Atlas which, together with powerful measuring machines and computers, has opened new possibilities for staging the drama of the universe.

The topics and papers given below are acknowledgements to our coworkers who are not mentioned as coauthors.

Amplifier: Budell, R. 1992, in *Astronomical Photography 1990*, ed. J.L. Heudier, Université de Nice-Sophia-Antipolis, P. 23.

Astrometry: Tucholke, H.-J., Schuecker, P. 1992, *PASP* **104**, 704; Tucholke, H.-J., Hiesgen, M. 1991, in IAU Symp. 148, *The Magellanic Clouds*, eds. R. Haynes, D. Milne, Kluwer, Dordrecht, p. 491; Winkelkoetter, H. 1992, Diploma Thesis Münster.

Colour-magnitude diagrams: Ritzmann, B.-M. 1992, Diploma Thesis Münster.

Fluctuation analysis: Schuecker, P., Ott, H.-A. 1991, *ApJ* **378**, L1.

Hubble Constant: Duemmler, R. 1992, *A&A* **261**, 1.

Morphological classification: Spiekermann, G. 1992, *AJ* **103**, 2102.

Photometry: Cunow B. 1992, *MNRAS* **258**, 251; 1993a, b, *A&A*, in press.

Quasars: Meijer, J. 1991, Diploma Thesis Münster; Nolze, W. 1993, Diploma Thesis Münster.

Redshifts: Schuecker, P. 1993, *ApJS* **84**, 39.

Software and Hardware: Teuber, D. 1989, in *Reviews in Modern Astronomy 2*, ed. G. Klare, Springer, Berlin, p. 229.

Star/galaxy separation: Horstmann, H. 1992, Doctoral Thesis Münster.

First Technical Run of the COME-ON-PLUS at the ESO 3.6-m Telescope

N. HUBIN, ESO
G. ROUSSET, ONERA, Châtillon, France
J.L. BEUZIT, DESPA, Observatoire de Paris, France
C. BOYER, Laserdot, Marcoussis, France
J.C. RICHARD, Laboratoire d'Electronique Philips, Limeil-Brévannes

From December 6 to 15, 1992, the new VLT adaptive optics prototype system, the so-called Come-On-Plus system, was tested at the 3.6-metre telescope (Fig. 1). This system [1, 2, 3] is an upgraded version of the previous prototype, Come-On [4].

The main characteristics are its 52-actuator deformable mirror, the photon counting wavefront sensor using an Electron Bombarded CCD and the modal control [1, 2, 3]. During this run two visible wavefront sensors were used, one for visible magnitudes up to 9.5 and one for visible magnitudes up to 16. The imaging channel was equipped for this run with a 32×32 InSb infrared camera from the DESPA/Observatoire de Paris working in J, H, K, L, M bands. The scale was 50 milliarcsec/pixel which provides a field of view of 1.6 arcsec.

Long and short exposure images in the J, H and K bands were obtained with

Figure 1.

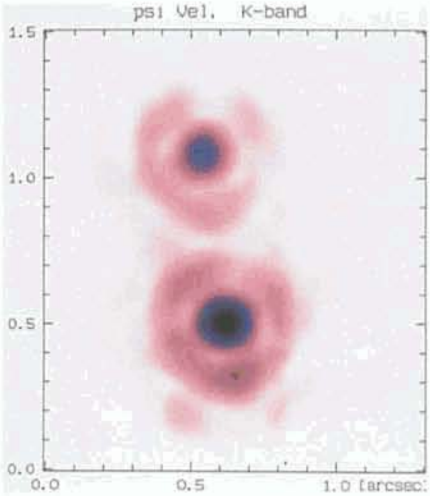

Figure 2.

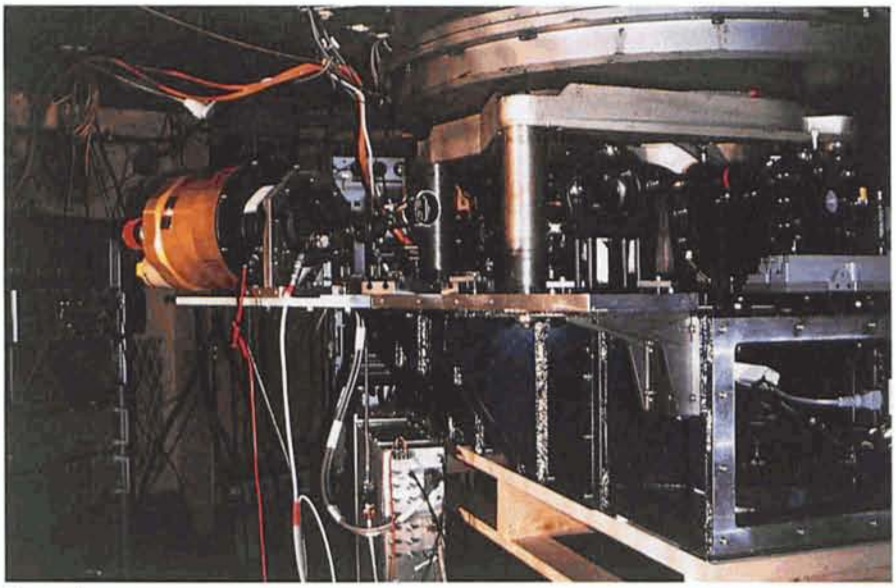

Figure 3.

a high correction efficiency using the "high flux wavefront sensor" (Fig. 2). Isoplanatic patch measurements were performed with star separation up to 20 arcsec still showing a good correction for the off-axis star in the K band. With this wavefront sensor a 30 Hz open loop bandwidth at 0 dB was reached.

Using the photon counting wavefront sensor, long exposure images in the K and L bands were recorded. The powerful capability of the modal control was used to optimize the correction depending on the star magnitude, the seeing condition, the average wind speed of the turbulent layers and consequently to minimize the noise propagation on the different modes. The system bandwidth (modal gain) was adjusted versus the signal-to-noise ratio. For instance, only tilts, defocus and astigmatisms were corrected with a 14th magnitude star (spectral type M). For magnitude 16 (spectral type M) only the tip-tilt was corrected allowing us to reduce the FWHM by a factor of 2.

At the end of this technical run a 512×512 cooled CCD camera was implemented in order to evaluate the partial correction capability of the system in the I band (Fig. 3). The scale was 20 milliarcsec/pixel with a field of view of 10 arcsec.

For the wavefront sensing, stars of visible magnitude between 4 and 6 were used and long exposure images were recorded. Double stars with separations of 0.33, 0.55, 0.8 and 2.6 arcsec were observed (Fig. 4). An average of 0.2 to 0.3 arcsec FWHM was obtained in the I band during this test under poor seeing conditions (seeing >1arcsec and average wind speed >10 m/s).

A detailed analysis of the results collected during this technical run is now under way and will provide important information for the second technical run foreseen in April. People interested in the detailed results are kindly invited to attend the next ESO Conference on Adaptive Optics in August.

Acknowledgements

The authors would like to thank many colleagues from ONERA, Observatoire

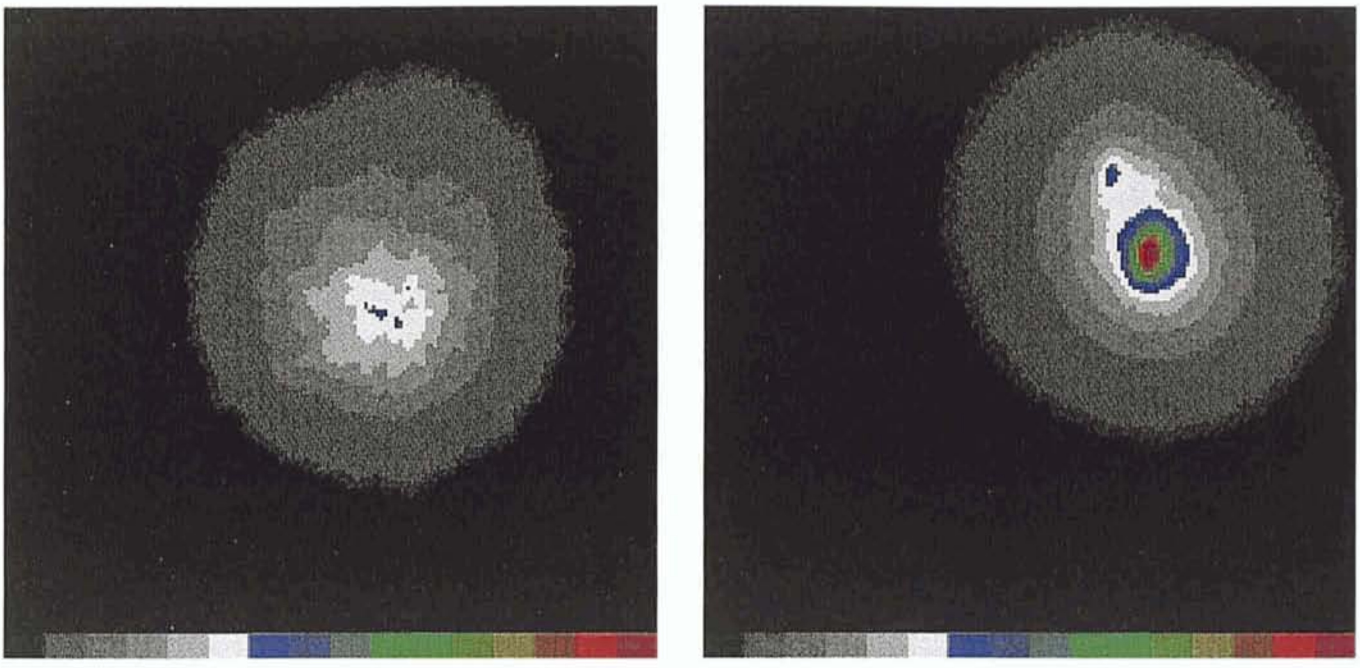

Figure 4: *Double star with separation of 0.3 arcsec observed in the I band, uncorrected (left) and corrected (right).*

de Paris, Laserdot, LEP and ESO-La Silla who have contributed to the design, construction and test of this instrument. In particular, we are thankful to Sen Wang and Pierre Gigan of the Observatoire de Paris for the optical and electronic integration performed during this run.

References

[1] Hubin et al. (1992): New adaptive optics prototype system for the ESO 3.6-m telescope: Come-On-Plus, 1992, *SPIE* 1780.

[2] Rousset et al. (1992): "The COME-ON-PLUS project: an adaptive optics system for a 4 m class telescope" ESO Conference Proc. No. 42, 403.

[3] Gendron et al. (1991): The Come-On-Plus project: an upgrade of the Come-On Adaptive Optics prototype system, *SPIE* 1542.

[4] Rigaut et al. (1991): "Adaptive optics on a 3.6-m telescope: results and performance", *Astron. Astrophys.* **250**, 280.

ADONIS – a User Friendly Adaptive Optics System for the 3.6-m Telescope

J.L. BEUZIT, DESPA, Observatoire de Paris, France

N. HUBIN, ESO

Last November a contract was signed between ESO and the Observatoire de Paris for the "design, development, manufacturing and installation at the ESO 3.6-m telescope at La Silla-Chile of the COME-ON+ upgraded to a user-friendly instrument called ADONIS". ADONIS stands for ADaptive Optics Near Infrared System.

This represents the third phase in the development of the VLT adaptive optics prototype. The very first version, COME-ON, constructed by the consortium ESO – Observatoire de Paris – ONERA – Laserdot, has already achieved routinely diffraction limited images in the near infrared on the ESO 3.6-m telescope (Rousset et al. 1990, *Astron. Astrophys.* **230**, L29; Rigaut et al. 1991, *Astron. Astrophys.* **250**, 280).

During five observing runs in 1990–1991 COME-ON obtained significant astrophysical results such as the determination of the rotation axis of the asteroid Ceres (Saint-Pé et al. *Icarus*, submitted), the first direct images of a disk-like structure around the young star Z CMa (Malbet et al., *The Messenger* No. **66** and *Astron. Astrophys.*, in press) and the images of Eta Car, showing a very complex structure (*Physics Today*, April 92).

A first upgrade of COME-ON, called COME-ON+, was recently tested on the 3.6-m telescope. The efficiency and performances of the instrument have increased significantly (see the report on page 50). However, COME-ON+ remains a prototype, its operation procedures are complex and a qualified team is required to operate the whole system in an efficient way.

In fact, several parameters have to be optimized (number of corrected modes, band-pass, choice of wavefront sensor) according to astronomical requirements (wavelength of observation, magnitude of object) and external inputs such as atmospheric turbulence (amplitude and temporal spectrum), magnitude, spectral type and angular distance of the reference star. This has led to the necessity of implementing an automated system which will do the settings and optimization much better and with greater regularity, thus helping the observer to take the basic operation decisions in an efficient way with respect to the more efficient use of telescope time.

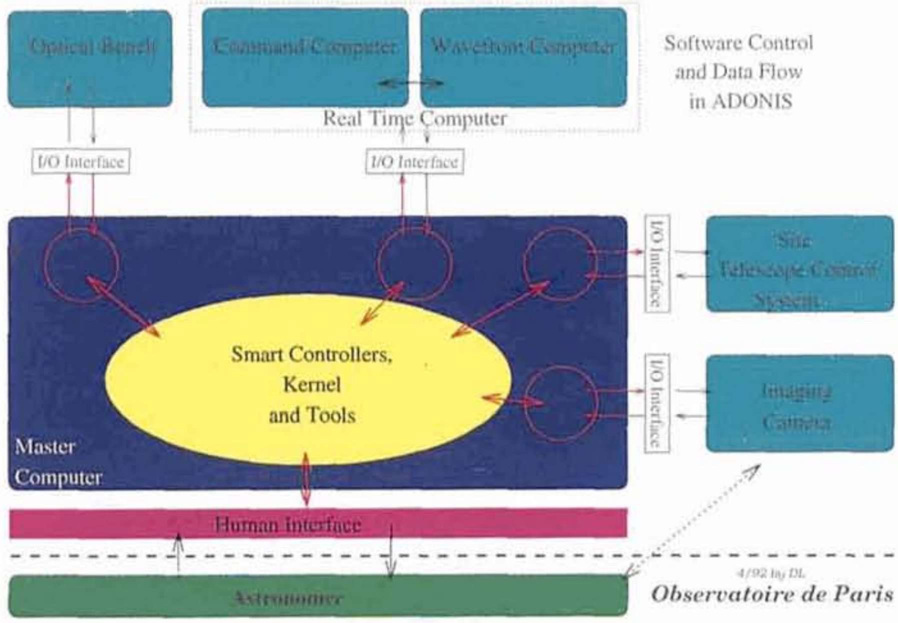

To perform this, a smart software control system will be generated, with interfaces (data acquisition or direct control) with all subsystems such as optomechanical bench, real-time computer, infrared camera, telescope control system, site sensors (seeing, meteo), databases and user interface (see figure).

In addition, a dedicated 128×128 infrared imaging camera, covering the 1–5-μm region, will be installed to take full advantage of this powerful adaptive optics system. Two interchangeable scales (0.035″/pixel and 0.1″/pixel) are selectable to match the diffraction patterns respectively in J (1.2 μm) and L (3.6) bands.

ADONIS will also offer the possibility to accommodate many different imaging devices, for instance the Nicmos camera of the MPI/MPE Garching which will already be used on COME-ON-PLUS in April 1993. Moreover, the possibility for visiting observers to bring along special equipment will be possible by the definition of a simple and open interface on the output F/45 beam. An ADONIS interface manual will be published for this purpose.

ADONIS should progressively become available to the community during the period 1993–1995. In addition to the scientific use at La Silla, ADONIS will bring a substantial gain in optimizing the operation of an adaptive optics system, particularly important for the VLT prospect. ADONIS continues to rely on the collaborative action with ONERA and Laserdot which made the success of its predecessors. The continuing adaptive optics development programme is currently the only one which is solely dedicated for nighttime astronomy and which has produced significant astrophysical results.

Nonlinearity Problems with Generation-3 CCD Controllers

H. E. SCHWARZ and T. M. C. ABBOTT, ESO-La Silla

Introduction

At present, there are 20 CCDs from five manufacturers running under three different control systems in use at La Silla. Recently, during an observing run at the 2.2-m telescope, a nonlinearity in the response of CCD #8 was discovered (Remy et al., 1992). This short article is intended to describe the problem, set limits on its first possible occurrence, inform the reader about its solution and request contacts from interested parties.

The Problem

During the observing run of 27.2.1992 to 1.3.1992 at the 2.2-m telescope with EFOSC2, with observers Surdej et al. for Key Programme 2-003-43K, a nonlinearity in the CCD response was found. The effect shows up as a feature in the plot of signal variance versus mean signal (the transfer curve, Janesick et al., 1987). For a properly functioning system this plot should be a straight line in the photon shot noise dominated regime whose slope is the inverse of the system conversion factor in electrons per ADU. Figure 1 shows the nonlinear behaviour. A similar feature is also present in the linearity curve for the CCD (mean counts versus integration time), with a total excursion from linearity of 4 % peak-to-peak.

Investigation of the problem revealed that the fault was with the analogue to digital converter board in the Gen3 system, not the CCDs themselves. These boards replaced the previous model boards because of their lower noise performance. Replacing the new boards with the old cured the problem. Figure 2 shows the same plot as Figure 1, but after installing the old boards which have all been in place since 6.4.1992. Since the old boards were originally replaced in 1986, we must also determine when the nonlinearity first appeared and which CCDs were affected.

Which Systems Have Been Affected?

Only instruments using Gen3 systems have been affected. There were 4 such

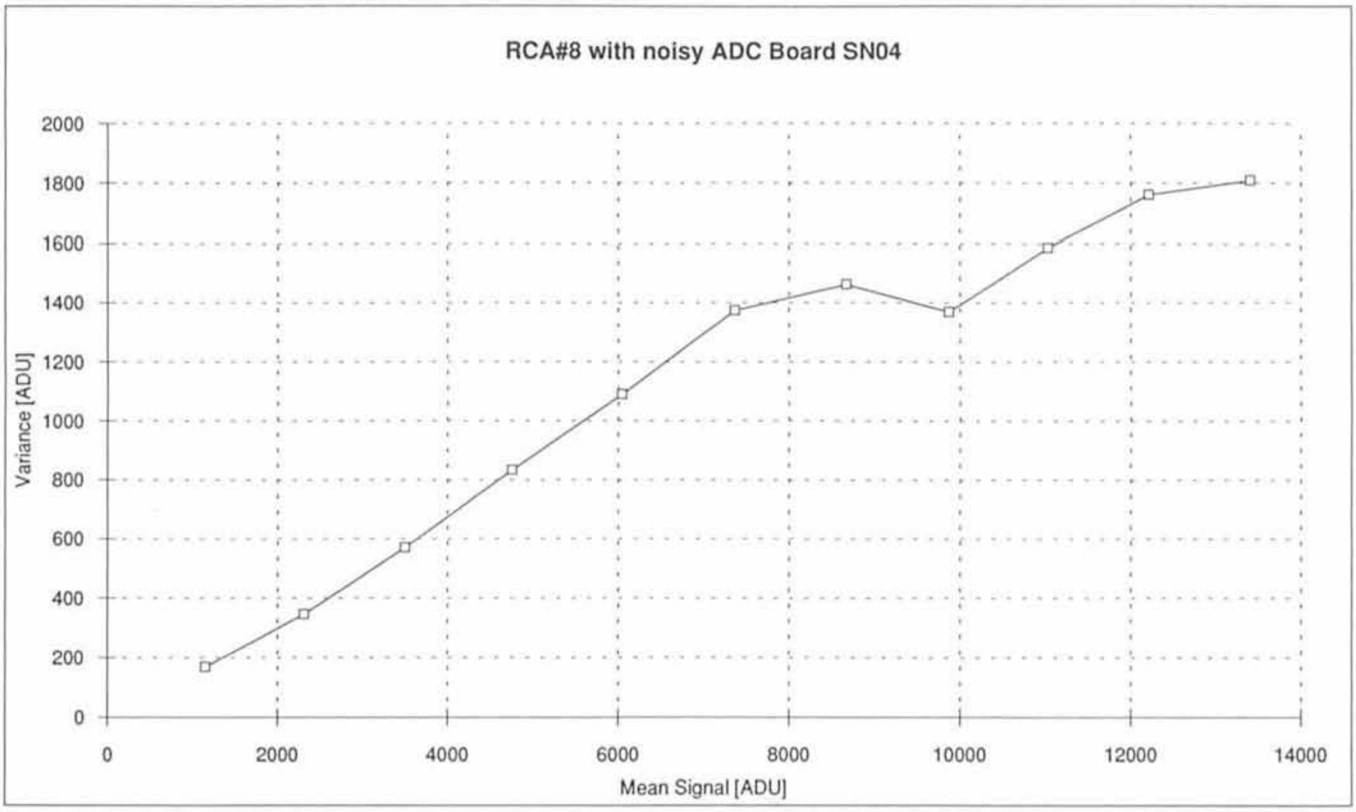

Figure 1.

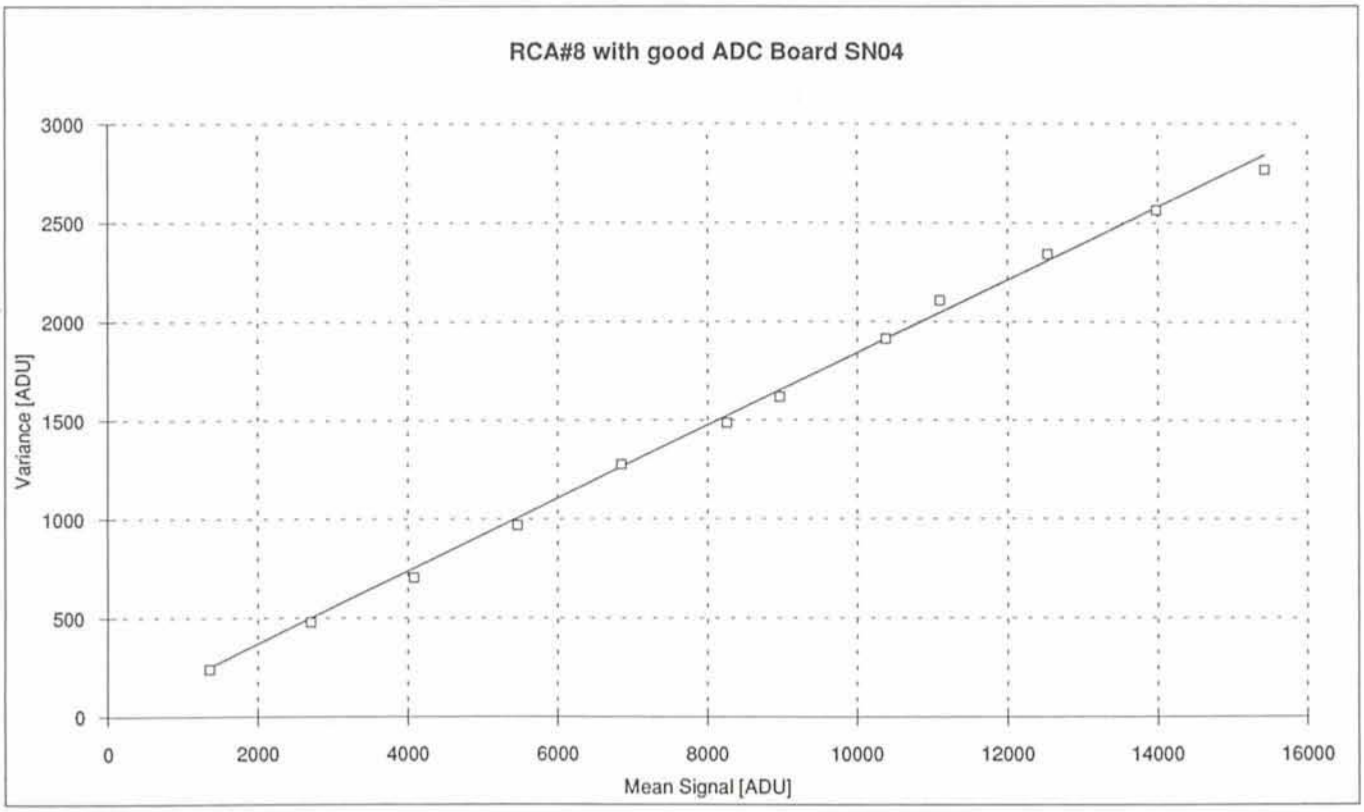

Figure 2.

sets of CCD electronics in use at La Silla:
(a) 2.2-m with adapter, EFOSC2 and Boller and Chivens. CCD used: #8
(b) 1.54-m Danish with adapter. CCDs used: #5, 15.
(c) 1.52-m with Boller and Chivens and Echelec. CCD used: #13.
(d) 0.91-m Dutch, since July 1991. CCDs: #14 (briefly in July 1991), #7.

Note that none of the Gen5 or VME systems have been affected by the problem at any time. Therefore data from Ford, Thomson and Tektronix CCDs have not been affected.

When Did the Problem First Occur?

To determine the first occurrence of the nonlinearity, data have been analysed at La Silla. The earliest known affected data were taken on the 1.54-m Danish telescope in February 1991 with CCD #15 – the effect is only marginally present. Data from 1988, 1989, and 1990 are being investigated.

What was the Nature of the Problem?

It has been found that there is an extra noise component present in the system which contributes in the range 6,000 to 10,000 ADU, just the range in which the nonlinearity occurred (Fig. 1). This measurement was made using a CCD video simulator which produces a signal with noise independent of the signal level, unlike astronomical signals where the noise varies with the square root of the signal level (shot noise). For the old (good) boards the result was a variance which was constant with signal level; the new (bad) boards showed the additional noise component. It is therefore clear that the excess noise component is linked to the observed nonlinearity.

After solving the main problem, further investigations have revealed that there are still low-level nonlinearities present which are still being studied.

Further Information

For further information, please contact the authors (hschwarz@eso.org and tabbott@eso.org) and watch *The Messenger* for further articles concerning CCDs at La Silla.

References

J.R. Janesick, T. Elliot, S. Collins, M.M. Blouke, J. Freeman, 1987, *Opt. Eng.*, **26**, 692.
M. Remy, P. Magain, A. Smette, J. Surdej, 1992, private communication.

CASPEC Improvements

L. PASQUINI and A. GILLIOTTE, ESO-La Silla

Introduction

CASPEC, the high-resolution spectrograph mounted at the Cassegrain Focus of the 3.6-m telescope, has been the object of almost constant upgrading in the last three years (Pasquini et al. 1991, 1992).

CASPEC is the only high-resolution spectrograph at La Silla which offers a broad range of options: a rather high resolving power coupled with a large spectral coverage, the possibility to easily change the central wavelength and the capability to observe in the blue and UV up to the atmospheric cut off (Baade and Crane 1990, Molaro et al. 1992). These characteristics, coupled with the large telescope aperture, have made of CASPEC a powerful and versatile instrument used by a large number of observers.

During 1992 CASPEC was not

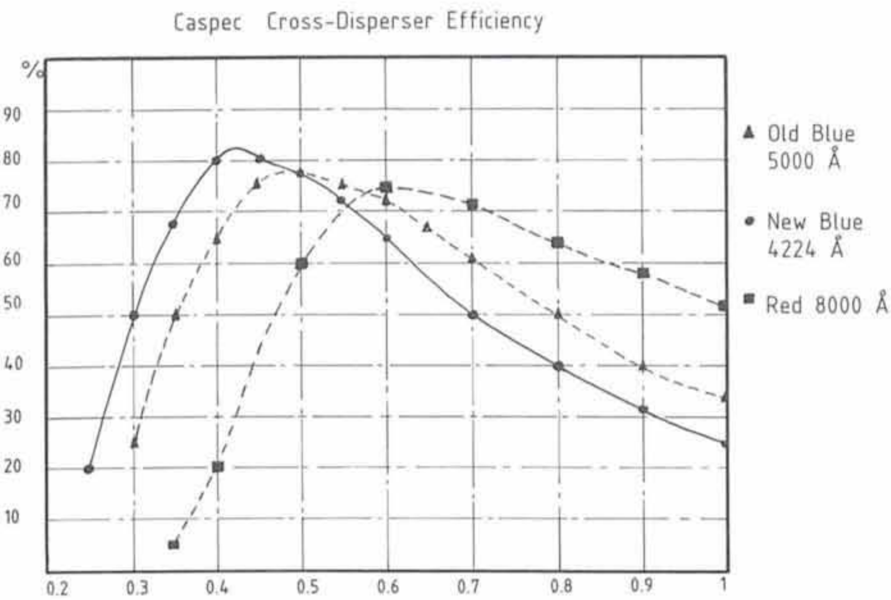

Figure 1: *Efficiency curves for (a): The new Blue crossdisperser (filled dots):; (b): The old Blue crossdisperser (filled triangles); (c): The Red crossdisperser (filled squares).*

mounted at the telescope for three months, in the period August–November. This opportunity was taken to upgrade the instrument through two major changes: a remastering of the old Blue crossdisperser and the mounting of a new, more sensitive CCD.

A new remastering of the Blue crossdisperser was necesarry for mainly two reasons:

(1) Due to the inclined position in the CASPEC mounting, the optical surfaces of the crossdisperser gratings were quite degraded, after 10 years of use. This did affect the efficiency of the instrument and its general performances, increasing the presence of stray light and optical blemishes.

(2) With the implementation of the Red crossdisperser of CASPEC and of the High-Resolution mode on EMMI at the NTT (Melnick et al. 1982), these two spectrographs resulted in a very good performance at wavelengths longer than ~ 5500 and 4500 Å respectively. As a consequence, the CASPEC performances should be enhanced in the Blue-UV region, where EMMI cannot work at a comparable resolution. The first step towards this goal was the replacement of the old Blue CASPEC crossdisperser, which was blazed at 5000 Å, with a new one with a bluer blaze peak.

The New Blue Crossdisperser

The new crossdisperser is, as the old one, a mosaic of two gratings, whose characteristics are summarized in Table 1. In Figure 1 the grating efficiency as function of wavelength is given (filled dots), together with those of the old Blue crossdisperser (filled triangles) and of the Red crossdisperser (filled squares). The blaze peak of the new Blue crossdisperser is at 4224 Å and Figure 1 shows that it is more efficient than the old one in the 3000–4800 Å wavelength range, and only for longer wavelengths the performances are comparable or lower; the expected efficiency is doubled at 3000 Å.

Considering that above 5500 Å the Red crossdisperser can be used, the new Blue crossdisperser will represent a significative advance in the instrument performance. The dispersion of the new gratings being the same as the old ones, the spectral coverage is maintained to ~ 1400 Å per frame.

Table 1: *Characteristics of the new Blue crossdisperser gratings.*

Type	Milton Roy 3563/90
Groove density	300/mm
Blaze wavelength	4224 Å
Blaze angle	3°36'

In order to limit costs and manpower, the two gratings forming the crossdisperser mosaic were remastered on the old blanks.

As soon as they came back from the manufacturer, the gratings were assembled into the mosaic. This assembling was performed at La Silla and the results were checked through interferograms.

The CCD

Together with the new crossdisperser, also a new CCD was installed on CASPEC: the 512×512 Tektronix ESO CCD #32, whose characteristics are given in Table 2, and whose response curve is shown in Figure 2. This CCD has an excellent efficiency over a broad wavelength range: the Relative Quantum Efficiency peaks at 76 % at 6500 Å, is almost 50 % at 3600 Å and it drops to 23 % at 3200 Å (see Fig. 2). It does not need UV flooding to enhance its blue sensitivity. The other CCD parameters are very similar to those of the CCD #16 previously mounted on CASPEC. The Dark Current and Read Out Noise are higher than expected, however the CCD

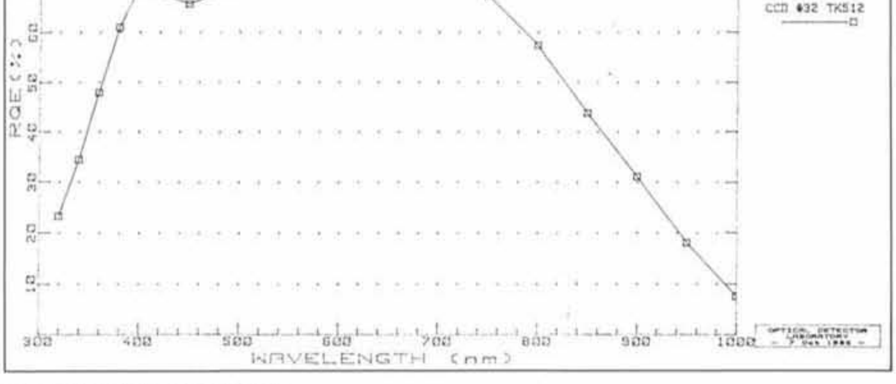

Figure 2: *R.Q.E. of CCD #32*

Table 2: *CCD #32 characteristics*

Type: Tektronix TK 512 CB, thinned, Ar-Coated, MPP	
Serial number:	BR 1456-12-10
Format:	512×512, 50 pre-scan pixel in horizontal direction
Pixel size:	27×27 μm
Conversion factor:	normally used at 3.85 e⁻/ADU
Noise level:	~10e⁻ (measured at telescope)
Linearity	±1.2 % up to 55,000 e⁻/pixel
Blemishes:	In high-level exposures in the RED a weak cold line at x=386 and a warm patch from x=366, y=146 to x=391, y=127. Those blemishes are erasable with flat fielding.
Dark current:	10±2 e⁻/pixel/hour at 162 K.
Charge transfer efficiency:	CTE is 0.9999989 (parallel) and 0.9999969 (serial)
R.Q.E.:	See Figure 3
Operating temperature:	162 K
Cosmic ray events:	3.55 ± 0.30 events/min/cm^2

team at La Silla will carry out a large programme of CCD optimization in the next months, which should improve that situation.

Tests at the Telescope

The new set-up was tested in one photometric night in December 1992, using the Short Camera and both, the 31.6 and 52 lines/mm echelle.

The mounting of the crossdisperser and of the CCD was quite successful, and no major problems occurred. It was possible to obtain a homogeneous focus over the whole chip and no ghosts appeared. Only for wavelengths above ~ 6400Å some traces of the second order of the crossdisperser were present at a low level, but, if necessary, these can be easily filtered out using the colour filters available in the CASPEC filter wheel.

The efficiency of the telescope + instrument was measured observing spectrophotometric standards from the list of Hamuy et al. 1992, and the results are shown in Figure 3, for both the 31.6 (filled squares) and the 52 lines/mm (filled triangles) echelle. Note that the efficiency refers to the peak of the order blaze. For the bluest orders of the 31.6 line/mm echelle the overall efficiency is somewhat higher than in Figure 3, due to the large order overlap achievable with this configuration.

The important gain obtained after these last improvements can be appreciated by comparing our new results with those obtained with the old configuration, which are also shown in Figure 3 (open squares).

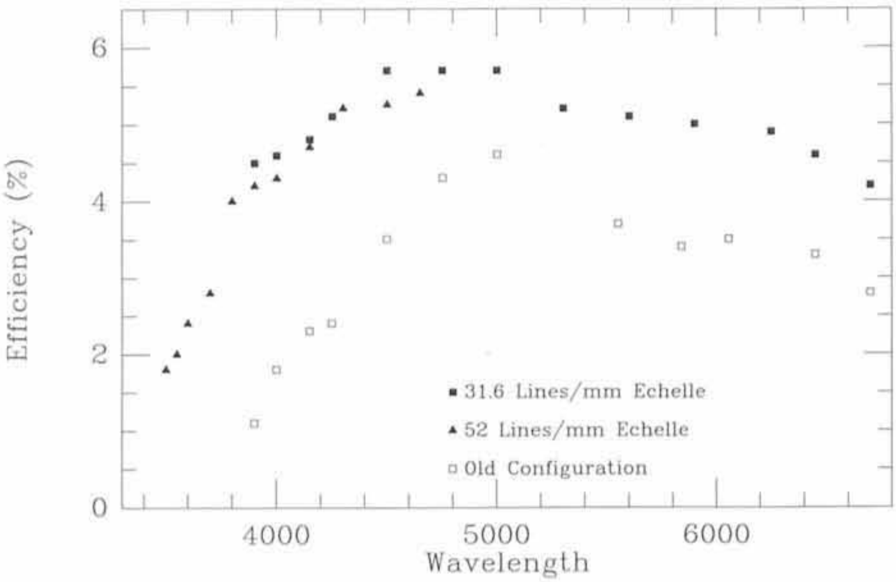

Figure 3: *Overall efficiency curve for the 3.6-m telescope + CASPEC and the new Blue crossdisperser. Short Camera plus 31.6 lines/mm echelle (filled squares) and 52 lines/mm echelle (filled triangles). The results obtained with the old configuration are also shown (open squares) for comparison.*

CASPEC is now working at high performance over the whole visual and blue spectral ranges and it has already been successfully used by several visiting astronomers.

Acknowledgements

Special thanks go to the members of the detector groups at La Silla (P. Moore, P. Sinclaire) and Garching (S. Deiries and R. Reiss) who have tested and prepared CCD #32.

References

Baade, D., Crane, P. 1990: *The Messenger* **61**, 49.

Hamuy, M. et al. 1992: *PASP* **104**, 533.

Melnick, J., Dekker, H., D'Odorico, S. 1992: *EMMI&SUSI* ESO Operating Manual, in preparation.

Molaro, P., Castelli, F., Pasquini, L. 1992: in "Origin and Evolution of the Elements", in press.

Pasquini, L., Gilliotte, A. 1991: *The Messenger* **65**, 50.

Pasquini, L., Rupprecht, G., Gilliotte, A., Lizon, J.L. 1992: *The Messenger*, **67**, 50.

STAFF MOVEMENTS

Arrivals

Europe

CIMATTI, Andrea (I), Student
DUBATH, Pierre (CH), Associate
FENDT, Michael (D), Engineer (Systems)
MAGANA BÄRNTHALER, Anne (F/USA), Secretary/Administrative Assist. to the Director General
MORTENSEN, Lars (DK), Mechanical Engineer
MOUREAU, Serge (B), Electronic Technical Engineer
WOLOHAN, Deirdre (IRL), Administrative Clerk (Personnel)

Chile

KNEIB, Jean Paul (F), Coopérant
VAN DER BLIEK, Nicole (NL), Student

Departures

Europe

GEHRING, George (D), Student
GOUIFFES, Christian (F), Fellow
MERKLE, Fritz (D), Optical Engineer
PIENEMAN, Henk (NL), Accounting Assistant
VAN DER LAAN, Heike Renate (D), Executive Assistant/Head of Secretariat of the Director General
WILSON, Ray (GB), Senior Physicist

Chile

BECHMANN, Erling (DK), Foreman
JANSSON, Borgar (S), Electronics Maintenance Engineer

First Images from DFOSC

A new instrument for the Danish 1.54-metre telescope at La Silla has just been successfully tested. DFOSC (= Danish Faint Object Camera and Spectrograph) is similar in concept and performance to the ESO instruments EFOSC and EFOSC2, and it offers the same possibilities for direct imaging and low dispersion spectroscopy (including an echelle mode).

The image shown here, a 30-second, exposure of the 30 Doradus area in the Gunn r filtre, was obtained on Dec. 6, 1992 by Per Kjaergaard Rasmussen (PI) and Michael Andersen from the Copenhagen University Observatory. South is up and east is to the right. A logarithmic intensity scale has been used.

The detector is a 1000 x 1000 Thomson CCD which gives a 8.5 x 8.5 arcmin^2 field. The instrument will eventually be equipped with a 2000 x 2000 Ford CCD which will give a field of 13.7 x 13.7 arcmin^2.

DFOSC may possibly be offered to the ESO community later this year. A short description of the instrument will be published in a forthcoming number of *The Messenger.*

P. KJAERGAARD, Astronomical Observatory, Copenhagen University, Denmark

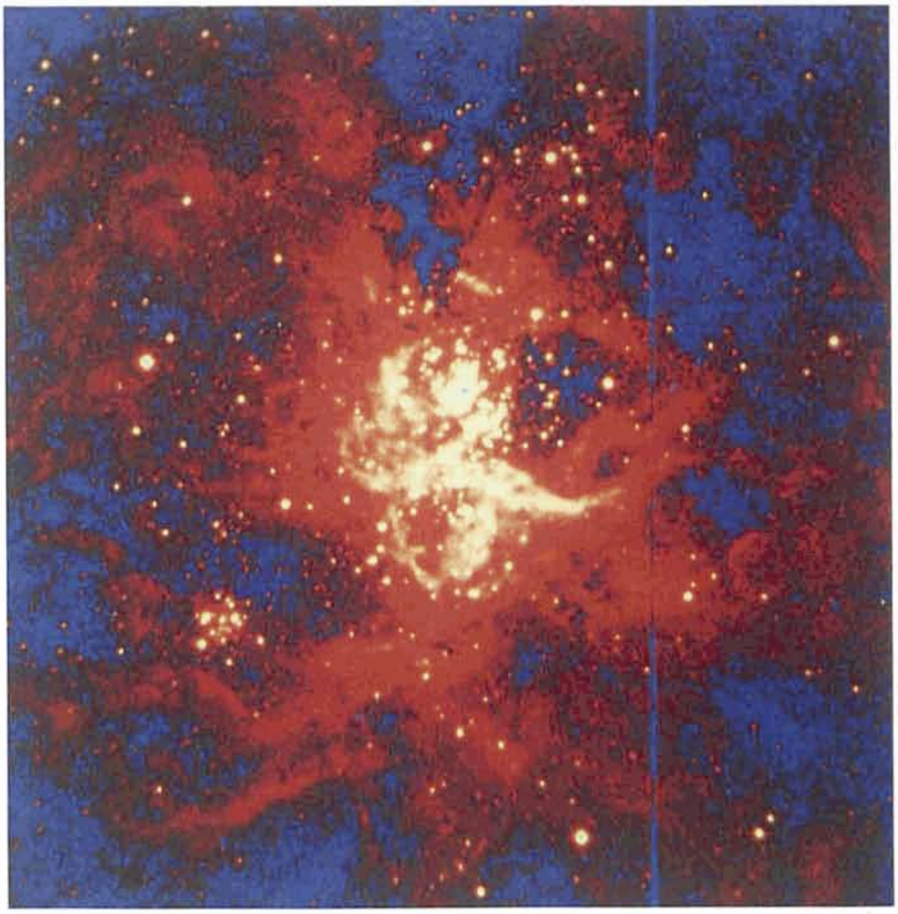

A New Fine-Grain Photographic Emulsion

T.A. BIRULYA[1], D.K. MIKHAILOV[2], P.V. SHEGLOV[1]

[1]Sternberg Astronomical Institute, Moscow University, Moscow, Russia; [2]"Slavitch" A.S., Moscow, Russia

Photographic observations continue to play an important role in astronomy in our part of the world, although we of course hope that in the future more and more CCD detectors may become available at observatories in the republics on the territory of the former Soviet Union. For certain purposes like accurate astrometry, however, the photographic emulsion is still superior to the digital detectors, thanks to its great stability and large area.

It would clearly be very useful to further improve the photographic emulsions which are available for astronomers. For this reason, astronomical photographical plates with quasi-T AgBr crystals have been experimentally produced during the past four years and progressively improved at the "Slavitch" A.S. factory near Moscow. This emulsion is fine grain and must be hypersensitized by hydrogen soaking before the observations. It is coated on accurately polished glass of 2.6 mm thickness for astrometric purposes, and is also available on 1.3 and 1.7 mm thick glass at sizes up to 30×30 and 30×36 cm. The hypersensitizing of these plates was made by T.A. BIRULYA at the Sternberg Institute.

Several research programmes are now underway at the Sternberg Astronomical Institute with these plates. For instance, Dr. Yurij Shokin has been using them during the past four years with the 23-cm astrometric refractor (f–2300 mm) at the field station of the Sternberg Institute at Mount Majdanak (Uzbekistan) to greatly improve the positional accuracy of the reference stars and hence the Martian moons, Phobos and Deimos. He has also used them for the determination of the positions of optical counterparts of radio sources.

The achievable astrometric accuracy has been compared with that obtainable on ORWO ZU-21 plates which were used earlier for these programmes. A certain improvement is noted, especially when the very stable, 2.6 mm thick plates are used; these are much flatter than the ZU-21 coated on 1.6-mm glass, then bending resulting from the gelefication of the emulsion.

Dr. Goransky has also used the new plates to obtain photographs of the Andromeda Nebula by means of a 50-cm Maksutov camera (f=2000 mm), located at the Sternberg station on Crimea. With

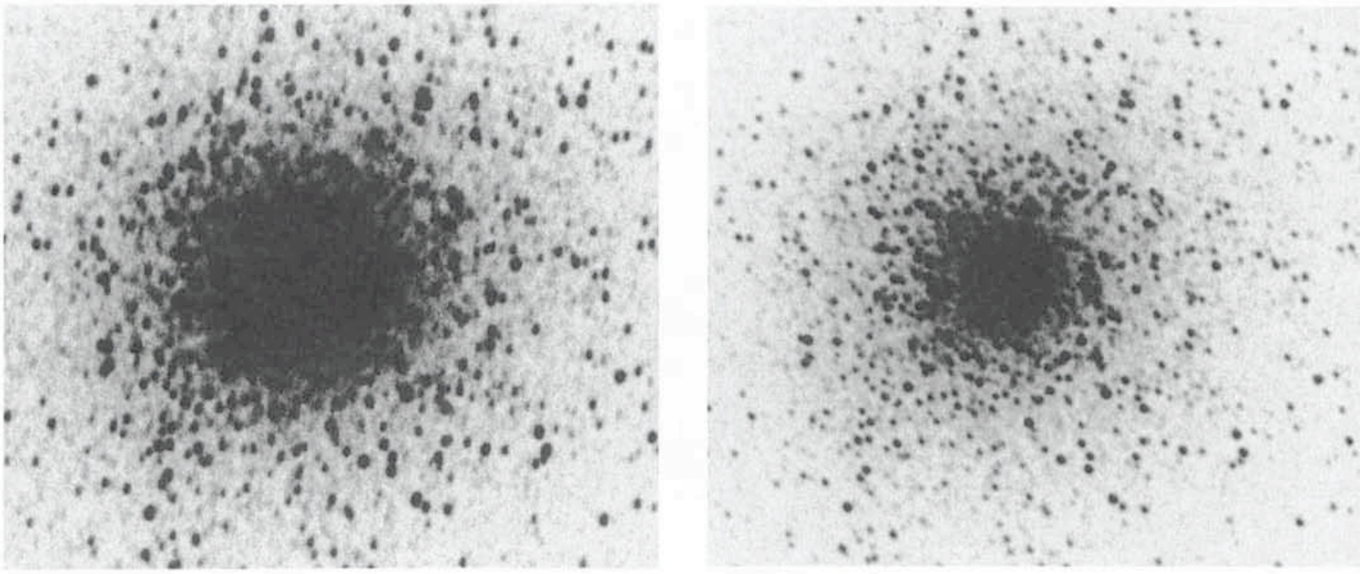

Figure 1: *A comparison between the new T-emulsion (right) described in this article, and the ORWO ZU-21 (left) which was much used before. Both photos were obtained by A. Martys with the 50-cm Maksutov telescope at the Crimean field station of the Sternberg Astronomical Institute and show the central part of the globular cluster Messier 13. The photographic reproductions from the original plates were made by H.-H. Heyer at the ESO Headquarters.*

an exposure of 60 min under good conditions and through a B filtre, he reaches a limiting stellar magnitude which according to Dr. Sharov is near 19.5, and the plates show many individual stars on the nebular background.

With the same instrument, Dr. A. Martys took several T-plates of the globular cluster M13 for plate evaluation and they were compared to ZU-21 plates. The new plates reach a limiting magnitude of about 20.5 in a 60-min exposure.

Using the new emulsion, Dr. N. Chernykh of the Crimean observatory reached magnitude 18 in 30 min with the Zeiss astrograph (D=40 cm, f=160 cm) and measured the positions of (4179) Toutatis even though it was very close to the horizon. On ORWO ZU-21 this asteroid could not be found.

At the Tashkent Observatory (Uzbekistan), Drs. A. Latypov and E. Mirmachmudov made some tests in May 1991 of the new emulsion with the Carte du Ciel astrograph (D=33 cm, f=344 cm). This astrograph is subject to heavy light pollution, since the observatory which was founded in 1873 is now situated near the centre of a town of 2 million inhabitants. Still, with an exposure of 20 min, they measured images of stars down to 15.5; measurable images of Pluto were also obtained. During March 1991, Dr. Bronnikova at Pulkova Observatory used the Carte du Ciel astrograph there to photograph Pluto with the new plates. Measurable images of the planet (15.5 pg) were obtained with an exposure of 30 minutes, also under heavy light pollution conditions. So, the new T-crystal plates appear to be useful for the revitalization of the Carte du Ciel astrographs, of which several have excellent first epoch collections.

At the 6-metre telescope, Dr. Yu. Glagolewsky has used the new plates for coudé spectroscopy with a Zeeman analyser. He reports that the graininess of the new plate is much finer than of the Kodak 103aO plate, improving the limiting magnitude.

CORRECTION

On the Dead-Time Constant in Photon-Counting Systems

In *The Messenger* **68**, page 52, I drew attention to a practical method to determine the dead-time constant τ in photoelectric photometry. In that paper n_τ, the number of photons which arrive in a time interval shorter than τ, was calculated to be

$$n_\tau = N \int_0^\tau \lambda e^{-\lambda t} dt,$$

where N is the total number of photons arrived during the measurement time and λ is the arrival frequency of the photons. This equation was derived from the Bose-Einstein statistics. However, this approach is not valid since to observe the effects of Bose-Einstein clumping it is necessary to use much faster equipment and much more monochromatic light than we have in ordinary astronomical photometry. Actually, the arrival of photons can be considered as independent events and Poisson statistics can satisfactorily fit the distribution of intervals between an event and the next one, as R. D. Evans makes clear in his fundamental textbook *The Atomic Nucleus* (1955, Mc Graw Hill Publ.).

In such a distribution, the probability that the duration of an interval will be between t and t + dt is

$$dP_t = \lambda e^{-\lambda t} dt.$$

The number of intervals greater than t_1 but less than t_2 is obtained by integrating

$$n = N \int_{t1}^{t2} dP_t = N \int_{t1}^{t2} \lambda e^{-\lambda t} dt.$$

Resolving for $t_1 = 0$ and $t_2 = \tau$ we obtain the same equation as with the Bose-Einstein approach. Of course, the subsequent approximations are again valid, leading to the same practical formula.

Thanks are due to Andy Young who prompted these remarks on the incorrect approach.

E. PORETTI,
Osservatorio Astronomico di Brera, Milano, Italy

Astronomy Acknowledgement Index 1992

D. A. VERNER, Kapteyn Astronomical Institute, Groningen, the Netherlands, and Space Research Institute, Moscow, Russia

Last year we announced the creation of *Astronomy Acknowledgement Index (AAI)*, which included bibliographical references to all personal acknowledgements from 7 leading journals in astronomy and astrophysics. The aim of this project is to give, in addition to the *Science Citation Index*, the useful informational tool for astrosociology and history of astronomy. Since the publication of the statistical overview of *AAI*-1991 (D. A. Verner, 1992, *The Messenger* No. 67, p. 61, hereafter Paper I), we have received many comments and some requests for *AAI*-1991 data.

Table 1. *General statistics of AAI*-1992. *N_{pap} is the number of papers, N_{ack}* the number of acknowledgements.

	ApJ	*ApJS*	*A&A*	*A&AS*	*MNRAS*	*AJ*	*Nat*	*PASP*	Total
N_{pap}	1680	119	1127	173	507	362	104	149	4221
N_{ack}	5540	509	3003	688	1148	1179	280	608	12955
N_{ack}/N_{pap}	3.30	4.28	2.66	3.98	2.26	3.26	2.69	4.08	3.07

Table 2. *The 21 most-acknowledged scientists from astronomy and astrophysics journals in 1992.*

Name	Affiliation	*ApJ*	*ApJS*	*A&A*	*A&AS*	*MNRAS*	*AJ*	*Nat*	*PASP*	Total
E. Bertschinger	MIT, Cambridge, USA	14				4				18
R.D. Blandford	Caltech, Pasadena, USA	14				4	1	1		20
D. Burstein	Arizona State Univ., Tempe, USA	11	2	1	1		2		1	18
B.T. Draine	Princeton University, USA	10	1	3		1				15
G.J. Ferland	Ohio State Univ., Columbus, USA	18	4	2		5	2	1		32
J.E. Gunn	Princeton University, USA	12	1			1	3			17
J.P. Huchra	CfA, Cambridge, USA	10				4	2		1	17
R.L. Kurucz	CfA, Cambridge, USA	7		8	1		3			19
J.P. Ostriker	Princeton University, USA	26	1	1		3				31
B. Paczyński	Princeton University, USA	17				1		3	1	22
P.J.E. Peebles	Princeton University, USA	21				2				23
E.S. Phinney	Caltech, Pasadena, USA	12	1			6	1			20
M.J. Rees	Cambridge University, UK	14		2		9		1	1	27
P.L. Schechter	MIT, Cambridge, USA	4	2		1	3	6		2	18
S.N. Shore	NASA/Goddard, Greenbelt, USA	10		3			1		1	15
P.B. Stetson	DAO, Victoria, Canada	5	3		1		5		5	19
M.A. Strauss	Caltech, Pasadena, USA	14	2			3	2			21
S. Tremaine	CITA, Torontó, Canada	18	1				1		1	21
E.L. Turner	Princeton University, USA	19				2	3			24
S.D.M. White	Cambridge University, UK	13		1		5	1	2	1	23
S.E. Woosley	Univ. of California, Santa Cruz, USA	18		1		1	1	1		22

In 1992, we included in our compilation the eighth journal, *Publications of the Astronomical Society of the Pacific (PASP)*. References to personal acknowledgements from 1991 PASP papers have been added to *AAI*-1991 as well. In 1991, *PASP* published 158 papers, which included 442 acknowledgements (in average, 2.80 per paper).

Table 2 of Paper I presented the names of scientists who were acknowledged in 15 or more papers in 1991. Taking into account the data from *PASP*, this table should be completed by two names. P. B. Stetson (Dominion Astrophysical Observatory, Canada) got 15 acknowledgements in 1991 (*ApJ*-3, *ApJS*-1, *A&A*-1, *AJ*-6, *PASP*-4), and R. E. Williams (Cerro-Tololo Interamerican Observatory) got 16 (*ApJ*-5, *A&A*-1, *A&AS*-1, *MNRAS*-3, *AJ*-2, *Nat*-1, *PASP*-3). Also, additional gratitudes in the 1991 *PASP* papers were addressed to the following scientists from Table 2 in Paper I: G. J. Ferland (1), J. P. Huchra (1), J. E. Pringle (1), and J. C. Raymond (3).

Now we present some statistics based on *AAI*-1992. The total amount of data in *AAI*-1992 is 12996 bibliographical references (110 % of the 1991 data). We have used the same as in 1991 threshold of 15 papers for including a scientist in the list of most-acknowledged persons. As in 1991, papers in American journals contain more acknowledgements (in average, 3.40 per paper) than papers in European ones (2.68). That is one of the reasons, why American scientists have dominant positions in the Table 2. The most-acknowledged astronomers from the ESO countries are A. Renzini (University of Bologna, Italy) – 14 (*ApJ*-3, *A&A*-5, *A&AS*-1, *MNRAS*-2, *AJ*-3) and C. M. Walmsley (Max-Planck-Institut für Radioastronomie, Bonn, Germany) – 14 (*ApJ*-4, *A&A*-10). Note that 13 of 21 names (62 %) appeared in the Table 2 the second year. Six scientists from this table are affiliated to Princeton University, and the seventh, M. A. Strauss, is affiliated to Princeton Institute for Advanced Study (in his last 1992 papers only).

Data from *AAI*-1991 and *AAI*-1992 are available upon request (Internet: dverner @kapteyn.astro.rug.nl). *AAI*-1993 is being compiled now.

Amateur Astronomy with CCDs

P. ANIOL, Sternwarte Cessertshausen, Germany

Watch out professionals, the amateurs are coming!

In the last few years a dream came true for the amateur astronomers. With the arrival of relatively low-cost CCD cameras on the market, it became possible to join the astronomical imaging revolution. At the same time, amateurs have begun to have access to powerful imaging tools, similar to those used by professional astronomers at ESO and around the world for their work.

All amateur CCD cameras of the first generation are based on the same Texas Instruments chip (TC-211) with 192 by 165 pixels, each measuring 13.3 by 16 micron. Although this chip has a surface of only 2.5 by 2.5 mm and because of the rather high electronic readout-noise, it is still possible to obtain really impressive results when compared to conventional photography. Richard Berry, the former editor of *Astronomy* has written some image processor programmes (ImagePro, QuickPix and ColorPix) for the most popular amateur CCD cameras on the market.

So all you need to do amateur observations is a good telescope, the CCD camera and a PC. If you are the happy owner of a Laptop computer it is also possible to go outside with a portable telescope and to benefit from the dark skies in the Alps or somewhere else.

For the images shown here, I used the Lynxx CCD camera from Spectra Source; it is the only first-generation camera with 12-bit resolution, all the other cameras have only 8 bits. It can easily be attached to any telephoto lens or telescope, making it possible to convert the CCD head from a wide-angle camera into a high-resolution planetary camera within a few minutes.

For example, the images of comet P/Swift-Tuttle (Figs. 1 and 2) were obtained with a 500-mm telephoto lens with a resulting field width of 16 arcminutes. the image of Saturn (Fig. 3) was made with an effective focal length of six metres, which corresponds to 0.4 arcsec per pixel.

It is also possible to create colour pictures by superposing in the computer three single exposures taken through three different colour filters.

The Lynxx CCD camera was also used at the 1.06-metre amateur telescope in Puimichel in southern France. This telescope was completely built by the Belgian amateur astronomer and mirror maker Dany Cardoen. The Amateur Observatory Puimichel lies in a beautiful landscape with many clear dark nights near the professional Haute-Provence Observatory in Southern France.

In the meantime, the next generation of amateur CCDs has begun to appear on the market and the future in digital imaging for amateurs looks extremely promising!

Larger chips and more sophisticated electronics and programmes now provide possibilities to which only professional astronomers had access a few years ago. For example, the new ST-6 camera from SBIG works with a CCD, which is 8 times larger than the TC-211 and has 16 bit resolution. Next year another Lynxx model with a 500 pixel CCD may become available. With these cameras one can do really serious, qualitative work at prices which are reasonably affordable for Western amateurs.

My personal goal in the coming years is to construct a large mobile telescope which will allow conventional photography with a relatively large field on the sky of 2 by 2 degrees as well as CCD imaging. It will be a 0.86 metre Newtonian f/3.4 telescope on a fork mounting with computer-controlled drive and positioning system. The telescope will be fully transportable and will be mounted on a trailer. With this instrument, which

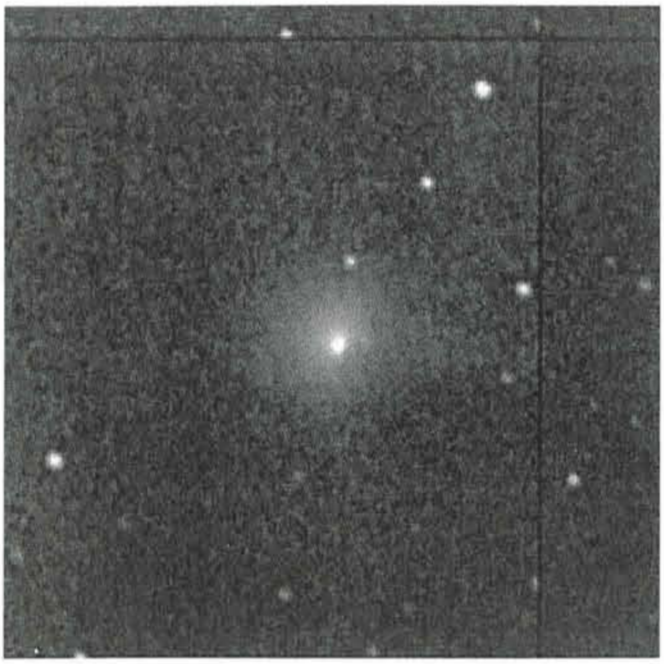

Figure 1: *Comet P/Swift-Tuttle 1992t on October 30, 1992 at 17:55 UT, exposure: 300 sec; scale: 5 arcseconds per pixel; estimated total magnitude of coma: 7.2 mags.*

Figure 2: *Comet P/Swift-Tuttle 1992t on November 6, 1992 at 17:25 UT, exposure: 600sec; scale: 5 arcseconds per pixel; estimated total magnitude of coma: 6.5 mags. Both comet exposures were made through a 500-mm telephoto lens with f/8.0*

Figure 3: *Saturn on August 8, 1992 at 21:30 UT. Composite image of three single images made through Wratten filter 23A for red, 56 for green and 38A for blue light. Exposure time: 0.5 sec, 1 sec and 3 sec for red, green and blue light respectively. The seeing was mediocre (about 2 arcseconds) and the image was taken at the 1.06-m Newton telescope in Puimichel.* ▶

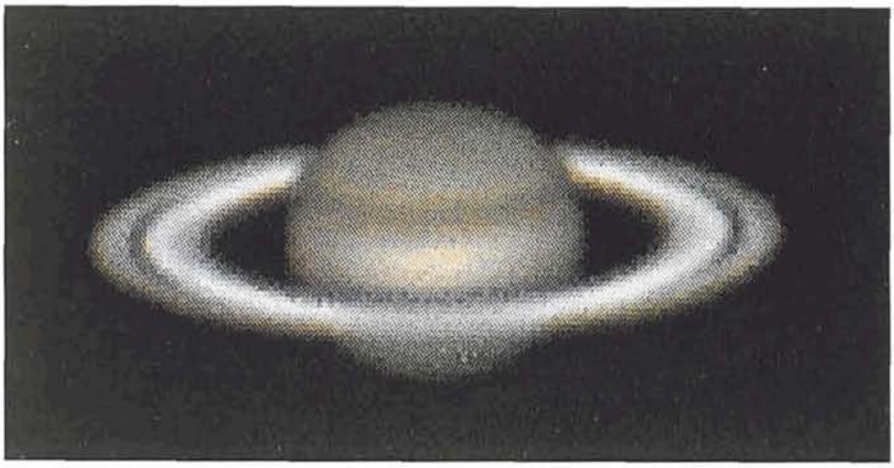

is already under construction, I intend to travel to the best places for astronomy in the world, including northern Chile. This will obviously not be easy, but with the help of friends nothing is impossible.

"First light" for the new telescope will be in the first half of 1993. Maybe I will have the opportunity to inform the readers of *The Messenger* about the progress of this project and the results from the future observations.

I want to thank the *Messenger* editor, who invited me to write about some aspects of CCD astronomy, as it is used by non-professionals. I also want to thank the ESO Image Processing Group for preparing my images shown in the article.

Development of ESO Publications

Introduction

The readers of *The Messenger* are probably aware that ESO is one of the world's major astronomical institutes, and most of the readers also know that, apart from some advance information published in *The Messenger*, the results of the scientific research performed at ESO are published in the well-known astronomical journals like *Astronomy and Astrophysics, Monthly Notices, Astrophysical Journal*, etc.

But not so many people realize that, in addition to *The Messenger*, ESO produces many other publications as well and is also a registered "publishing house". The number of these publications and especially their volume has increased over the years, reflecting the increasing scientific and technical activities of this Organization. In this article, the development of ESO's main publications will be described – primarily with regard to the increase of pages from 1974 – the first year of service of the undersigned – to 1992. It would be too time-consuming to compare the page numbers for each of these years. Therefore only the following four years – 1974, 1980, 1986 and 1992 – will be considered here. The six-year intervals have been randomly chosen, and there are certainly fluctuations from one year to the other between these reference years, but the general tendency is obvious: the number of ESO publications has been steadily increasing.

Which Are These Publications?

The most important ESO publications are *The Messenger*, the Annual Report, the ESO Conference and Workshop Proceedings and the Scientific and Technical Preprints. Other series are the VLT Reports, the Scientific Reports, the Technical Reports, the ESO Users Manual, the Operating Manuals and the Maintenance Manuals. In addition to these series, ESO also publishes information material for PR purposes – e.g. press releases and posters – and, from time to time, books like "Evolution in the Universe", "The ESO/Uppsala Survey of the ESO (B) Atlas", "ESO's Early History", etc. The term "main" or "important" publication in this connection only refers to the effort and time required to prepare them for publication. It does not take into account the sometimes enormous efforts of the authors and other people involved (secretaries, photographers, draftsmen, etc.) to draft and type the manuscript and to provide the accompanying illustrations. Information leaflets, posters and similar material (though their preparation can be rather time-consuming) will not be included in this comparison. Their relatively small number of pages does not reflect the time involved and would not have much influence on the total number of pages given hereafter.

In the early years of ESO there existed two other series whose publication was discontinued in the 1970s: *The ESO Bulletin* and the *Communications of the European Southern Observatory*. The former mostly contained infomation of a more technical nature like reports on instrumentation or meteorological reports, and the latter consisted of reprints of articles published in the scientific journals by ESO researchers.

The Messenger

The Messenger was launched in May 1974 by Prof. A. Blaauw (then Director General of ESO) in order "... to promote the participation of ESO staff in what goes on in the Organization, especially at places of duty other than our own. Moreover, *The Messenger* may give the world outside some impression of what happens inside ESO..." It may be useful to remind the reader that in 1974 the ESO Headquarters in Garching did not yet exist and that the European activities of ESO were dispersed over Hamburg (Office of the Director General and Administration) and Geneva (Telescope Project Division and Sky Atlas Laboratory).

The first issue of *The Messenger* had six pages, the one of December 1992, 88 – the record so far attained. The circulation at the beginning was about 1000 copies, today it is 4200, with new subscriptions being opened almost every day. If we except the first three issues, until now two editors have been responsible for the journal, Dr. R. M. West and Dr. P. Véron. *The Messenger* is now published under the responsibility of the ESO Information Service, to which the undersigned is also affiliated.

Two issues were published in 1974 with a total of 12 pages. In 1980 there were only three issues instead of the four originally planned: No. 20 (12 pages), No. 21 (32 p.) and No. 22 (20 p.), amounting in total to 64 pages. The following issues were published in 1986: No. 43 (36 p.), No. 44 (40 p. [the first colour pictures appear!]), No. 45 (36 p.) and No. 46 (28 p.), which brings us to a total of 140 pages. In the last year of this comparison, 1992, there were also four issues: No. 67 (64 p.), No. 68 (56 p.), No. 69 (72 p.) and No. 70 (88 p.). With a total of 280 pages this is exactly twice the number of pages as in 1986.

Total number of pages/issues published of the various ESO publications in the years 1974, 1980, 1986 and 1992.

Year	1974	1980	1986	1992
The Messenger (number of pages)	12	64	140	280
Annual Report (number of pages)	174[1]	112[2]	90[3]	130[4]
ESO Conference and Workshop Proceedings (number of pages)	398	654	1166	3128
ESO Preprints (number of issues)	–	57	69	93
Other publications (number of pages)	246	188	796	1520

[1]Total number of pages of the English (86 p.) and French (88 p.) versions of the Annual Report for 1973. – [2]Total number of pages of the English (56 p.) and French (56 p.) versions of the AR for 1979. – [3]"New" 3-language version of the AR for 1985. – [4]3-language version of the AR for 1991.

The Annual Report

According to the ESO Convention, the Director General "shall submit an annual report to the Council". The four reports compared in this account have been conceived by three different Directors General; note also that the reports published in 1974, 1980, 1986 and 1992, in fact refer to the years 1973, 1979, 1985 and 1991, respectively.

The 1973 and 1979 reports were still published in two versions, an English version and a French one that usually followed about half a year later. The English and French versions of the Annual Reports for the years 1973 and 1979 amounted to 86 and 88 (total: 174), and 56 and 56 (112) pages, respectively. The drop in the number of pages is of course not due to a decrease in the activities of ESO, but to the arrival of a new Director General in 1975, Prof. L. Woltjer, who somewhat changed the style and compressed the format of the report. Later, with the Annual Report for 1980, the format of the report was changed again, and from then on it contained three languages, English, French and German, in one volume. The 1985 report, therefore, again increased to 90 pages, and the 1991 Annual Report, presented by the third Director General during the period under review, Prof. H. van der Laan, to 130 pages.

The ESO Conference and Workshop Proceedings

One of the aims of ESO stated in the Convention is "promoting and organizing co-operation in astronomical research". An important means to fulfill this requirement are the numerous colloquia, workshops and conferences organized by ESO and held at irregular intervals at ESO or at other institutes in the member States and elsewhere. The proceedings of these meetings constitute an increasingly important series of ESO publications. To allow speedy publication, the speakers at the meetings are requested to submit their contribution in camera-ready form. Responsibility for the editing is generally assumed by one or several of the organizers of the meeting. The first volume in this series, "ESO/CERN Conference on Large Telescope Design" appeared in 1971.

The first volume considered in this comparison was the No. 4 in the series, "ESO/SRC/CERN Conference on Research Programmes for the New Large Telescopes" (398 p.), published in 1974.

In 1980, the proceedings of three workshops were published: "ESO Workshop on Two Dimensional Photometry" (412 p.), "ESO Workshop on Methods of Abundance Determination for Stars" (56 p.) and "The First ESO/ESA Workshop on the Need for Coordinated Space and Ground-based Observations – Dwarf Galaxies" (186 p.), amounting in total to 654 pages.

In 1986, three proceedings volumes were published: the ESO-OHP Workshop on "The Optimization of the Use of CCD Detectors in Astronomy" (356 p.), the Second Workshop on "ESO's Very Large Telescope" (484 p.) and the Second ESO-CERN Symposium "Cosmology, Astronomy and Fundamental Physics" (326 p.). Taking them together brings us to 1166 pages.

The year 1992 brought about a new record. Five proceedings were published (including the one on "High-Resolution Imaging by Interferometry II" (1318 p.), the manuscripts of which had been submitted to the printer in July 1992, but – due to problems at the printers – the Proceedings were delivered only end of February 1993). The other four proceedings are: "4th ESO/ST-ECF Data Analysis Workshop" (188 p.), "High Resolution Spectroscopy with the VLT" (310 p.), "Progress in Telescope and Instrumentation Technologies" (778 p.) and "Astronomy from Large Data Bases II" (534 p.). So the total number of pages of the 1992 proceedings amounts to no less than 3128.

The ESO Preprints

The ESO Scientific Preprint series was initiated in 1976, and in 1988 the first Technical Preprint was published. In this comparison, however, no distinction will be made between these two series. The preprints reflect more than any other ESO publication the increasing scientific activities at ESO. They contain articles written by, or in collaboration with, ESO staff and which, normally, have been accepted for publication by one of the big scientific journals. The delay between submission and publication of these articles often amounts to several months, so that in general the results of the research carried out at ESO are made available to the astronomical community much earlier by means of the preprints.

Since a great number of preprints are no longer available, it is not possible to give the exact number of pages published in the years of reference. For this reason only the number of preprints can be given and not the number of pages as for the other publications.

In 1980 there were 57 Scientific Preprints (Nos. 75 – 131). In 1986 this number amounted to 69 (Nos. 411 – 479), and in 1992 there was a total of 93 preprints (Scientific Preprints Nos. 811 – 895 and Technical Preprints Nos. 43 – 50).

Other Publications

The other ESO publications will be treated jointly under this subheading.

In 1974, there were the ESO Bulletin No. 10 (40 p.) and five Technical Reports published by the Telescope Project Division at CERN in Geneva: No. 1 (46 p.), No. 2 (54 p.), No. 3 (38 p.), No. 4 (22 p.) and No. 5 (46 p.), summing up to a total of 246 pages.

in 1980 were published the Technical Report No. 12 (30 p.), Maintenance Manual No. 1 (78 p.), the User's Manual No. 1 (28 p.) and User's Manual No. 2 (52 p.). This series was later interrupted and succeeded by the "Operating Manual" to avoid confusion with the "big" Users Manual. The total number of pages of these publications amounts to 188.

In 1986 there were the Maintenance Manual No. 4 (50 p.) and the VLT Reports No. 43 (52 p.), No. 44 (172 p.), No. 45 (156 p.), No. 46 (100 p.), No. 47 (34 p.), No. 48 (20 p.), No. 49 (144 p.), No. 50 (16 p.), No. 51 (20 p.) and No. 52 (32 p.), which makes a total of 796 pages.

In 1992 the number of pages of these publications reached so far its highest point: 1520. There were first the Strasbourg-ESO Atlas of Galactic Planetary Nebulae – Part I and Part II – (1044 p.), the Scientific Report No. 11 (212 p.), the VLT Report No. 65 (132 p.) and the Operating Manuals No. 10 (44 p.), No. 14 (36 p.) and No. 16 (52 p.).

Concluding Remarks

Up to now it has been possible to avoid increasing the manpower concerned in spite of the considerable increase in volume of the ESO publications. To make this possible, it was necessary to transfer the PR activities which were previously taken care of by the undersigned to other members of the Information Service. So there is still only one man acting as "interface" between authors and editors, on the one hand, and the printers, on the other. Today, however, it seems that the limit of what is possible within the present system and with the present manpower has been attained. The 40-hour week has become a rare exception and longer delays are often unavoidable. Nevertheless, authors of papers for the Conference and Workshop Proceedings and to a certain extent also the authors of preprint articles and the editors of manuals have the possibility to alleviate this situation somewhat, by really making their papers camera-ready. Indeed, a number of authors have recently made great efforts in this sense, and it is hoped that others will follow their example. This could in many cases help reduce delays.

I should like to take this opportunity to thank the authors and editors for their patience and comprehension, especially in those cases where the preparation of their publication took longer than expected.

K. KJÄR, ESO

Written-Off Items Available at ESO Garching

The following electronic parts, in good condition for further use, have recently been written off at ESO, Garching, and are immediately available for donation to Scientific Institutes provided that:

- a formal request is presented to ESO, Contracts and Procurement (Mr. F. Palma, Tel.: 0049-89-32006-205, Fax: 0049-89-3207327), before April 30, 1993,
- the Institute takes charge with own means of picking up the equipment in the place, state and condition where the item is located; alternatively, the Institute can request delivery from ESO to a given destination at no warranty, bearing, however, the costs of removal, packing and transport.

Assignments will be done

- in order of presentation of a formal request up to exhausting items;
- giving priority to Institutes in the ESO Member States;
- giving preference to Institutes located in other countries, for which no export licence from Germany is necessary.

F. PALMA, ESO

Manufact.	Description	Part Number	S/N	Year of Manuf.
Kennedy	Magnet Tape	MT23Ken.9300	211–4387	1983
Kennedy	Magnet Tape	MT15	102–2422	1981
Kennedy	Magnet Tape	MT14	102–2421	1981
Kennedy	Magnet Tape	MT13	001–1394	1981
Kennedy	Magnet Tape	MT12	002–1463	1981
Hewlett Packard	Disc Controller	DC4HP13037B	1808F00470	1978
Hewlett Packard	Disc Controller	DC6HP13037C	1944A07543	1980
Hewlett Packard	Disc Drive	D21HP7914R	2413F00694	1984
Hewlett Packard	Disc Drive	D4HP7920A	1752A01479	1978
Hewlett Packard	Disc Drive	D9HP7920B	2028A02341	1980

(continued on page 64)

The ESO MESSENGER is published four times a year: normally in March, June, September and December. ESO also publishes Conference Proceedings, Preprints, Technical Notes and other material connected to its activities. Press Releases inform the media about particular events. For further information, contact the ESO Information Service at the following address:

EUROPEAN
SOUTHERN OBSERVATORY
Karl-Schwarzschild-Str. 2
D-8046 Garching bei München
Germany
Tel. (089) 32006-0
Telex 5-28282-0 eo d
Telefax: (089) 3202362
ips@eso.org (internet)
ESOMC0::IPS (decnet)

The ESO Messenger:
Editor: Richard M. West
Technical editor: Kurt Kjär

Printed by Universitäts-Druckerei
Dr. C. Wolf & Sohn
Heidemannstraße 166
8000 München 45
Germany

ISSN 0722-6691

Manufact.	Description	Part Number	S/N	Year of Manuf.
Hewlett Packard	Terminal	T59HP2621B	2309F03131	1983
Hewlett Packard	Terminal	T40HP2621P	2023W01286	1981
Hewlett Packard	Terminal	T49	2023W00735	1981
Hewlett Packard	Terminal	T58HP2626A	2245F01460	1983
Hewlett Packard	Terminal	T18HP2648A	1817F00268	1978
Hewlett Packard	Terminal	T13	1817F00181	1978
Hewlett Packard	Terminal	T44HP2621A	1942W02262	1981
Hewlett Packard	Terminal	T46HP2621A	1942W01976	1981
Hewlett Packard	Terminal	T22HP2621A	1920A05566	1979
Hewlett Packard	Terminal	T41HP2621A	1942W02282	1981
Hewlett Packard	Terminal	T43HP2621A	1942W02388	1981
Hewlett Packard	Terminal	T48HP2621A	1942W02013	1981
Hewlett Packard	Terminal	T47HP2621A	1942W01989	1981
Hewlett Packard	Terminal	T45HP2621A	1942W02022	1981
Hewlett Packard	Terminal	T42HP2621A	1942W02287	1981
Hewlett Packard	Terminal	T29HP2621A	1920A05572	1979
Hewlett Packard	Terminal	T28HP2621A	1920A05582	1979
Hewlett Packard	Terminal	T27HP2621A	1920A05565	1979
Hewlett Packard	Terminal	T24HP2621A	1920A05577	1979
Hewlett Packard	Terminal	T26HP2621A	1920A05562	1979

Contents